UNIVERSIDADE ESTADUAL DE CAMPINAS

INSTITUTO DE BIOLOGIA

Alexandre Bruni Cardoso

Envolvimento de Metaloproteinases de Matriz no Desenvolvimento e na Regressão da Próstata Ventral de Roedores

Este exemplar corresponde à redação final da tese defendida pelo(a) candidato (a)

Alexandre Bruni Cardoso

e aprovada pela Comissão Julgadora.

Tese apresentada ao Instituto de Biologia para obtenção do Título de Doutor em Biologia Celular e Estrutural, na área de Biologia Celular

Orientador: Prof. Dr. Hernandes F. Carvalho

Campinas, 2010

Campinas, 24 de fevereiro de 2010.

BANCA EXAMINADORA

Prof. Dr. Hernandes Faustino de Carvalho (Orientador)

_____
Assinatura

Profa. Dra. Helena Bonciani Nader

_____
Assinatura

Prof. Dr. Ruy Gastaldoni Jaeger

_____
Assinatura

Profa. Dra. Maria Christina Werneck de Avellar

_____
Assinatura

Prof. Dr. Sérgio Luis Felisbino

_____
Assinatura

Prof. Dr. Claudio Chrysostomo Werneck

_____
Assinatura

Prof. Dr. Willian Fernando Zambuzzi

_____
Assinatura

Profa. Dra. Luciana Bolsoni Lourenço Morandini

_____
Assinatura

Agradecimentos

Estou muito feliz e plenamente satisfeito com o trabalho que realizei durante esses quatro anos, e digo com certeza que não chegaria a esses resultados se não fosse à ajuda de diversas pessoas. Pessoas em que pude contar em todos os momentos da execução dessa tese. Portanto, agradeço de coração a todos aqueles que de forma direta ou indireta colaboraram para que essa tese fosse concluída.

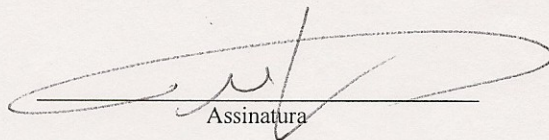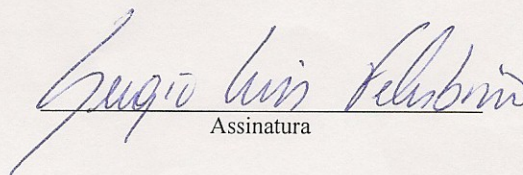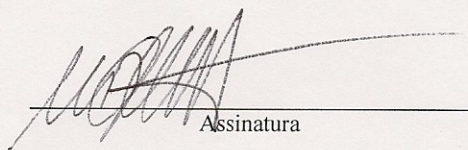Agradeço de forma muito especial o Prof. Hernandes F. Carvalho por ter me aceito como aluno de mestrado em 2004, ter continuado como meu orientador de doutorado e ter dado todo o suporte estrutural e intelectual em todas as etapas de execução do meu projeto. Muito obrigado Hernandes por ter me contagiado com o seu entusiasmo, rigor e curiosidade científica. Você é um exemplo de profissional e ser humano.

Aos Professores que aceitaram fazer parte da banca examinadora da minha tese: Dra. Helena Bonciani Nader, Profa. Dra. Maria Christina Werneck Avellar, Dr. Ruy Gastaldoni Jaeger, Dr. Sérgio Luís Felisbino e aos suplentes: Dr. Claudio Chrysostomo Werneck, Dr. William Fernando Zambuzzi, Dra. Luciana Bonsoni Lourenço.

Aos Professores Dr. Claudio Chrysostomo, Dr. Luciana Bonsoni Lourenço e Dr. Tiago Campos Pereira, pelo cuidado e senso crítico com que analisaram o meu projeto de qualificação.

Aos amigos e colaboradores, Profa. Dra Carmen V. Ferreira, Profa. Dra Dagmar Ruth Stach-Machado, Prof. Dr. Carlos Lenz Cézar Dr. Willian Zambuzzi, Márcio Lorencini, Juliete Francisco, Vinicius Pascoal e AndréThomaz.

A todos os integrantes do Laboratório de Matriz Extracelular: Guilherme, Taize, Rafaela, Danilo, Augusto, Rony, Fabiana, e as pessoas que já não mais trabalham no laboratório: Liliam, Silvia, Eliane, Helene, Manuel, Henrique, Rafael, Helene, Heloísa, Elusa e Daniele. Sou muito grato ao companheirismo, ajuda e ensinamentos que compartilhei com vocês.

À Profª Dra. Lynn Matrisian por ter me aceito para um estágio de 6 meses em seu laboratório na Vanderbilt University e pelo tratamento especial concedido a esse forasteiro.

Agradeço a todos os integrantes do laboratório de Biologia do Câncer da Vanderbilt University: Amy, Ashley, Barbara, Conor, Oliver, Michelle, Mike Lee. Especialmente sou grato ao Prof. Dr. Conor C. Lynch, por ter supervisionado meu trabalho no lab. Biologia do Câncer, pela amizade, pela ajuda e generosidade durante meu período em solo norte-americano.

Agradeço à FAPESP por ter concedido a minha bolsa de estudos (processo: 2005/04631-9) e por ter financiado todo o meu projeto.

A todos os Professores, funcionários e alunos do Departamento de Anatomia, Biologia Celular, Fisiologia e Biofísica. Obrigado pelos ensinamentos e pela grande colaboração

Ao Prof. Dr. Sebastião Roberto Taboga e a todos os integrantes do Laboratório de Microscopia e Microanálise da UNESP de São José do Rio Preto, onde tudo teve início na minha vida de biologista celular.

À Prof^a. Laurecir Gomes, coordenadora do Programa de pós-graduação em Biologia Celular e Estrutural. Um agradecimento muito especial à Liliam Panagio, secretária do Programa, pela prontidão e eficiência.

Aos meus companheiros do CatcherClub, em especial aos amigos Ernesto e José Luís, pelas amizade, risadas, cervejas e centenas de histórias.

À toda a minha família , aos meus pais Benedito e Malvina que sempre acreditaram em mim e apoiaram incondicionalmente com muito amor e dedicação os sonhos e pretensões de um "moleque doído" que sempre quis ser cientista. Meus pais, para mim vocês são os grandes exemplos de dedicação, amor ao próximo e perseverança.

Aos meus irmãos Leandro, Fernando e Tio Cosme e ao meu sobrinho Vinicius. Devo muito do que sou como pessoa a esses caras, que nunca me deixaram esquecer que há na vida muito mais do que livros e microscópios.

Sou muito grato de todo o coração a Andréia, minha esposa e eterna namorada, que sempre me apoiou desde o começo do doutorado, compreensível nas minhas ausências, dedicada e comprometida a construir uma vida inteira junto comigo. Muito obrigado minha Lindinha.

Aos meus pais Benedito e Malvina e à Andréia,
dedico essa tese

Índice

RESUMO

Importante glândula acessória do trato reprodutor de mamíferos, a próstata é um órgão alvo de várias doenças benignas e malignas, que ocorrem principalmente com o envelhecimento. Tanto o desenvolvimento prostático pós-natal como a regressão da glândula após a ablação hormonal são caracterizados por intensa modificação no comportamento das células e remodelação da matriz extracelular (MEC). As metaloproteinases de matriz (MMP) constituem uma família de enzimas que degradam principalmente componentes de MEC. Portanto, pareceu-nos plausível que as MMPs tenham papel crucial na remodelação tecidual que ocorre em decorrência dos eventos morfogenéticos da próstata ventral (PV) e na progressiva regressão prostática pós-castração. Assim, o objetivo desse trabalho foi investigar o papel da MMP-2 no desenvolvimento prostático pós-natal em roedores e das MMP-2, -7 e -9 na regressão da PV de ratos pós-castração. Para isso, foram empregadas técnicas moleculares, bioquímicas e análises morfológicas. A aplicação do siRNA específico para MMP-2 comprometeu o crescimento, a ramificação, a formação de lúmen e a proliferação de células epiteliais da PV de ratos *in vitro*, além de provocar um acúmulo de fibras colagênicas no compartimento estromal. A PV do camundongo MMP-2$^{-/-}$ adultos apresentou peso relativo reduzido e um menor volume epitelial, que resultaram de menor proliferação epitelial, menor ramificação ductal e maior estabilização da matriz colagênica durante a primeira semana de desenvolvimento pós-natal. Na regressão da próstata ventral de ratos após a castração encontraram-se múltiplas ondas de morte celular e uma relação direta entre a expressão e atividade das MMP-2, -7 e -9 e o pico de apoptose que ocorre 11 dias após a castração. Conclui-se através dos resultados apresentados neste trabalho, que tanto o desenvolvimento prostático pós-natal, como a regressão prostática pós-castração são dependentes da expressão e atividade das MMPs.

ABSTRACT

The prostate is an important gland of the reproductive tract of mammals, which is a target of several benign and malign diseases affecting the elder. Both postnatal prostate development and prostate regression after androgenic ablation are characterized by intense modification in cell behavior and remodeling of extracellular matrix (ECM). MMPs constitute a family of endopeptidases which are able to cleave preferentially ECM components. Thus, it seems reasonable that these enzymes play a crucial role in tissue remodeling that happens during the ventral prostate (VP) morphogenesis and in the prostate regression after castration. In this study, we aimed to define the involvment of MMP-2 in the postnatal prostate development of rodent and the involvement of MMP-2, -7 and -9 rat ventral prostate regression after castration. For this aim, we have used molecular, biochemical and morphological approaches. siRNA specific for MMP-2 compromised the rat VP growth, branching, lumen formation and epithelial cell proliferation, besides leading an accumulation of collagen fibers in the stroma. MMP-2$^{-/-}$ VP showed a reduced relative weight and epithelial volume, besides displaying a decreased epithelial proliferation and branching and a stabilization of collagen matrix at the end of the first postnatal week. In the prostate regression after castration, we found multiple waves of cell death and a direct association between activity and expression of MMP-2, -7 and -9 and an apoptotic peak that occurs at the 11$^{\underline{th}}$ Day after castration. In conclusion, the results presented here showed that both postnatal prostate development and prostate regression after castration are dependent on the expression and activity of MMPs.

LISTA DE ABREVIATURAS

Ac-DEVD-pNA: acetyl-Asp-Glu-Val-Asp p-nitroanilide

AIF: apoptosis-inducing factor

ANOVA: análise de variância

AR: androgen receptor

ARE: androgen-responsive element

BM: basal medium

BMP: bone morphogenetic protein

BSA: Bovine Serum Albumin

Cas: castrated

CML: célula muscular lisa

Ct: control

C$_T$: threshold cycle

DAPI: 4'-6-diamidino-2- phenylindole

DMSO: dimethyl sulfoxide

Dox: doxycycline

dUTP: deoxyuridine-triphosphate

EGF: epidermal growth factor

ELISA: enzyme linked immuno sorbent assay

ER: receptor de estrógeno

ECM: extracellular matrix

EMT: epithelial-to-mesenchymal transition

FAK: focal adhesion kinase

FAS: apoptosis stimulating fragment

FASL: FAS ligand

FGF: fibroblast growth factor

Fox: forkhead box protein

FST: follistatin

GFP: green fluorescent protein

GHR: growth hormone receptor

Gli: gliotactin family

Gli2: gliotactin family zinc finger 2

HC: hydrocortisone

HGF: hepatocyte growth factor

HOX: homeobox

HS: heparam sulfato

HSP: heat shock protein

IGF: insulin like growth factor

IgG: immunoglobulin G

INHBA: inhibin β A

KO: knockout

LAPC4: linhagem de células de câncer de próstata humana

LNCaP: linhagem de células de câncer de próstata humana

MEC: matriz extracelular

MMP: marix metalloproteinase

MT-MMP: membrane MMP

NKX3.1: NK3 homeobox 1

PPAR: peroxissome proliferator-activated receptor

PBS: phosphate buffer saline

pNA: p-nitroaniline

PTFE: politetrafluoretileno

PV: próstata ventral

RT-PCR: reverse transcription-polymerase chain reaction

qRT-PCR: quantitative reverse transcription-polymerase chain reaction

RAR: acid retinoic receptor

SD: standard deviation

SDS: sodium dodecyl sulfate

SEM: standard error of the mean

Ser: serine

SHG: second harmonic generation

SFRP-1: secreted frizzled-related protein 1

SHH: sonic hedgehog

siRNA: small interference RNA

SMC: smooth muscle cell

SMO: smoothened

SRD5A2: steroid 5 alpha-reductase type 2

SUG: seio urogenital

TBS: tris-buffered saline

TBS-T: tris- buffered saline- tween 20

Tfm: testicular feminized

TGF: transforming growth factor

TβRIII: TGF-β type III receptor

TIMP: inibidor tecidual de MMPs

TRPM-2: Testosterone-Repressed Prostate Message-2

TUNEL: terminal deoxynucleotidyltransferase [TdT]-mediated deoxy-UTP nick end labeling

VP: ventral Prostate

WB: Western blotting

WNT: wingless-type MMTV integration site family

1. INTRODUÇÃO

1.1. A Próstata

Exclusivamente encontrada em mamíferos, a próstata é uma glândula que secreta várias proteínas (incluindo várias enzimas), frutose, íons zinco e citrato, que ajudam a neutralizar a acidez do trato vaginal, contribuem com a capacitação e sobrevivência dos espermatozóides, e afetam propriedades físico-químicas do sêmen (Price, 1963). Em camundongos, a próstata produz proteínas importantes para a formação do "plug" copulatório (Cunha *et al.*, 1987). A motivação para a investigação da regulação do crescimento e fisiologia prostática dá-se pela existência de várias complicações patológicas que afetam essa glândula, sendo ela o sítio de vários tipos de inflamações, e alterações proliferativas malignas e benignas que se apresentam principalmente com o envelhecimento (Pfau *et al.,* 1980). Além disso, a glândula prostática constitui-se num excelente modelo para o estudo de interações celulares, decorrente dos diferentes tipos celulares encontrados no órgão e interações entre células e matriz extracelular.

A próstata é um órgão constituído de vários componentes glandulares e não glandulares (McNeal *et al.*, 1988). O componente glandular é formado por um conjunto de estruturas epiteliais túbulo-alveolares, envolvidas por um estroma muscular contrátil não glandular. Em roedores a próstata é lobulada, sendo esses lóbulos denominados: próstata ventral (PV), próstata dorsolateral e próstata anterior (ou glândula de coagulação) (Aümuller *et al.,* 1979). A próstata humana não apresenta essa distinção lobular, embora seja subdivida em três zonas: central, periférica e de transição (McNeal, 1980).

Na próstata ventral de rato, cada lobo prostático consiste de oito conjuntos de ductos que se originam a partir da uretra como uma estrutura tubular simples ramificada e contorcida distalmente. Esse conjunto de ductos é dividido em três regiões morfológica e funcionalmente distintas, denominadas proximal, intermediária e distal, de acordo com sua posição em relação à uretra (Lee *et al.,* 1990; Shabsigh *et al.,* 1999). Nas porções terminais dos ductos encontra-se uma maior quantidade de fibroblastos e poucas células musculares lisas (CML), associadas à proliferação de células epiteliais. Um epitélio com grande atividade secretória na porção intermediária circundado por uma camada contínua de CML. Nas porções proximais há uma

menor quantidade de fibroblastos e uma maior quantidade de CML, associadas à maior incidência de morte das células epiteliais, sugerindo que os arranjos assumidos pelas células estromais possam estar relacionados com o fenótipo das células epiteliais (Nemeth e Lee, 1996). Independente da região prostática, todo o estroma é rico em componentes de matriz extracelular como colágenos, elastina, glicoproteínas adesivas e proteoglicanos dentre outros (Carvalho *et al.*,1997a; Carvalho *et al.*, 1997b; Augusto *et al.*, 2008).

Originada a partir do seio urogenital (SUG), os primeiros sinais de formação da próstata são observados no 17º dia de desenvolvimento embrionário em camundongos, no 18º dia em ratos, e aproximadamente 10 semanas em humanos (Thomson, 2001) em resposta ao aparecimento de testosterona produzida pelos testículos (Timms *et al.,* 1994). O epitélio prostático é derivado da endoderme embrionária, ao contrário das estruturas Wolffianas tais como a vesícula seminal, ductos deferentes e epidídimos que são oriundos do mesoderma. As diferentes origens desses órgãos podem ter relevância no entendimento de mecanismos de crescimento diferentes entre próstata e órgãos derivados do ducto de Wollfian, embora todos mostrem crescimento dependente de andrógenos (Thomson, 2001). É importante ressaltar que, ao contrário da próstata, a vesícula seminal raramente desenvolve alterações proliferativas benignas ou malignas (Lee *et al.,* 2007).

A iniciação, o crescimento, a diferenciação, a produção de secreção e a manutenção da próstata são controlados principalmente pelos andrógenos testosterona e diidrotestosterona (Cunha *et al.,* 1987). A testosterona é produzida principalmente pelos testículos, mas é convertida em diidrotestosterona na próstata, através da ação da enzima 5-α redutase (Andersson *et al.,* 1999; Mahendroo *et al.,* 2001). A diidrotestosterona é um potente andrógeno, possuindo maior afinidade ao receptor de andrógeno (AR) que a testosterona propriamente dita (Aggarwal *et al.,* 2009). O AR é o fator responsável pelos efeitos dos andrógenos na transcrição gênica. Nesse contexto, foi demonstrado que o uso de finasterida, um inibidor farmacológico da 5-α redutase, provoca a regressão da glândula prostática (Aggarwal *et al.,* 2009).

Tanto o epitélio do seio urogenital como os primeiros brotos prostáticos não apresentam receptor de andrógeno funcional em níveis detectáveis, enquanto o mesênquima do seio urogenital e o mesênquima/estroma da próstata em formação apresentam grande quantidade deste receptor (Cunha *et al.,* 1987). Portanto durante o desenvolvimento, o primeiro tecido alvo de andrógenos é

o mesênquima do seio urogenital, que direciona o brotamento, ramificação e diferenciação epitelial por intermédio de fatores parácrinos. Por outro lado, o epitélio em desenvolvimento induz a diferenciação e o padrão morfológico de desenvolvimento do músculo liso.

O papel das interações entre epitélio e mesênquima no SUG foi extensivamente estudado por Cunha e colaboradores (Cunha e Chung, 1981), usando métodos de recombinação de tecidos. A recombinação de tecidos consiste na separação de rudimentos do órgão em mesênquima e epitélio seguido pela associação de um desses compartimentos (agora denominado enxerto) a um compartimento hospedeiro, permitindo o seu crescimento *in vivo*. Para esse método, podem-se utilizar compartimentos teciduais de doadores de vários "backgrounds" genéticos de uma linhagem particular de camundongo ou linhagens de camundongos "knockouts". Como exemplo, o camundongo Tfm carrega uma mutação no AR, o que inibe a sua função resultando na ausência de desenvolvimento prostático (He *et al*., 1991). Os camundongos machos Tfm apresentam testículos desenvolvidos, mas não apresentam as glândulas acessórias e têm a genitália externa feminilizada. O epitélio e o mesênquima provenientes desses camundongos foram utilizados para examinar o papel do AR no desenvolvimento prostático. Quando tecidos recombinantes foram feitos com o epitélio de Tfm e mesênquima contendo o AR selvagem, a glândula prostática foi formada na presença de andrógenos. Por outro lado, quando o epitélio derivado de camundongo selvagem e mesênquima de Tfm foram recombinados, não houve o desenvolvimento da próstata (Donjacour e Cunha, 1993). Esses resultados demonstraram que o AR expresso pelas células mesenquimais é suficiente para o desenvolvimento prostático, enquanto o AR epitelial deve estar associado à função secretora do epitélio.

Portanto essa interação entre epitélio e mesênquima/estroma é bidirecional (Cunha *et al*, 1987). Como já mencionado, a iniciação prostática é influenciada pela ação androgênica pré-natal (Timms *et al.,* 1994). As subseqüentes ramificação, crescimento, canalização e citodiferenciação epitelial também necessitam de estimulação androgênica e estão associadas a um aumento perinatal transitório na concentração de testosterona (Corbier, 1992).

Em ratos, a PV apresenta cordões epiteliais compactos e pouco ramificados no dia do nascimento (Bruni-Cardoso e Carvalho, 2007, Pu *et al.,* 2007). Entretanto, na primeira semana de desenvolvimento pós-natal, esses cordões crescem em resposta a intensa proliferação celular,

invadem o mesênquima/estroma, bifurcam-se em ramos laterais e canalizam-se (Sugimura *et al.*, 1986; Bruni-Cardoso e Carvalho, 2007). A medida que as estruturas epiteliais crescem e ramificam-se, ocorre um rearranjo do estroma subjacente. Esse processo parece ser resultante da expressão e atividade proteolítica localizada das metaloproteinases de matriz (MMP) -2 e -9 encontradas nessas regiões (Bruni-Cardoso *et al.,* 2008). Entretanto, os mecanismos moleculares que permeiam esse processo ainda não estão completamente esclarecidos.

O processo de canalização das estruturas epiteliais inicia-se logo no primeiro dia de vida e é devido, em grande parte, à morte das células localizadas no centro do epitélio, que deixam os espaços necessários para a formação do lúmen (Bruni-Cardoso e Carvalho, 2007). Entretanto, os fatores morfogenéticos que regulam esse processo permanecem desconhecidos. Concomitante à formação do lúmen, as células epiteliais que estão em contato com a lâmina basal diferenciam-se, adquirindo microvilosidades, organelas e vesículas de secreção (Bruni-Cardoso e Carvalho, 2007). Conforme os cordões epiteliais se canalizam o epitélio se reorganiza em duas populações celulares distintas: uma camada descontínua de células epiteliais basais ao longo da lâmina basal que expressam citoqueratinas 5 e 14 e p63, e uma população de células luminais colunares altas que expressam citoqueratinas 8 e 18 (Hayward *et al.*, 1996a, Wang *et al.,* 2001)

Ao mesmo tempo em que as células epiteliais diferenciam-se, as células mesenquimais diferenciam-se em uma camada de célula muscular lisa que envolve as estruturas epiteliais, e passam a expressar desmina, miosina, laminina e α-actina de músculo liso (Hayward *et al.*, 1996b).

Na próstata de roedores o padrão de ramificação é substancialmente diferente nos diferentes lobos, entretanto os mecanismos moleculares envolvidos nesses padrões diferenciados de ramificação ainda não estão bem estabelecidos. Foi demonstrado que 80% da ramificação do epitélio prostático é completada durante os primeiros 10 dias de vida em roedores (Donjacour e Cunha, 1988).

O AR e os receptores de estrógeno (ER) são responsáveis pela mediação dos efeitos fisiológicos dos andrógenos e estrógenos respectivamente (Gelmann, 2002 e Sasaki *et al.,* 2003). O AR atua fundamentalmente como fator de transcrição. Ele localiza-se no citoplasma e com a

ligação da testosterona ou da diidrotestosterona, dissocia-se de uma proteína HSP ("Heat Shock Protein"), dimeriza-se, e é translocado para o núcleo, onde, em conjunto com uma série de co-ativadores e co-repressores, ativa ou inativa diferentes conjuntos de genes (Li e Al-Azzawi 2009). O AR possui várias características em comum com os membros da família dos receptores nucleares, como os receptores de estrógeno, de progesterona, dos hormônios da tireóide e com os PPAR (receptores para os ativadores da proliferação dos peroxissomos) (Jacobs *et al.,* 2003).

O ER, assim como o AR, também pertence à família dos receptores nucleares e apresenta dois subtipos, ERα e ERβ, que podem ter papéis fisiológicos distintos (Altundag *et al.,* 2004). Os dois receptores compartilham homologia entre si, mas são produtos de diferentes genes (Zhao *et al.,* 2008). Os dois receptores de estrógeno ERα e ERβ estão presentes na próstata. No animal adulto, o ERα é predominante no estroma e o ERβ expresso principalmente no epitélio (Weihua *et al.,* 2001), indicando influencia local dos estrógenos no desenvolvimento e função prostática.

O desenvolvimento e o funcionamento prostático também são modulados diretamente por hormônios somatotróficos (como insulina, prolactina e hormônio do crescimento) e ácido retinóico (Webber, 1981; Prins, 2001), o que torna bastante complexo o mecanismo da regulação da fisiologia prostática.

Além disso, está bem estabelecido que alguns dos andrógenos circulantes são convertidos a estrógenos em vários órgãos, através da enzima aromatase (Simpson *et al.,* 1999). Essa enzima foi identificada na próstata humana, sugerindo um local de aromatização e conseqüentemente uma possível fonte local de estrógeno (Tsugaya *et al.,* 1996).

A breve exposição de roedores a estrógenos durante o desenvolvimento neonatal provoca um efeito irreversível ("imprinting" estrogênico) e dose dependente na morfologia, organização celular e função prostática (Prins *et al.,* 2001). Recentemente, nosso grupo demonstrou que a exposição ao 17β- estradiol no período neonatal resulta em diminuição da expressão gênica, remodelação e compactação da cromatina, reduzida atividade nucleolar e síntese de ribossomos, e também bloqueio da síntese protéica nas células epiteliais da próstata ventral de ratos, em decorrência de inibição epigenética por metilação do DNA ribossomal (Augusto *et al.,* 2009). Entretanto, a ação dos estrógenos na morfogênese e diferenciação celular da próstata ainda não

está exatamente esclarecida. Exposição a baixas doses de estrógeno durante a gestação em camundongos provoca aumento do peso da próstata no adulto, na quantidade do receptor de andrógeno e também um aumento do brotamento (Nonneman *et al.,* 1992).

Acredita-se que o "imprinting" estrogênico decorra de alterações nas concentrações de andrógeno via inativação do eixo hipotalâmico-hipófisiário-gonadal e de efeitos diretos na próstata (Huang *et al.,* 2004). Estudos realizados em cultura de próstata ventral (cultura de órgão) demonstraram que altas doses de estrógenos inibem o crescimento e diferenciação celular no desenvolvimento prostático (Jarred *et al.,* 2000), sugerindo que isso possa ocorrer *in vivo* em adição aos efeitos indiretos via supressão do eixo hipotalâmico-hipófisiário-gonadal.

No desenvolvimento normal prostático (proliferação e diferenciação celular e ramificação ductal), assim como em outros órgãos ramificados, tais como vesículas seminais, rim, pulmão, glândula mamária, glândulas salivares há envolvimento de fatores de crescimento e fatores morfogenéticos tais como, FGF-10 e -7, TGFβ, BMP-4, SHH (Thomsom, 2001 e Huang *et al,* 2005). Apesar da aparente similaridade, o controle molecular sobre a ramificação da próstata e desses outros órgãos ramificados parece ser somente parcialmente conservado. Portanto, não está totalmente esclarecido se há mecanismos conservados que regulam a ramificação epitelial de todos os órgãos.

A figura 1 esquematiza o perfil de expressão gênica (variação na concentração de transcritos) de diversos fatores durante todo o período de desenvolvimento prostático e a tabela 1 consiste de uma revisão dos fatores reconhecidamente envolvidos na ramificação dessa glândula.
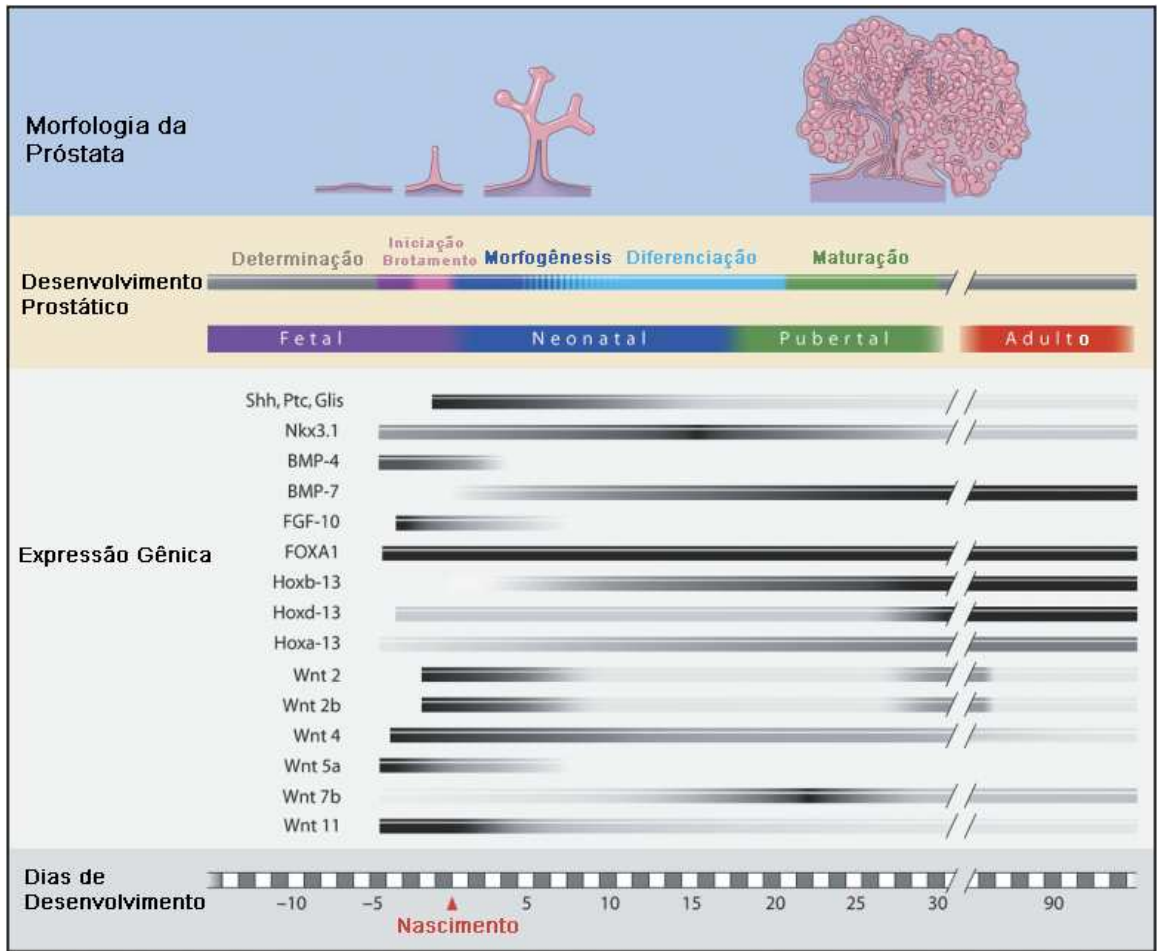
Figura 1. *Expressão de genes morforegulatórios durante o desenvolvimento prostático. Os dias desenvolvimento pré-natal e pós-natal são posicionados na parte inferior do esquema. A morfogênese da próstata ventral e seus estágios de desenvolvimento (parte superior) são seqüencialmente alinhados aos dias de desenvolvimento correspondentes. O padrão de expressão temporal dos genes (variação na concentração de transcritos) é representado por barras horizontais onde cores mais escuras demonstram maior expressão relativa do gene, conforme determinada por RT-PCR em tempo real. (Esquema adaptado de Prins e Putz, 2008). Os nomes completos referentes às abreviaturas dos genes aqui citados podem ser encontrados na lista de abreviaturas.*

Tabela 1 Proteínas que interferem na ramificação da próstata

Proteína	Papel na ramificação	Evidências a partir de Estudos		Referências
		in vitro	genéticos	
Activina A	Inibe	*X*		Cancilla *et al.* (2001)
AR	Promove	X	X	Takeda *et al.* (1986), Brown *et al.* (1998), Lubahn *et al.* (1989), Charest *et al.* (1991), Gaspar *et al.* (1991), He *et al* (1981)
BMP-4	Inibe	X	X	Lamm *et al.* (2001) Almahbobi *et al.* (2004)
BMP-7	Inibe	X	X	Grishina *et al* (2005)
EGF	Depende do Contexto	X		Kim *et al.* (1999)
ERα	Promove		X	Omoto *et al.* (2005)
Erβ	Depende do Contexto		X	Omoto *et al.* (2005)
Fosfatidina	Promove	X		Cancilla *et al.* (2001)
FGF-7	Promove	X	X	Alarid *et al.* (1994), Sugimura *et al.* (1996), Thomson e Cunha (1999), Donjacour *et al.* (2003)
FGF-10	Promove	X	X	Thomson e Cunha (1999) Donjacour *et al.* (2003)
Foxa	Promove		X	Gao et. (2005)
FST	Promove	X		Cancilla *et al.* (2001)
GHR	Promove		X	Ruan *et al.* (1999)
Gli2	Promove	X		Doles *et al.* (2006)
HGF	Promove	X		Sasaki *et al.* (1999)
HOXA-10	Promove		X	Podlasek *et al.* (1999a)
HOXA-13	Promove		X	Podlasek *et al.* (1999b)
HOXB-13	Promove		X	Economides e Capecchi (2003)
HOXD-13	Promove		X	Podlasek *et al.* (1997), Economides and Capecchi (2003)
IGF-1	Promove		X	Ruan *et al.* (1999)
INHBA	Inibe	X		Cancilla *et al.* (2001)
NKX3.1	Promove		X	Bathia-Gaur *et al.* (1999), Sheneider *et al.* (2000), Tanaka *et al.* (2000)
Noggin	Promove	X	X	Cook *et al.* (2007)
	Promove		X	Wang *et al.* 2006

Notch				
p63	Promove		X	Signoretti *et al.* (2000)
SFRP-1	Promove	X		Joesting *et al.* (2008)
RARs	Promove		X	Vezina *et al.* (2008) Vezina *et al.* (2009)
Pro- Proteína Convertases	Promove	X		Uchida *et al.* (2007)
TGF-β	Inibe	X	X	Itoh *et al.* (1998), Tomlinson *et al.* (2004)
SHH	Depende do Contexto	X	X	Podlasek *et al.* (1999c), Haraguchi *et al.* (2001) Freestone *et al.* (2003), Wang *et al.* (2003), Lamm *et al.* (2002), Berman *et al.* (2004), Doles *et al.* (2006)
SMO	Depende do Contexto	X	X	Podlasek *et al.* (1999c), Freestone *et al.* (2003), Wang *et al.* (2003), Lamm *et al.* (2002), Berman *et al.* (2004), Doles *et al.* (2006)
SRD5A2	Promove		X	Andersson *et al.* (1991), Mahendroo *et al.* (2001)
WNT5a	Promove	X		Huang *et al.* (2009)

A interação entre esses diversos fatores (Fig. 1 e Tabela 1) e sua relação direta com os mecanismos de sinalização celular durante o desenvolvimento prostático são pouco conhecidos. Entretanto, Prins e colaboradores estudaram intensivamente a interação das proteínas morfogenéticas FGF-10 ("fibroblast growth factor"-10), Gli (Gliotactina) e SHH ("sonic hedgehog"), (via de sinalização FGF-10-Gli-SHH), e a associação dessa via com a BMP-4 ("bone morphogenetic protein"-4) e propuseram um modelo para a regulação da morfogênese da ramificação prostática em ratos (Pu *et al.,* 2004), que é esquematizado a seguir (Fig. 2). O *Shh* é expresso localmente em foco discreto pelas células (em vermelho) no centro das extremidades dos cordões epiteliais em crescimento. Quando essas células entram em contato com as células mesenquimais, que expressam *Fgf-10* (círculos verdes), o SHH secretado (b, seta vermelha) ativa o seu receptor "patched" nas células mesenquimais regulando negativamente a expressão de *Fgf-10* (b, perda do verde). A supressão local da expressão de *Fgf-10* resulta em subdomínios laterais de alta expressão de *Fgf-10* adjacente ao foco de *Shh*, que por sua vez resulta em sua auto-ativação (c, seta verde) e proliferação das células epiteliais adjacentes. Em adição, o SHH secretado estimula a expressão de *Bmp-4* nas células mesenquimais imediatamente adjacentes ao foco de *Shh*, que

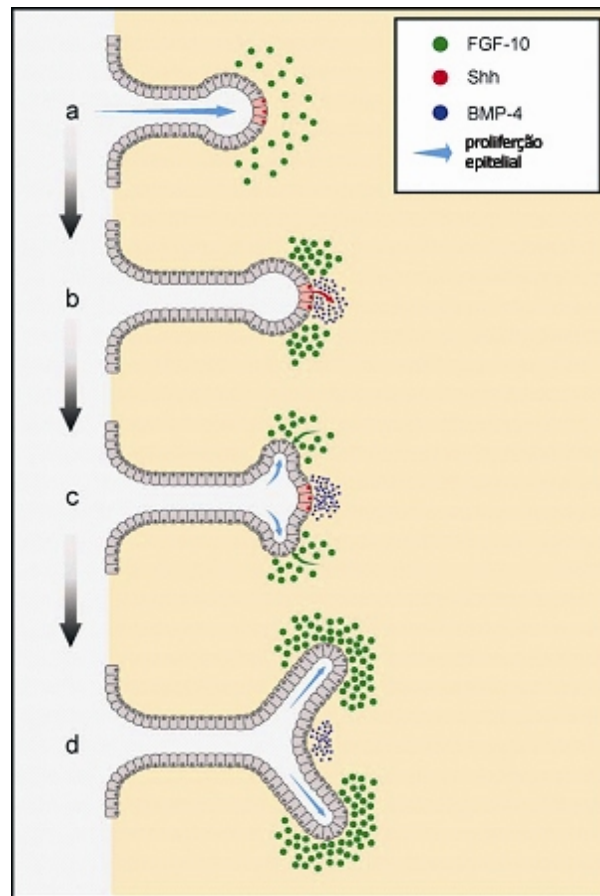suprime a proliferação celular na região central das extremidades dos cordões epiteliais (Pu *et al.*, 2004).

Figura 2. *Representação esquemática da via de sinalização FGF10-SHH-BMP4 processo de ramificação ductal no desenvolvimento prostático. Modificado de Pu et al., (2004).*

Uma boa correlação entre as propriedades de invasão tumoral e o crescimento normal das estruturas epiteliais foi estabelecido para a glândula mamária (Wiseman e Werb, 2002) e para o pulmão (Kheradmand *et al.,* 2002), pelo menos no que se refere a um estado proliferativo aumentado do epitélio, à necessidade de degradação da matriz extracelular adjacente e a colonização de espaços anteriormente ocupados pelo estroma. Este quadro parece ser também verdadeiro na angiogênese (Feng *et al.,* 1999), quando a membrana basal é degradada e substituída por uma matriz provisória de fibrina, na qual as células endoteliais proliferam invadem o tecido adjacente. Além disso, Cunha *et al.* (2004) propuseram que os mecanismos envolvidos na

organogênese prostática, no que diz respeito a aspectos de diferenciação celular e interações epitélio-estroma, podem ter relevância na gênese e biologia do câncer de próstata, sugerindo que o desenvolvimento tumoral prostático recapitule a ontogenia desse órgão.

O carcinoma prostático é uma das mais importantes doenças malignas diagnosticadas nos homens, principalmente a partir dos 50 anos. Pacientes em condições inoperáveis, devido à idade, são tratados com terapia hormonal ou radiação. A terapia hormonal mais comum para o câncer de próstata é a privação androgênica. Isto se deve ao fato de que a maioria dos tumores de próstata origina-se das células epiteliais glandulares da região periférica da próstata, as quais são dependentes de andrógenos para sobreviver e proliferar (Cunha *et al.,* 1987 Kambara *et al.,* 2009).

Decorrente da privação androgênica, a involução prostática configura um capítulo a parte no estudo da biologia desse órgão. Devido à alta dependência aos andrógenos, após a castração cirúrgica a glândula prostática sofre grande redução, principalmente em resposta a diminuição do fluxo sanguíneo (Shabisigh *et al.,* 1998), à morte por apoptose das células epiteliais, redução das vesículas e organelas de secreção (Heyns, 1990), eliminação constante da secreção luminal e extensa remodelação estromal, que inclui alterações fenotípicas das células musculares lisas (Antonioli *et al.,* 2004; Antonioli *et al.,* 2007), modificações no sistema elástico (Carvalho *et al.,*1997a), no colágeno VI (Carvalho *et. al*., 1997b) e na quantidade e tipos de glicosaminoglicanos (GAGs) (Kofoed *et al.*, 1971; Terry e Clark, 1996; Augusto *et al.,* 2008).

Acredita-se que algumas enzimas que degradam componentes de matriz extracelular tenham atuação importante nesse processo de remodelação do estroma prostático após a ablação androgênica. Como exemplo, Augusto *et al* (2008) demonstraram que a heparanase-1, uma endoglucosidase que cliva cadeias de heparam sulfato (HS) tem expressão aumentada após a castração, e que esse processo é associado com uma diminuição na quantidade de HS. Além disso, tanto a MMP-7 (Powell *et al.,* 1996; Powell *et al.,* 1999) como o ativador de plasminogênio do tipo uroquinase (Freeman *et al.*, 1990) parecem estar envolvidos na regressão prostática.

A cinética de morte das células epiteliais após a castração de roedores caracteriza-se por um pico de apoptose 72 horas após a cirurgia (Kurita *et al.,* 2001; Garcia-Florez *et al.,* 2005). Entretanto, estudos levando-se em consideração um período longo e uma investigação diária da

taxa de apoptose ainda não foram realizados. Sandford *et al*. (1984) detectaram a ocorrência de sucessivas ondas de apoptose na próstata ventral de ratos. Todavia, esses autores estavam se referindo a capacidade da glândula de animais castrados se rege nerar após a reposição de testosterona e alterar a cinética de morte celular por deslocar o pico clássico de apoptose de 72 horas para 48 horas após a cirurgia, depois de repetidos ciclos de administração de testosterona.

Na progressão tumoral, a degradação dos componentes da membrana basal e de outros componentes da matriz extracelular é um passo crítico entre os múltiplos eventos da cascata que levam à metástase. As células tumorais degradam estes componentes utilizando uma variedade de enzimas, destacando-se as metaloproteinases de matriz (MMPs). As MMPs são de enorme importância em eventos que incluem a remodelação tecidual, assim como na ovulação, erupção dental, cicatrização, inflamação, doenças autoimunes, processos degenerativos da cartilagem e no desenvolvimento de diversos órgãos (Heikinheimo e Salo, 1995; Bagavandoss, 1998; Tanney *et al.,* 1998; Ishizuya-Oka *et al.,* 2000). Portanto, torná-se claro o interesse em conhecer o envolvimento destas proteases durante eventos fisiológicos direcionados, como o desenvolvimento e a regressão da próstata.

1.2. As metaloproteinases de matriz

As MMPs formam uma família de enzimas dependentes de metais catiônicos bivalentes, principalmente zinco e cálcio. São capazes de degradar os componentes da matriz extracelular, tais como colágeno, elastina, laminina, fibronectina e proteoglicanos (Alexander e Werb, 1991; VanSaun e Matrisian, 2006).

Pelo menos 25 MMPs já foram descritas (Matrisian, 1990; Llano *et al*. 1997; Giambernardi *et al*., 1998; Grant, 1999; Velasco *et al*., 1999; Llano *et al*., 1999; Lohi *et al*., 2000; Marchenko e Strongin, 2001; Hannas *et al.,* 2007), sendo divididas em 5 grupos principais (Figura 3):

a. as colagenases intersticiais (MMPs -1, -8 e -13 e -18),

b. as gelatinases (MMPs -2 e -9),

c. as estromelisinas (MMPs -3, -10 e -11),

d. as metaloproteinases de membrana (MMPs -14, -15, -16, -17, -24 e -25) e

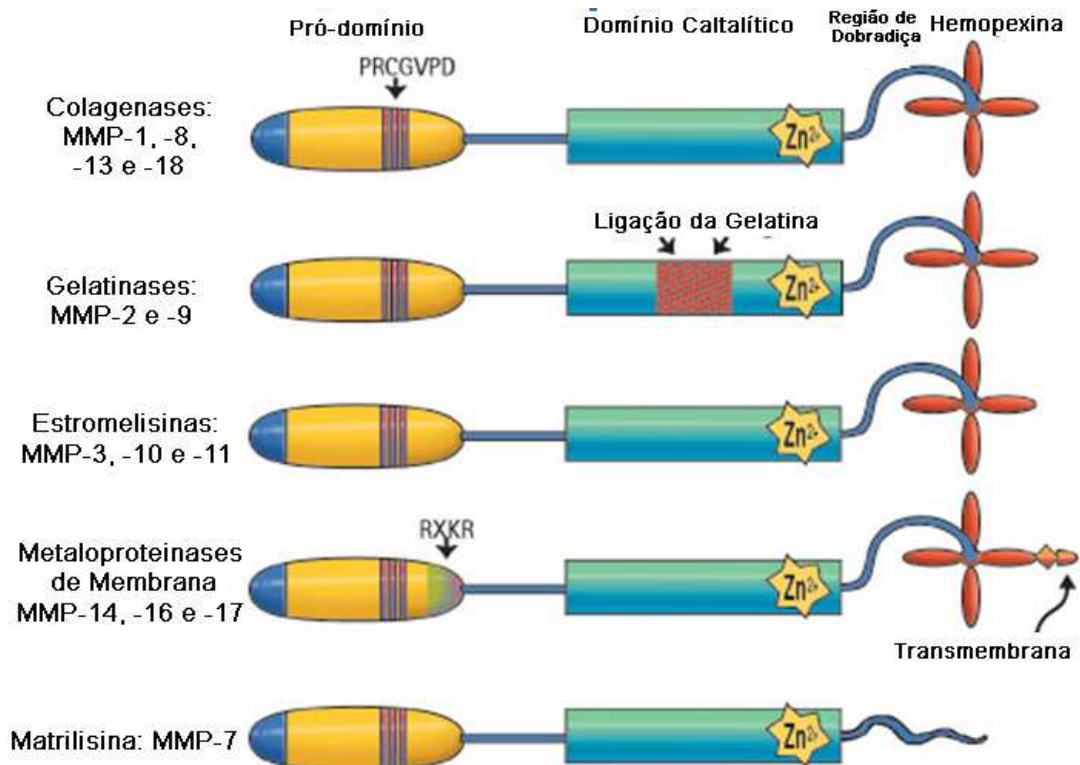**e.** MMPs que não se enquadram em nenhum dos grupos anteriores (MMPs -7, -12, -18, -19, -20, -21 -23, -26, -27 e - 28

Figura 3. *Estrutura básica dos cinco grupos principais de MMPs (http://www.merckbiosciences.co.uk/).*

As MMPs são secretadas em uma forma inativa, necessitando serem clivadas por outras proteases ou se autoprocessarem para se tornarem ativas. Além disso, as células secretam inibidores endógenos de MMPs. Estes inibidores endógenos são conhecidos como inibidores teciduais de metaloproteinases (TIMPs). Há quatro tipos de TIMP: TIMP-1, -2, -3 e -4 (Chang e Werb, 2001).

A existência de proteases, envolvidas na degradação de componentes da matriz extracelular e na ativação de outras proteases, e a interação com os seus inibidores demonstra a existência de um mecanismo finamente regulado de remodelação da matriz extracelular.

Como exemplo desta regulação, temos a MMP-2, que degrada preferencialmente o colágeno tipo IV, um dos principais constituintes das membranas basais. A MMP-2 é secretada na forma inativa de 72 kDa, sendo clivada em uma molécula ativa de 62 kDa pela ação de outras MMPs, como a MT1-MMP (também chamada de MMP-14). A MT1-MMP é uma metaloproteinase de membrana, conhecida como um ativador de pró-MMP-2. Além disso, a atividade da MMP-2 também é regulada pela inibição por TIMP-2 (Matrisian, 1990; Chang e Werb, 2001).

Estudos com animais transgênicos têm demonstrado alguns resultados contraditórios no papel das MMPs no desenvolvimento de tumores. Camundongos "knockout" (KO) para MMPs demonstraram tumorigênese reduzida (Wilson *et al.,* 1997): menos metástases ósseas em animais KO para MMP-7; menos fibrosarcomas induzidos em animais KO para MMP-19 (Pendás *et al.,* 2004), e menos melanomas para KO MMP-2- e MMP-9 (Itoh *et al.,* 1998). Por outro lado, outros KO manifestaram um aumento na tumorigênese, como exemplo KO MMP-8 e MMP-3 em câncer de pele induzidos quimicamente (Balbín *et al*., 2003; McCawley *et al*., 2004). Nesse contexto, vários estudos demonstraram uma associação entre o aumento da produção de MMPs (MMP-2, -3, -7 -9, e -14) e a progressão maligna do câncer de próstata (Hashimoto *et al.,* 1998; Upadhyay *et al.,* 1999; Nagakawa *et al.,* 2000). Além disso, foi observada uma correlação direta entre a intensidade de expressão da MMP-2 e o grau de progressão tumoral segundo a classificação de Gleason (Stearns e Wang, 1993; Sterns e Sterns, 1996).

Nos tumores, as MMPs podem ser produzidas tanto por células estromais (Poulsom *et al.,* 1992; Pyke *et al.,* 1993; Wood *et al.,* 1997) como por células epiteliais (Yoshimoto *et al.,* 1993), ou mesmo a cooperação entre estes dois tipos celulares (Ohtani, 1998; Lynch *et al.,* 2005).

Com estas expressivas evidências quanto à participação das MMPs no caráter metastático dos tumores, a inibição da atividade das MMPs, por inibidores naturais ou sintéticos, pode ser um importante caminho para o tratamento do câncer de próstata independente de hormônios. É neste

sentido que modelos experimentais são extremamente importantes para a investigação da expressão destas enzimas e de seus elementos de regulação, frente ao status hormonal dos indivíduos e sua associação com a proliferação tumoral.

Apesar dos tradicionais substratos das MMPs serem componentes da matriz extracelular, novas descobertas têm estendido a ação dessas enzimas a vários receptores, ligantes e moléculas de adesão, sendo hoje, portanto, creditado às MMPs importante papel nos processos de migração e proliferação celular (Sternlicht e Werb, 2001; Mott e Werb, 2004; VanSaun e Matrisian, 2006).

A participação das MMPs durante a regressão da PV de roedores ainda não está completamente esclarecida. Foi demonstrado o envolvimento da matrilisina (MMP-7) no processo de involução prostática de camundongos (Powell *et al.,* 1996). A MMP-7 foi implicada na clivagem e liberação do ligante de FAS (FAS-L), que poderia resultar na indução de apoptose das células epiteliais (Powell *et al.,* 1999). Além disso, Limaye *et al.* (2008) demonstraram um aumento na expressão de RNAm de MMP-2, -9 e TIMP-1 e -2 após a castração, e sugeriram que a atividade desses genes é suprimida por andrógenos na próstata. Entretanto, as células tumorais prostáticas LNCaP e LAPC-4 tem a expressão de MMP-2 regulada positivamente, de uma maneira dose-dependente por andrógenos via AR (Liao *et al.,* 2003). Foi demonstrado a existência de um elemento responsivo ao andrógeno no promotor do gene dessa enzima (Li *et al.,* 2007). Por outro lado, em células derivadas de fibroblastos tratadas com estrógeno apresentaram diminuição da expressão de MMP-2 (Moalli *et al.,* 2002). Esses dados sugerem que os hormônios androgênicos e estrogênicos atuam de forma complexa na regulação da expressão de MMPs e de seus inbidores na glândula prostática.

Nesse contexto, nós decidimos investigar e enteder o papel das MMPs em dois modelos, o de desenvolvimento pós-natal da próstata ventral e o de regressão prostática pós-castração cirurgica, que embora distintos, compartilham semelhanças no que diz respeito à dinâmica de eventos celulares e remodelação tecidual.

2. **Objetivos**

Os objetivos desse trabalho foram:

1. Definir o papel da MMP-2 nos processos de morfogênese pós-natal da próstata ventral de ratos e camundongos.

2. Compreender a dinâmica da morte celular epitelial e o envolvimento das MMP-2, -7 e -9 na regressão da próstata ventral de ratos após a castração cirúrgica.

3. RESULTADOS

Os resultados desta tese foram distribuídos em três manuscritos apresentados na forma de artigos cientíticos:

Artigo 1: MMP-2 regulates rat ventral prostate epithelial *in vitro*. (Developmental Dynamics, 2010, 239:737-46).

Artigo 2: MMP-2 contributes to the development of the mouse ventral prostate by impacting epithelial growth and morphogenesis (Submetido).

Artigo 3: Stromal remodelling is required for progressive involution of the rat ventral prostate after castration: Identification of a matrix metalloproteinase-dependent apoptotic wave. (International Journal of Andrology, DOI: 10.1111/j.1365-2605.2009.01004.x).

RESEARCH ARTICLE

MMP-2 Regulates Rat Ventral Prostate Development In Vitro

Alexandre Bruni-Cardoso,[1] Rafaela Rosa-Ribeiro,[1] Vinicius D. B. Pascoal,[2] Andre A. De Thomaz,[3] Carlos L. Cesar,[3,4] and Hernandes F. Carvalho[1,4]*

We have hypothesized that epithelial growth, branching, and canalization in the rodent ventral prostate (VP) would require matrix remodeling, and hence matrix metalloproteinase (MMP) activity. Therefore, the aim of this study was to evaluate the impact of blocking MMP-2, using whole organ culture. siRNA was employed to inhibit MMP-2 expression, and this was compared to GM6001's (a broad-spectrum MMP inhibitor) inhibition of general MMPs. These blocks impaired VP morphogenesis. MMP-2 silencing reduced organ size, epithelial area, and the number of tips, as well as caused a dilation of the distal parts of the epithelium. Histology, 3-D reconstruction, biochemistry, and second harmonic generation (SHG) revealed that MMP-2 silencing affected VP architecture by interfering in epithelial cell proliferation, lumen formation, and cellular organization of both epithelium and stroma, besides intense accumulation of collagen fibers. These data suggest that MMP-2 plays important roles in prostate growth, being directly involved with epithelial morphogenesis. *Developmental Dynamics 239:737–746, 2010.* © 2010 Wiley-Liss, Inc.

INTRODUCTION

The rodent prostate gland shows significant growth and morphological changes immediately after birth, in response to a testosterone surge (Corbier et al., 1992). In this phase, the epithelial structures grow, differentiate, branch, and canalize (Sugimura et al., 1986a; Donjacour and Cunha, 1988; Bruni-Cardoso and Carvalho, 2007; Bruni-Cardoso et al., 2008). These processes involve cell proliferation (Sugimura et al., 1986b; Bruni-Cardoso and Carvalho, 2007), lumen formation (Vilamaior et al., 2006), epithelial and smooth-muscle cell differentiation, and colonization of spaces previously occupied by stromal components (Bruni-Cardoso and Carvalho, 2007), in addition to concentrating important events in prostatic morphogenesis that result in further growth of the prototype gland at puberty. This early postnatal developmental stage coincides with an important physiological window that will influence later prostate physiology and susceptibility to disease, especially in response to xenobiotics (Putz et al., 2001; Risbridger et al., 2005). MMPs constitute a family of zinc-dependent endopeptidases that preferentially cleave extracellular matrix (ECM) proteins. These enzymes play a key role in normal development and physiology (VanSaun and Matrisian, 2006; Page-McCaw et al., 2007; Wiseman et al., 2003; Bruni-Cardoso et al., 2008), as well as in cancer initiation and progression (Matrisian and Bowden, 1990; Sternlicht and Werb, 2001; Lynch et al., 2005). We have previously demonstrated a higher and localized expression of MMP-2 and -9 in the rat ventral prostate during the first week of postnatal development, and have hypothesized that these events are associated with remodeling of ECM to allow epithelial growth (Bruni-Cardoso et al., 2008). Thus, the aim of the present study was to evaluate aspects of MMP-2 function in the rat ventral-prostate (VP)

morphogenesis during the first post-natal week, using specific siRNA for MMP2 in parallel to overall inhibition by GM6001 in the whole ventral prostate in vitro. The efficiency of siRNA treatment was assessed with RT-PCR, qRT-PCR, and gelatin zymography. Both MMP-2 silencing and GM6001 treatment were evaluated by measuring the organ and epithelial area, by counting the number of epithelial tips on day 2 of culture, and by examining collagen distribution using second harmonic generation (SHG) in a multiphoton laser scanning microscope. In addition, siRNA-treated VPs were examined by 3D-reconstruction of serial sections, volume changes, and hydroxyproline quantification. Together, the data showed that MMPs in general and MMP-2 in particular are important elements during VP morphogenesis. Moreover, we show that siRNA is an applicable and efficient tool for studying gene function in the neonatal whole-prostate organ culture.

RESULTS

GM6001 Treatment Inhibits Ventral Prostate Morphogenesis

The VP glands cultured on floating membranes grew and differentiated, with branching morphogenesis similar to the in vivo situation (Fig. 1A). In order to investigate the role of MMPs in VP development, we blocked their activity with GM6001, a broad-spectrum MMP inhibitor. VPs treated with 20 μM GM6001 showed an initial growth delay observed on day 2, which was partially restored on day 6.

The whole organ, epithelial area, and fraction of the organ occupied by the epithelium were smaller than those measured for the control group (Fig. 1B–D) on day 2. Branching morphogenesis was also affected. Whereas the VP epithelium of the control group showed extensive branching, resulting in about 40 epithelial tips per gland, GM6001-treated organs showed fewer tips (∼20) per gland (Fig. 1E). The lower concentration (2.5 μM) of this inhibitor did not affect prostatic morphogenesis at any point of the experiment.
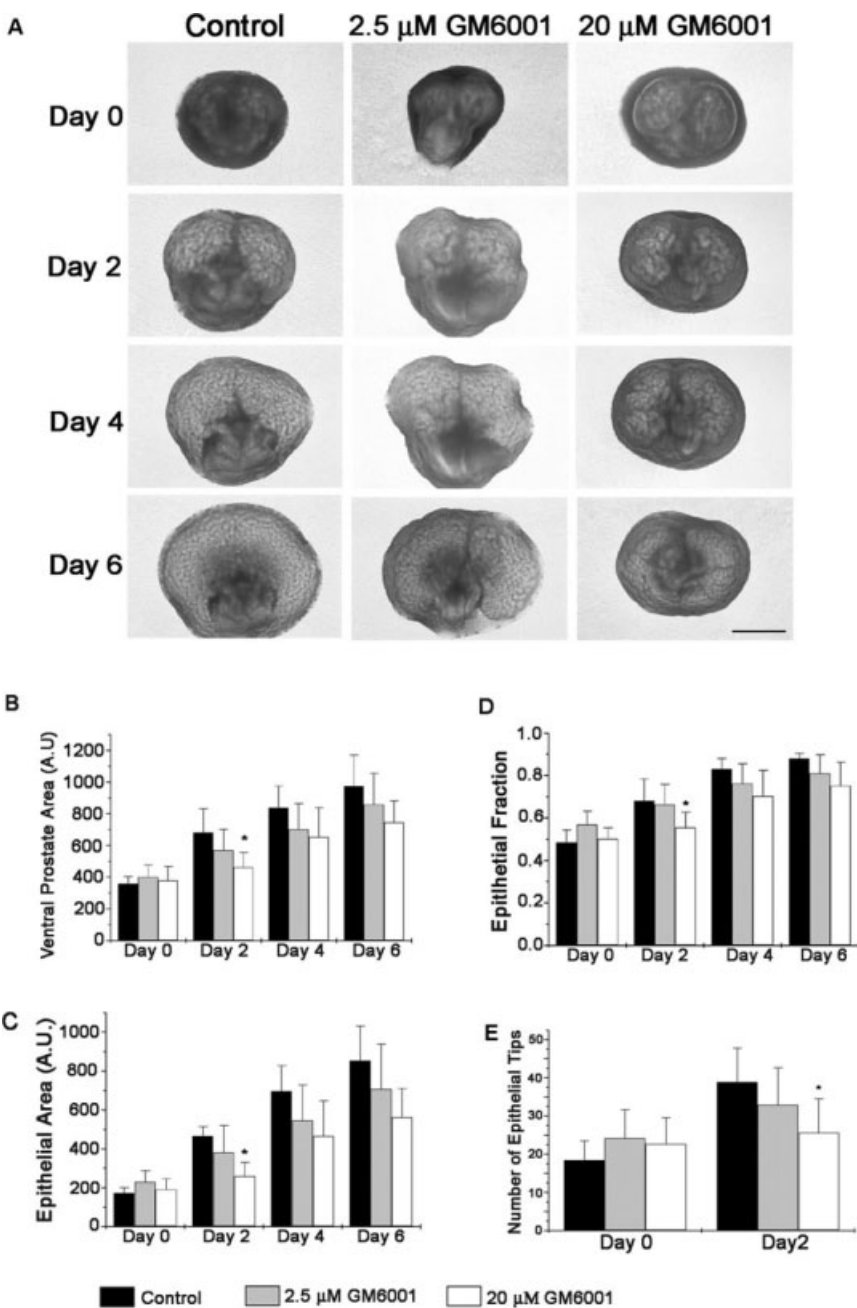

Fig. 1. **A**: Low-magnification optical-microscope views of ventral prostates from Control, 2.5-μM GM6001, and 20-μM GM6001 groups in culture. In these images, the morphogenesis of the translucent epithelium can be evaluated by following the same organ along the timeline of the experiment. The organ cultured with 20 μM GM6001 showed defective development (mainly in the epithelial structure) in comparison with the control group. Scale bar = 500 μm. B–E: Quantitative aspects of the VP development in culture from the vehicle (Control), 2.5-μM, and 20-μM GM6001 groups. Values are expressed as the mean ± standard deviation. **B**: Mean total area of VPs during their development in vitro. **C**: Mean area occupied by the epithelium. **D**: Mean fraction of the VP represented by the epithelial structures. The 20-μM GM6001 group showed a significantly smaller total and epithelial area, as well as epithelial/organ ratio, than those obtained for the Control group only on day 2 of development. **E**: Number of epithelial tips on days 0 and 2 of culture. The 20-μM GM6001 group had on day 2 practically the same number of epithelial tips found at day 0, whereas for the Control the number of these structures was doubled on day 2. Asterisks (*) indicate statistical differences ($P < 0.05$) between groups, as obtained using ANOVA followed by Tukey's test. A total of ten VPs per group was used for these measurements.

MMP-2 Silencing by siRNA Inhibits Ventral-Prostate Morphogenesis

To evaluate the importance of MMP-2 during the morphogenesis of the VP, we decided to block this enzyme using siRNA. The efficiency of this technique was evaluated by measuring MMP-2 mRNA and MMP-2 activity levels. siRNA-treated ventral prostates showed 90% less MMP-2 mRNA relative to the control and siGFP groups (Fig. 2A and B). Reproducibility was confirmed in two independent experiments. Off-target silencing was discarded by examining the expression levels of MMP-9 and heparanase-1, which showed no variation (fold-changes equal 1.1 and 1.0, respectively). Consistently, the siRNA-treated samples had less MMP-2 in comparison to the control groups. As assessed by zymography, the intensity of the entire set of MMP-2 bands diminished 57.3%, while the intensity of the active MMP-2 band was reduced 68.4% (Fig. 2C,E). Taken together, these results demonstrate that siRNA treatment of the cultured whole neonatal VP was efficient in blocking MMP-2 mRNA expression.

siRNA blocking of MMP-2 compromised VP gland growth (Fig. 3A). The treatment resulted in a smaller total organ area on day 6 of culture, and in a smaller epithelial area on days 4 and 6 of culture, as compared to the controls (Fig. 3B–D). In addition, epithelial branching was impaired in ventral prostates treated with siRNA against MMP-2, as assessed by counting epithelial tips on day 2. The siMMP-2 group showed about 20 epithelial tips, whereas the control groups had about 40 epithelial tips at this time point (Fig. 3E). It was also interesting to note that the epithelial tips doubled every 48 hr, starting with 20 tips on day two and ending up with about 160 tips on day 6.

The VP from control animals on day 6 showed tissue architecture very similar to that found in vivo, with branched and canalized epithelium surrounded by layers of smooth muscle cells (Fig. 4A–C). Apoptotic cells were identified in the regions of lumen formation (Fig. 4A and B), as observed in vivo (Bruni-Cardoso and Carvalho, 2007). Although the siMMP-2 group
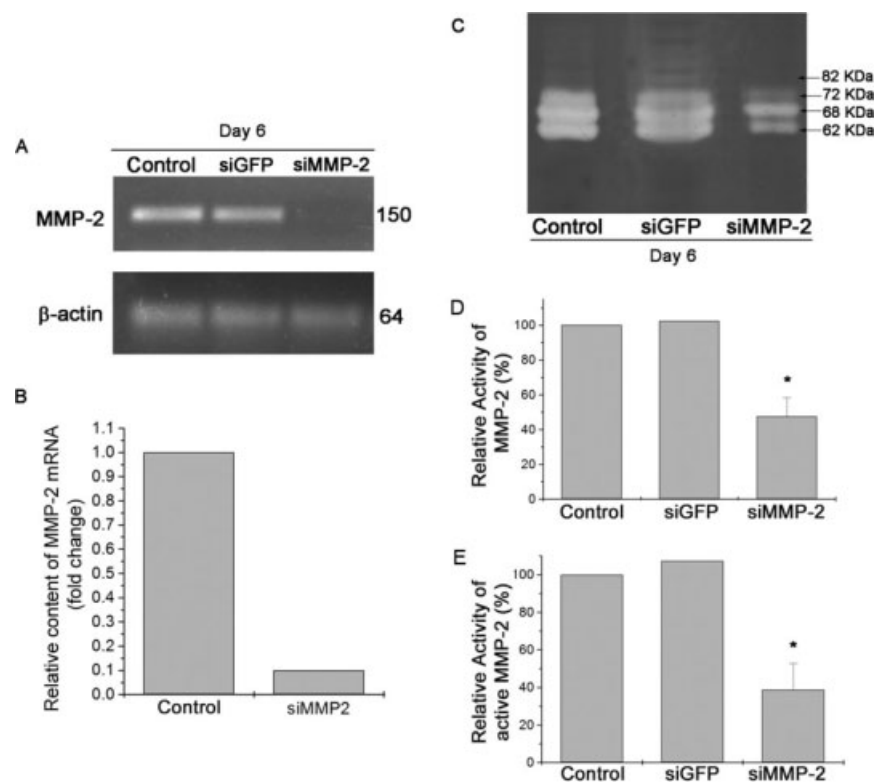

Fig. 2. **A**: Representative agarose gels loaded with MMP-2 (150 bp) and β-actin (64 bp) RT-PCR products from Control, siGFP, and siMMP-2 samples, and stained with ethidium bromide. The siMMP-2 group showed a faint band of the MMP-2 amplicon. **B**: Quantitative evaluation of MMP-2 mRNA levels, as assessed by Real-time PCR. The fold change value was obtained from the $2^{-\Delta\Delta Ct}$ equation using β-actin as the internal. The siMMP-2 group showed 90% less MMP-2 mRNA than the control groups. These experiments were performed in triplicate. **C**: Representative gelatin zymogram loaded with 20 μg protein from the Control, siGFP, and siMMP-2 groups on day 6 of culture. Three MMP-2 bands (latent: 72 KDa; intermediate: 68 KDa; and active: 62 KDa) were detected. **D**: Quantification of the relative intensity (mean ± standard deviation) of the three MMP-2 bands from the Control, siGFP, and siMMP-2 groups. The siMMP-2 samples contained less MMP-2 in comparison with the control groups. **E**: Percentage variation of the active MMP-2 band. The siMMP-2 group also showed weaker intensity of the active MMP-2 compared to the control groups. Asterisks (*) indicate significant differences ($P < 0.01$) obtained using ANOVA followed by Tukey's test. This experiment was done in quadruplicate.

also showed branched epithelium containing apoptotic cells, one could rarely find signs of lumen formation. Furthermore, unlike the controls, the stroma from the siMMP-2 group was not organized, and contained few smooth muscle cells (Fig. 4D and E). As the VP achieves a high complexity and this impaired analysis of the projected images, by conventional microscopy, we used serial historesin sections to obtain 3D-reconstructions of the whole gland (Fig. 4F and G, see Supp. videos S1 and S2, which are available online). This allowed the observation of the impact of MMP-2 knockdown on the gland, which was evident from the reduced volume of the gland and the epithelium, and the elongated and thinner proximal ducts and the presence of dilated distal

structures. Volume calculation showed that blocking MMP-2 expression resulted in a gland about 28% smaller (Fig. 4H). Significant reduction of the number of epithelial tips at day 6 was also documented (Fig. 4I). Evaluation of the proliferation rate showed that the percentage of mitotic cells, as identified by phospho-histone H3 immuno-histochemistry (Fig. 4J and K), was reduced about twofold (Fig. 4L).

Blocking Either Total MMPs or MMP-2 Resulted in Collagen-Fiber Accumulation in the VP Stroma

Collagen fibers appeared as a few thin fibers around the epithelium in both proximal and distal regions of the
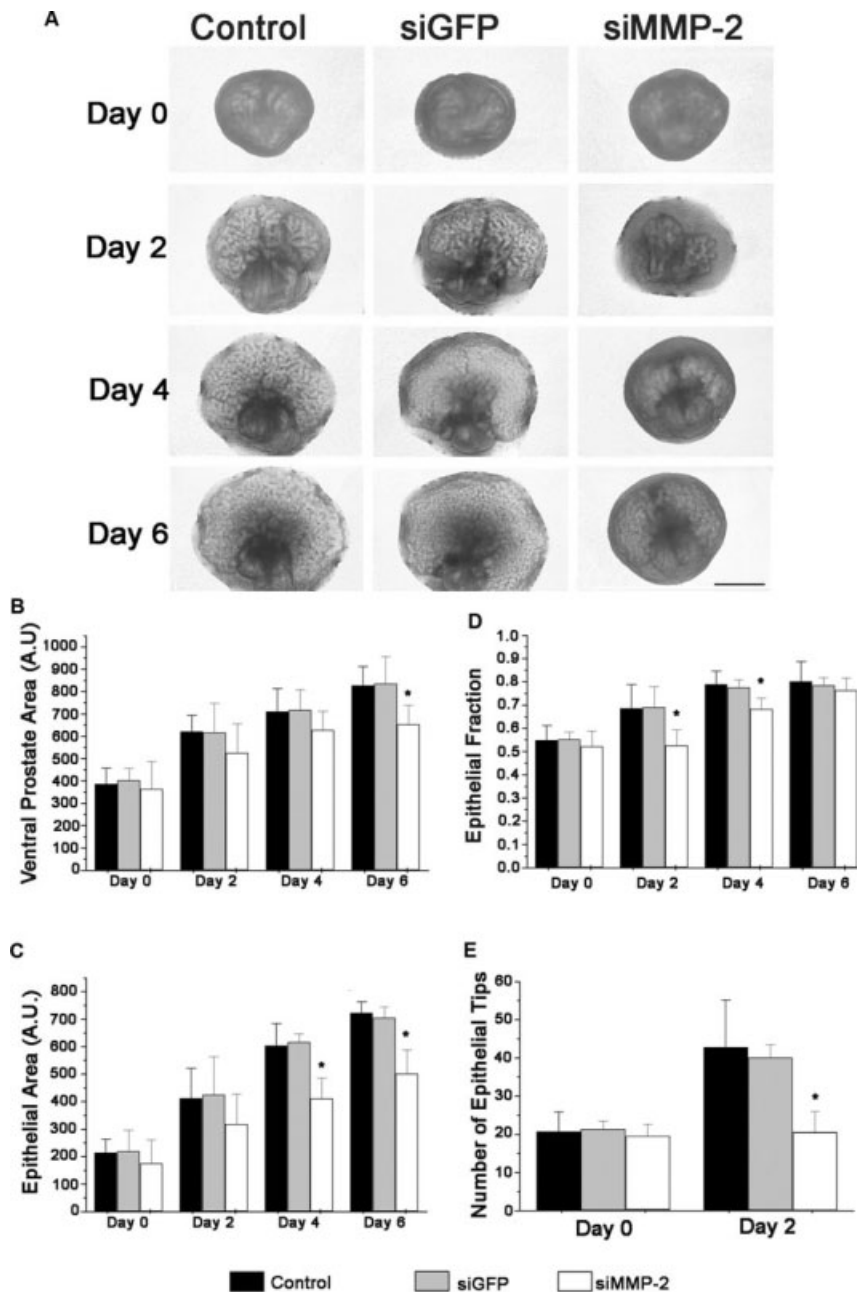
Fig. 3. A: Lower-magnification light-microscope views of ventral prostates from the Control, siGFP, and siMMP-2 groups recorded on days 0, 2, 4, and 6 of in vitro development. Observe that VPs from the siMMP-2 group showed reduced growth and compromising of epithelial morphogenesis, and had their development impaired, especially in epithelial structures. The treatment with siRNA against GFP did not affect prostate development. Scale bar = 500 μm. B–E: Quantitative parameters of the ventral prostate glands developed in vitro from the control, siGFP, and siMMP-2 groups. Values are expressed as mean ± standard deviation. **B**: Mean total area of VPs during their development in culture. **C**: Mean area occupied by the epithelial structures. The inhibition of MMP-2 affected the area size of the total VP only on day 6, and the epithelial area on days 4 and 6. **D**: Mean fraction of the VP occupied by the epithelial structures. The epithelial/organ ratio was reduced in the siMMP-2 on days 2 and 4. **E**: Number of epithelial tips on days 0 and 2. The number of these structures in folded on day 2 in the control and GFP groups, whereas the siMMP-2 group showed the same number shown by the VPs on day 0. The asterisks (*) indicate statistical differences ($P < 0.05$) between groups, as obtained using ANOVA followed by Tukey's multiple comparison test. A total of ten VP pictures per group was used for these measurements.

organ, as assessed by multiphoton SHG (Fig. 5A, B). The amount and density of collagen fibers in the stroma increased in response to GM6001 administration (Fig. 5C and D) and in response to siRNA expression blocking of MMP-2, in both proximal and distal regions (Fig. 5E and F), suggesting a stabilization of the extracellular matrix. siRNA silencing of MMP-2 also resulted in 40% increase in the concentration of hydroxyproline (Fig. 5G), confirming the structural analysis.

DISCUSSION

Extracellular matrix degradation is necessary for the creation of spaces that allow growth and invasion of developing and pathological tissues (VanSaun and Matrisian, 2006; Page-McCaw et al., 2007). Proteinases in general and MMPs in particular have critical roles in these processes. The morphogenesis of the rodent prostate is characterized by dynamic events, such as epithelial growth, branching, and canalization (Sugimura et al., 1986a,b; Hayward et al., 1996; Bruni-Cardoso et al., 2007), which require stromal remodeling and hence MMP activity. Furthermore, most of these events take place postnatally up to the third week after birth (Hayashi et al., 1991; Vilamaior et al., 2006; Huang et al., 2005; Pu et al., 2004; Bruni-Cardoso and Carvalho, 2007). In this context, we decided to investigate the role of MMP-2 in prostate morphogenesis during the first post-natal week, by inhibiting its expression and activity in organ cultures. This study demonstrated for the first time that MMP-2 is essential for normal prostate development, including epithelial cell proliferation, branching morphogenesis and canalization, as well as the organization of the stromal cells around the epithelial structures.

Several studies have reported the involvement of MMPs during the development of branched organs, such as kidney (Lelongt et al., 1997), mammary gland (Wiseman and Werb, 2002), lung (Kheradmand et al., 2002), and submandibular salivary gland (Steinberg et al., 2005). In fact, MMP2-null mice show reduced body size, reduced neovascularization
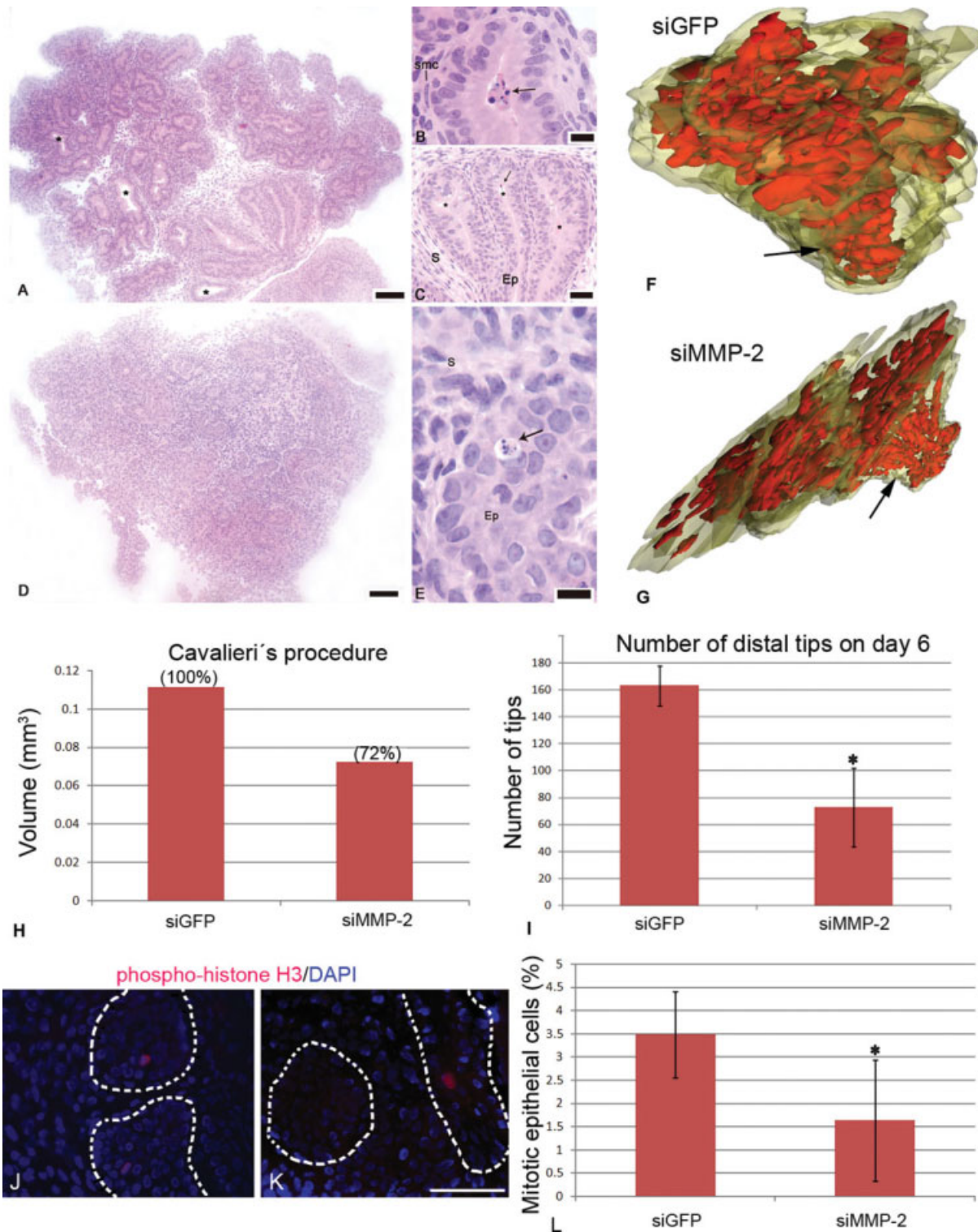
Fig. 4. Structural characterization of the VPs cultured in vitro and the effects of MMP-2 knockdown. A–E: Hematoxylin-eosin-stained historesin sections viewed under an optical microscope. **A**: Cross-section of a control gland, showing a branched and canalized epithelium (*). **B**: Histological aspects of a distal epithelial region, showing an apoptotic cell (arrow), and surrounding smooth-muscle cells (smc). **C**: Histology of three proximal epithelial ducts possessing apoptotic cells (arrow) and surrounded by a thick layer of stromal cells (S). **D**: Cross-section of a VP treated with specific siRNA for MMP-2, in which epithelial cells are not as organized as in the control VP. **E**: An apoptotic epithelial cell (arrow) is observed in a proximal epithelial cord, surrounded by undifferentiated stromal cells. Scale bars: A and D = 100 μm, B and E = 10 μm, and C = 30 μm. **F, G**: 3-D reconstruction of serial sections of the control (siGFP) and siMMP-2 groups (siMMP-2). The effect of silencing MMP-2 expression is evidenced as reduced growth, and thinner and elongated proximal ducts (arrows) (see also Supp. videos). **H**: Stereological determination of gland volume according to the Cavalieri procedure demonstrated a 28% reduction in the volume of the gland. **I**: Counting of epithelial tips on day 6 was possible on 3D-reconstructed images, and showed a significant reduction of the branching ($P < 0.05$). **J, K**: Immunohistochemical detection of phospho-histone H3 (red) in the control (siGFP) and siMMP-2 groups, respectively. Nuclei were stained with DAPI (blue). Epithelial areas were demarcated (traced white lines). Scale bar = 50 μm. **L**: Cell proliferation as assessed by the quantification of phospho-histone H3-positive cells in siMMP-2 groups was reduced to about 50% of the control (siGFP) group ($P < 0.05$).
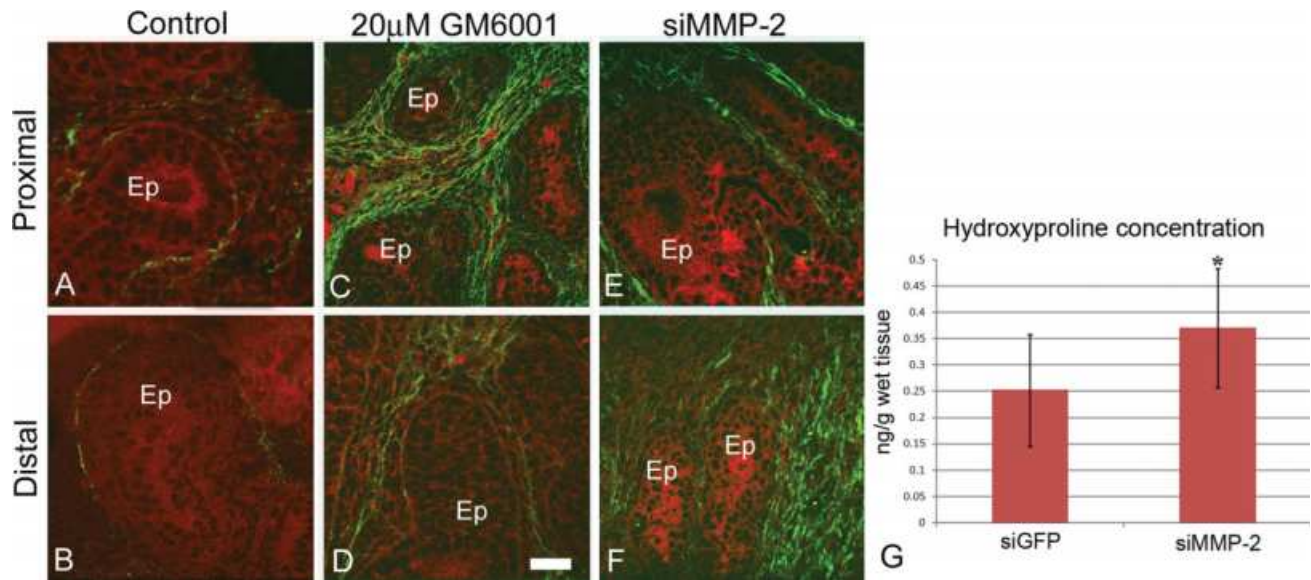
Fig. 5. Imaging of collagen fibers in the cultured ventral prostate by second harmonic generation (SHG) from the hematoxylin and eosin-stained sections shown in Figure 4. Eosin fluorescence was included in the images for allowing identification of the tissue structures, especially the epithelium (Ep). Collagen fibers in the control prostates appeared as a few thin fibers in the stroma, in both proximal (**A**) and distal regions (**B**). GM6001 (20 μM) treatment of the cultures resulted in marked accumulation of collagen fibers (**C, D**) and so did blocking of MMP-2 expression by siRNA (**E, F**). Scale bar = 30 μm. **G**: Determination of the concentration of hydroxyproline in the control (siGFP) and siMMP-2 group revealed a significant increase in response to MMP-2 silencing ($P < 0.05$).

(Kato et al., 2001), decreased primary ductal invasion in the mammary gland (Wiseman et al., 2003), and reduced lung saccular development (Kheradmand et al., 2002). We have recently shown that MMP-2 and -9 activities are higher and localized in the epithelium and at the epithelial/stromal interface of rat VP during the first postnatal week, and have suggested that this gelatinolytic activity is correlated with the ECM remodeling necessary for VP morphogenesis, in particular to permit epithelial growth and its projection into the surrounding stroma (Bruni-Cardoso et al., 2008).

In the present study, we found that inhibition of MMPs with 10 μM GM6001 significantly impaired VP growth and morphogenesis by day 2 of culture. Despite showing a dose-dependent effect, the GM6001 treatment did not significantly affect VP development concerning the evaluated parameters in the later stages. Because GM6001 is a specific broad-spectrum inhibitor, it is possible that some MMP activity could have an inhibitory effect on gland morphogenesis in the period studied, and their blocking would result in extended growth. Such an inhibitory effect

could manifest through degradation of extracellular matrix components contributing to gland development. In fact, it is known that some ECM elements promote branching morphogenesis, such as tenascin in lung (Gebb and Jones, 2003) and type III collagen in salivary gland (Nakanishi et al., 1998). We cannot rule out the possibility that MMP-activity is compensated by different proteases.

To assess the importance of MMP-2 in the morphogenesis of the ventral prostate, we silenced this enzyme with siRNA, using appropriate controls (either a transfecting agent or specific siRNA for GFP). The post-transcriptional silencing of MMP-2 by siRNA was highly effective, reaching 90% reduction of the corresponding mRNA (as obtained by qRT-PCR) and about 60% of the MMP-2 activity in gelatin zymograms. Probably, the discrepancy between these percentages results from MMP-2 protein stability in the extracellular spaces. The present study demonstrated reduced growth (at day 6) and compromised epithelial morphogenesis throughout the timeline of the experiment in the absence of MMP-2. As demonstrated by the histological evaluation, VPs developed in vitro showed similar

architecture as seen in vivo (Bruni-Cardoso and Carvalho, 2007; Bruni-Cardoso et al., 2008). Apoptotic cells were found inside the epithelial structures in the process of canalization. In spite of the presence of apoptotic cells in the siMMP-2 group, lumen formation was hindered. It is thus apparent that, in addition to the creation of spaces by epithelial cell deletion, the expansion and consolidation of luminal compartments require MMP-2 activity at the periphery of the epithelial structures consistent with gelatinolytic activity and MMP-2 location not only at the epithelial tips, but also at the base of the epithelium along the epithelial structures (Bruni-Cardoso et al., 2008).

BMP-4 and -7 play a key role in the VP development by inhibiting its morphogenesis (Huang et al., 2005; Cook et al., 2007; Prins and Putz, 2008). Interestingly, multiple BMP family members, including BMP-4 and BMP-7, induce an epithelial-to-mesenchymal transition (EMT) in the human pancreatic-cancer cell line Panc-1 (Gordon et al., 2008). Moreover, BMP-mediated EMT results in an increase in invasiveness of Panc-1 cells, in part through increased expression and activity of MMP-2

(Gordon et al., 2008). Accompanying EMT, BMP reduces the expression of the TGF-β type III receptor (TβRIII). TGF-β inhibits mammary-gland branching (Nelson et al., 2006) and epithelial mammary-cell EMT in 3D culture (Nelson et al., 2006, 2008). Sustained TβRIII expression inhibits BMP-mediated invasion and suppresses Smad1 activation. Furthermore, Smad1 is required for BMP-induced invasiveness and is partially responsible for BMP-mediated increases in MMP-2 activity. We believe that EMT might occur in the morphogenesis of ventral prostate, since we have recently found morphological features of this process at ventral-prostate epithelial growing tips such as a few cell junctions, non-polarized cells, and invadopodia/filopodia-like structures (Bruni-Cardoso et al., 2008).

We believe that the high testosterone levels occurring immediately after birth (Corbier et al., 1992) might regulate the expression of MMPs, especially MMP-2. Liao et al. (2003) showed that testosterone regulates MMP-2 expression in LNCaP and LAPC-4 cells in a dose-dependent manner. Although MMP-2 expression is constitutive, the levels of this enzyme can be altered during normal development and in processes of inflammation and tumor progression (Qin et al., 1999). In fact, there is an androgen-responsive element (ARE) in the MMP-2 promotor gene (Li et al., 2007), indicating that MMP-2 expression might be regulated by androgens during prostate development.

The present results demonstrated the stabilization of the collagen matrix in the prostate stroma. SHG revealed an accumulation of collagen fibers, which was confirmed by the quantification of hydroxyproline, in response to MMP-2 and overall MMP inhibition, thus compromising VP prostate morphogenesis, likely by restricting the growth of the epithelial structures.

Taken together, the results presented here indicate that MMP-2 plays an important role in epithelial growth and morphogenesis in the rat ventral prostate, and it became clear that collagen-fiber accumulation (and matrix stabilization) in response to

MMP-2 inhibition by siRNA and overall MMP-activity inhibition with GM6001 compromises VP morphogenesis. While this effect in itself could be responsible for the impaired epithelial growth and differentiation, we cannot rule out the participation of release of growth factors or cryptic regulatory molecules from the ECM. Thus, further analysis will be done regarding MMP-mediated ECM remodeling and/or shedding and activation of growth factors that are directly involved in VP morphogenesis and physiology.

EXPERIMENTAL PROCEDURES

Animals and Whole-Organ Culture

Eighty male Wistar rats were purchased from CEMIB-UNICAMP. The pups were decapitated on the day of delivery, and their VPs dissected under a stereoscopic microscope. Immediately after harvesting, the whole VPs were cultured for 6 days on PTFE membranes (Millipore Corp., Bedford, MA) floating in 500 μL of the basal medium (BM) constituted of DMEM/Ham's F-12 (1:1; vol:vol) supplemented with insulin-transferrin-selenium (Gibco, Grand Island, NY) and 10 nM of testosterone cypionate (Novaquímica, São Bernardo do Campo, SP, Brazil), according to Lopes et al. (1996).

For each assay, VP images were taken using a TM- C35DX Zeiss camera connected to an Axiovert S100 microscope (Zeiss, Thornwood, NY) at day 0 (the day of delivery and the first day of culture) and days 2, 4, and 6 of culture.

MMP Inhibition by GM6001

For experiments using the synthetic MMP inhibitor GM6001 (Sigma Chemical Co., Saint Louis, MO), the VPs from 30 animals (10 VPs per treatment) were cultured with either 2.5 or 20 μM GM6001 in BM. An equivalent volume of dimethylsulfoxide (DMSO, vehicle for GM6001) in basal medium was used as a control. The basal medium containing GM6001 was changed every 48 hr.

Post-Transcriptional Silencing of MMP-2 by Short Interference RNA (siRNA)

The oligonucleotides for MMP-2 siRNA were (sense) 5′- UGG UGU UGG GGG AGA UUC UCA- 3′ and (antisense) 5′- AGA AUC UCC CCC AAC ACC AGU - 3′, and for GFP siRNA were (sense) 5′- GAC GGG AAC UAC AAG ACA CGU - 3′ and (antisense) 5′- GUG UCU UGT AGU UCC CGU CAU - 3′. These were designed with software (http://lgm.fcm.unicamp.br:9001) as described previously (Pereira et al., 2007), using the NCBI sequence for the rat MMP-2 (access number: NM_031054.1). The lyophilized oligonucleotides (Integrated DNA Technologies, Coralville, IA) were dissolved (1 μg/μL) in DEPC water. Twenty-five micrograms of each oligonucleotide was mixed and incubated for 5 min at 95°C and cooled for 4 hr at room temperature, for annealing of the complementary strands.

Ventral Prostates from 30 animals (10 VPs per group) were treated in culture with 50 nM siRNA specific for MMP2 (siMMP-2 group), GFP (siGFP group), or only the transfecting agent lipofectamin 2000 (control group) (Invitrogen, Carlsbad, CA). In brief, 1.25 μL of the siRNA stock solution (20 μM) was mixed with the same volume of lipofectamin in 100 μL basal medium, according to the manufacturer's instructions. The siRNA/lipofectamin mixture was added to 400 μL of BM, and loaded on 24-well plates. The BM containing siRNA was changed every 24 hr.

The organs were harvested on day 6 of culture for RNA and protein extraction, and histological processing.

Evaluation of siRNA Silencing Efficiency and Off-Target Effects

The efficiency of MMP-2 silencing by siRNA was evaluated by RT-PCR, real-time RT-PCR, and gelatin zymography on day 6. Off-target silencing was assessed by determining the effect of siRNA treatment on the non-related genes MMP-9 and heparanase-1.

RNA Extraction and Reverse Transcription-Polymerase Chain Reaction (RT-PCR)

After culturing for 6 days, 4 VPs from each group (control, siGFP, and siMMP-2) were harvested and pooled, and the total RNA was extracted using the RNASpin Kit (GE Healthcare, Buckinghamshire, UK), quantified by spectrophotometry, and reverse-transcribed using 200 U of SuperScript III and Oligo $(dT)_{12-18}$ Primer (Invitrogen, São Paulo SP, Brazil) according to the manufacturer's instructions. β-actin was used as the internal control for the reactions. All the primers were designed with Gene Runner 3.05 Software and synthesized by Invitrogen, and their sequences were the following: for MMP-2 (forward) 5′ - CGA CCA CAG GAA GCC ATC - 3′ and (reverse) 5′ - TCG CCC ATC ATC AAG TTC - 3′and for β-actin (forward) 5′- CTG GCC TCA CTG TCC ACC TT - 3′ and (reverse) 5′- GGG CCG GAC TCA TCG TAC T - 3′.

The cycling conditions were (1) initial step of 5 min at 94°C; (2) 30 cycles of 1 min at 94°C, 1 min at 60°C (for β-actin) or 58°C (for MMP-2), and 1 min and 30 sec at 74°C; and (3) final step of 7 min at 74°C. The reactions occurred in 13 μL final volume containing 110 ng of cDNA, 0.39 U Taq DNA Polymerase (Promega, Madison WI), 2 mM $MgCl_2$ and 1.5 μM of each primer. The reaction product was electrophoresed in 2% agarose gel and stained with ethidium bromide. Images were taken with a digital camera. Each experiment was repeated three times.

Quantitative RT-PCR

Real-time quantitative RT–PCR was performed using TaqMan Universal PCR Master Mix (Applied Biosystems, Foster City, CA) in the Applied Biosystems 7300. Inventoried assays (Primer and FAM-conjugated probes) for β-actin (Rn02532334_s1), β2-microglobulin (Rn00560865_m1) MMP-2 (Rn00667869_m1), MMP-9 (Rn00578162_m1), and heparanase-1 (Rn00575080_m1) were purchased from Applied Biosystems. cDNA (20 ng) was used in each reaction, according to universal cycling conditions for the TaqMan system. The results were normalized using the C_T (threshold cycle) values of the internal control β-actin on the same plate. The equation $\Delta C_T = C_T$ (target gene) $- C_T$ (internal control) was employed for normalization of the results. In order to quantify and acquire the fold-change variation of MMP-2, the mathematical model $2^{-\Delta\Delta CT}$ was utilized. Both the MMP-2 and β-actin assays had their efficiency calculated through the equation: $E = 10^{(-1/slope)}$, with resulting values of 1.05 and 1.03 for MMP-2 and β-actin, respectively. The same procedure was applied for measuring expression levels of MMP-9 and heparanase-1, considering the internal control β2-microglobulin, this latter chosen because it showed the best efficiency for the former two genes. All reactions were performed in technical triplicate on the same plate for each pool, and the experiment was repeated twice.

MMP Extraction and Gelatin Zymography

Twelve VPs cultured for 6 days in each group were pooled (4 pools, 3 VPs each) and homogenized in 50 mM Tris–HCl, pH 7.4, 0.2 M NaCl, 0.1% Triton, 10 mM $CaCl_2$, and 1% protease inhibitor cocktail (Sigma Chemical Co.). The homogenates were then incubated for 2 hr at 4°C and centrifuged at 2,080g for 20 min at 4°C. The supernatants were reserved, and the pellets were suspended once again in the same solution, heated to 60°C for 5 min, and centrifuged at 2,080g for 20 min at 4°C. The two supernatants were pooled, and the soluble protein was quantified using the Bradford dye binding assay kit (BioAgency, São Paulo, SP, Brazil). Twenty micrograms of protein from each sample was electrophoresed on 10% SDS polyacrylamide gel containing 0.1% gelatin (used as the substrate) at 4°C under nonreducing conditions. After electrophoresis, the gel was washed twice, and then gently shaken in 2.5% Triton X-100 for 30 min at room temperature to remove the SDS. The gel was incubated overnight in a 50 mM Tris–HCl buffer pH 7.4, containing 10 nM $CaCl_2$ and 0.1 M NaCl, at 37°C. The gel was then stained with Coomassie brilliant blue R (0.5% dye in 20% methanol and 10% acetic acid) for 1 hr. Unstained bands indicating gelatinolytic activity were seen after slight destaining with 30% ethanol and 10% acetic acid. Quantitative assessment of band intensity was done by densitometry, using the software Scion Image (Scion Corporation, Frederick, MD). The activity determined for the control group was used as the reference (100%). The experiments were done in quadruplicate. Statistical comparison of the results was done using ANOVA followed by post-hoc Tukey's test, with the level of significance set at $P < 0.05$, using the Mini Tab 14 statistical software.

Morphometric Analysis and Counting of Epithelial Ducts

A total of 10 digitalized images of the whole organ were assessed for each experimental condition on days 0, 2, 4, and 6 of culture. The epithelial area was outlined and measured using the Image Pro Plus software. A similar outline of the whole VP was utilized to estimate the organ area and the fraction of the VP occupied by the epithelium (epithelial fraction = epithelium area/organ area ratio), as described previously (Pu et al., 2007). The number of epithelial tips and main epithelial ducts on day 2 was counted using the Adobe Photoshop 7.0 program, according to Cook et al. (2007).

Measurements were submitted to ANOVA followed by the post-hoc Tukey's test, using the Mini Tab 14 statistical software. Values of $P < 0.05$ were considered statistically different.

Historesin Embedding, Histology, 3D-Reconstruction, Tip Counting, Volume Calculation, and Second Harmonic Generation (SHG)

At day 6 in culture, the ventral prostates were fixed with 4% paraformaldehyde in phosphate-buffered saline for 16 hr. After dehydration in ethanol, the material was embedded in Leica historesin (Leica, Heidelberg, Germany) following the manufacturer's instructions. Serial two-micrometer

Developmental Dynamics

sections were cut, stained with hematoxylin-eosin, and analyzed under a light microscope for histology. Serial sections were used for both 3D-reconstruction and volume calculation. Serial reconstruction was done by using the free software Reconstruct (http://synapses.clm.utexas.edu/tools/reconstruct/reconstruct.stm). Thirty to 70 sections were employed, and varied according to the position of the organ with respect to the sectioning plane. Three reconstructions were obtained for the control (siGFP) and siMMP-2 organs. Distal tips were counted manually on the resulting reconstructions. The volume of the glands was calculated by the Cavalieri procedure, after determination of the section area using the Leica Application Suite software (Leica, Heerbrugg, Switzerland).

SHG was identified using an Olympus confocal system (IX-81 inverted microscope, the FV300 scan head, the FV-5 COMB2 laser combiner, and two Hamamatsu model 3896 PMTs). SHG was examined by excitation with a Ti:Sapphire laser (Tsunami, Spectra Physics) at 800 nm and 80 MHz repetition rate, coupled to the scan head by an external port, and collected by the condenser in the forward direction with a bandpass filter at 400 nm (Oriel Corporation, Stratford, CT) and a blue shortpass filter to reject any fluorescence signal. The Fluoview software was used to reconstruct the images.

Proliferation Rate

Cultured VP were fixed in 4% paraformaldehyde, processed for routine paraffin embedding, and subjected to immunohistochemistry for phospho-histone H3 (ser10) mitosis marker. In brief, 5-μm sections were de-waxed and subjected to antigen retrieval by boiling in 10 mM citrate buffer pH 6.0 for 10 min in a microwave oven, and then treated for 20 min with 20 μg/mL proteinase K in 10 mM Tris-HCl, pH 7.4, buffer at room temperature. Sections were then blocked with 1% BSA and 5% donkey serum in blocking buffer (10 mM Tris-HCl, pH 7.4, containing 0.1 M $MgCl_2$, 0.5% Tween-20), before incubation with a rabbit anti-phospho-histone H3 (ser10) (Millipore, Temecula, CA) (diluted 1:250) in blocking solution overnight

at 4°C. After rinsing, sections were incubated with an Alexa-fluor 546-conjugated donkey anti-rabbit IgG (Invitrogen, Eugene, OR) (diluted 1:500) in blocking solution. Negative controls were effected by substituting the primary antibody with rabbit IgG at the same concentration as the primary antibody. Sections were then counterstained with DAPI. Mitotic index was determined by counting phospho-histone H3-positive nuclei with respect to the total number of epithelial cell nuclei in 10 microscope fields taken at random per animal (n=3) using a 40× objective in a Leica fluorescence microscope. At least 800 nuclei were counted per group.

Quantification of Hydroxyproline

Hydroxyproline content was determined for individual VP after treatments with siGFP (control) or siMMP-2, according to the procedure of Stegemann and Stalder (1967) after hydrolysis with 6N HCl at 115°C for 16 hr. To determine the tissue concentration of hydroxyproline, we used the gland volume calculated according to the Cavalieri procedure as described above and assuming the specific gravity of the gland as 1 g/mL, according to the determination for the adult VP by DeKlerk and Coffey (1978). The results were obtained for 4–5 individuals in each experimental group, and are presented as nanograms of hydroxyproline per gram of wet tissue.

REFERENCES

Bruni-Cardoso A, Carvalho HF. 2007. Dynamics of epithelium during canalization of the rat ventral prostate. Anat Rec 290:1223–1232.

Bruni-Cardoso A, Vilamaior PSL, Taboga SB, Carvalho HF. 2008. Localized matrix metalloproteinase (MMP) 2 and MMP-9 activity in the rat ventral prostate during the first week of postnatal. Histochem Cell Biol 129:805–815.

Cook C, Vezina CM, Allgeier SH, Shaw A, Yu M, Peterson RE, Bushman W. 2007. Noggin is required for normal lobe patterning and ductal budding in the mouse prostate. Dev Biol 312:217–230.

Corbier P, Edwards DA, Roffi J. 1992. The neonatal testosterone surge: a comparative study. Arch Int Physiol Biochim Biophys 100:127–131.

Donjacour AA, Cunha GR. 1988. The effect of androgen deprivation on branching morphogenesis in the mouse prostate. Dev Biol 128:1–14.

DeKlerk DP, Coffey DS. 1978. Quantitative determination of prostatic epithelial and stromal hyperplasia by a new technique biomorphometrics. Invest Urol 16:240–245.

Hayward SW, Baskin LS, Haughney PC, Cunha AR, Foster BC, Dahiya R, Prins GS, Cunha GR. 1996. Epithelial development in the rat ventral prostate, anterior prostate and seminal vesicle. Acta Anat 155:81–93.

Gebb SA, Jones PL. 2003. Hypoxia and lung branching morphogenesis. Adv Exp Med Biol 543:117–125.

Gordon KJ, Kirkbride KC, How T, Blobel GC. 2008. Bone morphogenetic proteins induce pancreatic cancer cell invasiveness through a Smad1-dependent mechanism that involves matrix metalloproteinase protein-2. Carcinogenesis 30:238–248.

Huang L, Pu Y, Alam S, Birch L, Prins GS. 2005. The role of Fgf10 signaling in branching morphogenesis and gene expression of the rat prostate gland: lobe-specific suppression by neonatal estrogens. Dev Biol 278:396–414.

Hayashi N, Sugimura Y, Kawamura J, Donjacour AA, Cunha GR. 1991. Morphological and functional heterogeneity in the rat prostatic gland. Biol Reprod 45:308–321.

Kato T, Kure T, Chang J, Gabison EE, Itoh T, Itohara S, Azar DT. 2001. Diminished corneal angiogenesis in gelatinase A-deficient mice. FEBS Lett 508:187–190.

Kheradmand F, Rishi K, Werb Z. 2002. Signaling through the EGF receptor controls lung morphogenesis in part by regulating MT1-MMP-mediated activation of gelatinase A/MMP2. J Cell Sci 115:839–848.

Lelongt B, Trugnan G, Murphy G, Ronco PM. 1997. Matrix metalloproteinases MMP2 and MMP9 are produced in early stages of kidney morphogenesis but only MMP9 is required for renal organogenesis in vitro. J Cell Biol 136:1363–1373.

Li BY, Liao XB, Fujito A, Thrasher JB, Shen FY, Xu PY. 2007. Dual androgen-response elements mediate androgen regulation of MMP-2 expression in prostate cancer cells. Asian J Androl 9: 41–50.

Developmental Dynamics

Liao X, Thrasher JB, Pelling J, Holzbeierlein J, Sang XQ, Li B. 2003. Androgen stimulates matrix metalloproteinase-2 expression in human prostate cancer. Endocrinology 144:1656–1663.

Lopes ES, Foster BA, Donjacour AA, Cunha GR. 1996. Initiation of secretory activity of rat prostatic epithelium in organ culture. Endocrinology 137: 4225–4234.

Lynch CC, Hikosaka A, Acuff BH, Martin MD, Kawai N, Singh RK, Vargo-Gogola TC, Begtrup JL, Peterson TE, Fingleton B, Tomoyuki S, Matrisian LM, Futakuchi M. 2005. MMP-7 promotes prostate cancer-induced osteolysis via the solubilization of RANKL. Cancer Cell 7: 485–496.

Matrisian LM, Bowden GT. 1990. Stromelysin/transin and tumor progression. Semin Cancer Biol 1:107–115.

Nakanishi Y, Nogawa H, Hashimoto Y, Kishi J, Hayakawa T. 1988. Accumulation of collagen III at the cleft points of developing mouse submandibular epithelium. Development 104:51–59.

Nelson CM, Vanduijn MM, Inman JL, Fletcher DA, Bissell MJ. 2006. Tissue geometry determines sites of mammary branching morphogenesis in organotypic cultures. Science 314: 298–300.

Nelson CM, Khauv D, Bissell MJ, Radisky DC. 2008. Change in cell shape is required for matrix metalloproteinase-induced epithelial-mesenchymal transition of mammary epithelial cells.. J Cell Biochem 105:25–33.

Page-McCaw A, Ewald AJ, Werb Z. 2007. Matrix metalloproteinases and the regulation of tissue remodeling. Nat Rev Mol Cell Biol 8:221–233.

Prins GS, Putz O. 2008. Molecular signaling pathways that regulate prostate gland development. Differentiation 76: 641–659.

Pu Y, Huang L, Prins GS. 2004. Sonic hedgehog-patched Gli signaling in the developing rat prostate gland: lobe-specific suppression by neonatal estrogens reduces ductal growth and branching. Dev Biol 273:257–275.

Pu Y, Huan L, Birch L, Prins GS. 2007. Androgen regulation of prostate morphoregulatory gene expression: Fgf10-dependent and -independent pathways. Endocrinology 148:1697–1706.

Putz O, Schwartz CB, Kim S, LeBlanc GA, Cooper RL, Prins GS. 2001. Neonatal low- and high-dose exposure to estradiol benzoate in the male rat: I. Effects on the prostate gland. Biol Reprod 65:1496–1505.

Qin H, Sun Y, Benveniste EN. 1999. The transcription factors Sp1, Sp3, and AP-2 are required for constitutive matrix metalloproteinase-2 gene expression in astroglioma cells. J Biol Chem 274: 29130–29137.

Risbridger GP, Almahbobi GA, Taylor RA. 2005. Early prostate development and its association with late-life prostate disease. Cell Tissue Res 322:173–181.

Stegemann H, Stalder K. 1967. Determination of hydroxyproline. Clin Chim Acta 18:267–273.

Steinberg Z, Myers C, Heim VM, Lathrop CA, Rebustini IT, Stewart JS, Larsen M, Hoffman MP. 2005. FGFR2b signaling regulates ex vivo submandibular gland epithelial cell proliferation and branching morphogenesis. Development 132:1223–1234.

Sternlicht MD, Werb Z. 2001How matrix metalloproteinases regulate cell behavior. Annu Rev Cell Dev Biol 17: 465–516.

Sugimura Y, Cunha GR, Donjacour AA. 1986a. Morphogenesis of ductal networks in the mouse prostate. Biol Reprod 34:961–971.

Sugimura Y, Cunha GR, Donjacour AA, Bigsby RM, Brody JR. 1986b. Whole-mount autoradiography study of DNA synthetic activity during postnatal development and androgen-induced regeneration in the mouse prostate. Biol Reprod 34:985–995.

VanSaun MN, Matrisian LM. 2006. Matrix metalloproteinases and cellular motility in development and disease. Birth Defects Res C Embryo Today 78: 69–79.

Vilamaior PS, Taboga SR, Carvalho HF. 2006. Alternating proliferative and secretory activities contribute to the postnatal growth of rat ventral prostate. Anat Rec A Discov Mol Cell Evol Biol 288:885–892.

Wiseman BS, Werb Z. 2002. Stromal effects on mammary gland development and breast cancer. Science 296: 1046–1049.

Wiseman BS, Sternlicht MD, Lund LR, Alexander CM, Mott J, Bissell MJ, Soloway P, Itohara S, Werb Z. 2003. Site-specific inductive and inhibitory activities of MMP-2 and MMP-3 orchestrate mammary gland branching morphogenesis. J Cell Biol 162:1123–1133.

MMP-2 contributes to the Development of the Mouse Ventral Prostate by impacting Epithelial Growth and Morphogenesis

Alexandre Bruni-Cardoso[1], Conor C. Lynch[2,3], Rafaela Rosa-Ribeiro[1], Lynn M. Matrisian[2] and Hernandes F. Carvalho[1,4]

[1]Department of Anatomy, Cell Biology, Physiology and Biophysics, State University of Campinas (UNICAMP), Campinas, SP, Brazil
[2]Department of Cancer Biology, Vanderbilt University, Nashville, TN, USA
[3]Department of Orthopaedics and Rehabilitation, Vanderbilt University, Nashville, TN, USA
[4]National Institute of Photonics Applied to Cell Biology (INFABIC), State University of Campinas (UNICAMP), Campinas, SP, Brazil

Running Title: MMP-2 knocking out impacts epithelial development

Key words: prostate development, MMP-2, MMP-9, reticulin fibers, ventral prostate

Corresponding author:

Hernandes F Carvalho

Department of Cell Biology – UNICAMP

CP 6109

13083-863 Campinas SP, Brazil

Tel. 55 19 3521-6118

Fax: 55 19 3521-6185

e-mail: hern@unicamp.br

Abstract

Epithelial growth, branching, and canalization are important morphogenetic events of the rodent ventral prostate (VP) that take place during the first postnatal week. In this study, we evaluated the effect of knocking out MMP-2 (MMP-2$^{-/-}$), by examining developmental and structural aspects of the VP in mice MMP-2$^{-/-}$ mice. Neonate (day 6) MMP-2$^{-/-}$ mice showed fewer epithelial tips, a lower epithelial cell proliferation rate, and also reticulin fiber accumulation. The VP of adult MMP-2$^{-/-}$ mice showed lower relative weight, smaller epithelial and smooth-muscle cell volume, and a larger amount of thicker reticulin fibers. No differences in cell proliferation or apoptotic index were noted between adult MMP-2$^{-/-}$ and wild-type mice. MMP-9 was found in the adult MMP-2$^{-/-}$, but not in the wild-type. In conclusion, MMP-2 function is essential for the epithelial morphogenesis of the mouse VP, and that compensation by MMP-9 is not sufficient for acquisition of the normal adult histology.

Introduction

The prostate is a branched gland accessory to the reproductive tract. In humans, prostate development takes place during the second and third trimester of gestation; whereas in rodents, the prostate gland displays significant growth and morphogenetic changes during the first postnatal week. In this period, the epithelial cells proliferate and differentiate, together with epithelial growth, branching, and canalization (Sugimura et al., 1986a; Donjacour and Cunha, 1988; Hayward et al., 1996; Bruni-Cardoso and Carvalho, 2007; Bruni-Cardoso et al., 2008). Epithelial growth involves colonization of spaces previously occupied by the mesenchyme/stroma (Bruni-Cardoso and Carvalho, 2007).

This early postnatal developmental period involves extensive extracellular matrix (ECM) remodeling and coincides with a physiological window in which the prostate is capable of responding to hormones and endocrine disruptors that can affect prostate physiology and susceptibility to diseases in adult life (Putz et al., 2001; Risbridger et al., 2005).

MMPs are a family of zinc-dependent endopeptidases that preferentially cleave ECM proteins, playing a key role in normal development and physiology (VanSaun and Matrisian, 2006; Wiseman et al., 2003; Page-McCaw et al., 2007), as well as in cancer initiation and progression (Matrisian and Bowden, 1990; Sternlicht and Werb, 2001; Lynch et al., 2005). Recently *in vitro* and *ex vivo* studies by our group have defined roles for MMP-2 in prostate canalization and morphogenesis (Bruni-Cardoso et al. 2009a) but to date the exact role for MMP-2 in the development of the organ *in vivo* remains unexplored. Given the prevalence of MMP-2 in the epithelialization of other organs such as the kidneys (Lelongt et al., 1997) and the mammary gland (Wiseman and Werb, 2002), the current study utilizes mice systemically null for MMP-2

in order to evaluate the role of MMP-2 in mouse ventral prostate morphogenesis by comparing

VP morphogenesis and structure in age matched neonatal (day 6) and adult (day 60) wild type

and MMP-2$^{-/-}$ mice on a C57BL/6 background. The data presented here demonstrate that the

ablation of MMP-2 activity resulted in compromised morphogenesis (less epithelial-cell

proliferation, fewer epithelial tips) and reduced weight and epithelial volume in adulthood.

Additionally, we also noted increased immunostaining for MMP-9, suggesting a compensatory

mechanism, which is, however, not sufficient to compensate for the role of MMP-2 in the growth

of the wild-type ventral prostate.

Material and Methods

Animals

C57BL/6 wild-type mice and homozygous MMP-2 null mice were housed with IACUC

approval to Dr. Matrisian at Vanderbilt University, Nashville, TN, USA. Breeding pairs were

mated for 24 hours after which males were removed. Pregnant females were isolated and

monitored. Litters were typically born at twenty one days postcoitus and the day of birth was

termed day 0. Males were euthanized on day 6 (neonate) by decapitation, or on day 60 (adult) by

CO_2 inhalation, and had their ventral prostates removed and processed for paraffin embedding.

We used five animals per group in each age point. All adult ventral prostates were weighed, and

their relative weight was calculated as a percentage of the animal body weight.

Stereology and counting of epithelial tips

The VPs were fixed in 4% formaldehyde, processed for routine paraffin embedding, stained with hematoxylin-eosin, and submitted to stereological analysis. Volume densities ($V_{v\%}$) and the volumes of the epithelium, lumen, and stroma were determined by the method of Weibel. A total of 144 dots/72 grid lanes were analyzed as described previously for the ventral prostate (Huttunen et al., 1981; Antonioli et al., 2004; Garcia-Florez et al., 2005; Antonioli et al., 2007). Four or five microscopic fields taken at random were analyzed per animal (n=4), resulting in 16–20 fields per group. Volume density was calculated by considering the number of points falling on a given compartment, epithelium, lumen, non-muscle stroma (which includes everything in the stroma except smooth-muscle cells), muscle stroma (smooth-muscle cells), and total stroma (which is a summation of non-muscle and muscle stroma) for the adult ventral prostate, and the epithelium, lumen, and stroma for the neonate ventral prostate, after conversion to percentages (144 points equal 100%). The number of epithelial profiles in the distal regions (Tips) was counted on 2 equatorial cross sections per animal (n=4).

Immunohistochemistry

Five-μm sections were de-waxed and subjected to antigen retrieval by boiling in 10 mM citrate buffer, pH 6.0 for 10 min in a microwave oven, and then treated for 20 min with 20 μg/mL proteinase K in 10 mM Tris-HCl, pH 7.4 buffer at room temperature. Sections were then blocked with blocking solution (1% BSA and 5% donkey serum in 10 mM Tris-HCl, pH 7.4 containing 0.1 M $MgCl_2$, 0.5% Tween-20), before incubation with rabbit anti-mouse MMP-2

(cat. ab7052), MMP-9 (cat. ab38898; Abcam, Cambridge, MA, USA) (diluted 1:500), mouse

monoclonal anti-Pan-Cytokeratin-26 (cat. ab6401; Abcam) (diluted 1:250) in blocking solution

overnight at 4^oC. After rinsing, except for MMP-9 staining, sections were incubated with an

Alexa-fluor 488-conjugated donkey anti-rabbit (cat. A11008) or anti-mouse IgG (cat. A11059;

Invitrogen, Eugene, OR, USA) (diluted 1:500) in blocking solution. MMP-9 staining was

performed by using the Vecstain Kit (cat. pk6100; Vector Laboratories, Burlingame, CA, USA),

before developing the reaction with 3,3′-diaminobenzidine tetrahydrochloride and

counterstaining with Mayer's hematoxylin. Negative controls were performed by substituting the

primary antibody with the appropriate rabbit or mouse IgG at the same concentration as the

primary antibody. Sections were then counterstained with 4'-6-diamidino-2-phenylindole

(DAPI).

Histological assessement of ventral prostate growth

Mitotic cells were identified by immunohistochemistry as described above, using a rabbit

anti phospho histone H3 (cat. 06570; Millipore, Temecula, CA, USA). For adult VP, at least two

equatorial sections per animal (n=4) were assessed by counting the total number of phospho-

histone H3-positive nuclei per section. For animals on day 6, the mitotic index was determined

by counting phospho-histone H3-positive nuclei with respect to the total number of epithelial or

stromal cell nuclei in 5 microscope fields taken at random per animal (n=4) using a 20X

objective, in a Leica DM 2500 microscope.

The TUNEL assay was performed in paraffin sections using the in situ cell-death

detection kit (Roche Diagnostics, Indianapolis, IN, USA), counterstained with DAPI and

analyzed in a Leica DM2500 fluorescence microscope, according to the manufacturer's

instructions. Five microscopic fields from equatorial sections of a VP from each of 4 animals per group were taken at random, and the frequency of apoptotic cells was counted and expressed as a percentage of the total number of epithelial cell nuclei.

Silver Impregnation for Reticulin Fibers

Ventral prostate paraffin sections submitted to Gömöri's silver impregnation staining were employed for the identification of reticulin fibers, as previously described (Bruni-Cardoso et al., 2008). Briefly, the procedure involves sequential treatment with 1% potassium permanganate, 3% oxalic acid, and 1% iron alumen followed by incubation with 10% ammoniacal silver. After the silver impregnation, reticulin fibers (mainly type III collagen fibrils) appear black. Measurements were taken after manual segmentation using the Image J (NIH free software) and the results are presented as the percentage of the sectional are occupied by reticulin fibers and as the reticulin-epithelium area ratio, by using at least 10 microscopic fields from at least three animals.

Statistical Analysis

Measurements were submitted to Student´s t-test using the Mini Tab 14 statistical software. Values of $p < 0.05$ were considered statistically different.

RESULTS

MMP-2 promotes branching and epithelial proliferation in VP development

Initially, we assessed the localization of MMP-2 in neonatal wild type and MMP-2$^{-/-}$ ventral prostates. Using immunohistochemistry, MMP-2 was found in the mouse ventral prostate on day 6, in both stroma and epithelium, being more concentrated in the epithelial distal regions (Fig. 1A), suggesting a role for this enzyme during epithelial branching and elongation, findings that are in agreement with our earlier *in vitro* and *ex vivo* studies in the rat (Bruni-Cardoso et al., 2008; 2009a). Tissue organization was determined by stereology. No difference was found in the volume density of the epithelium, lumen, and stroma at day 6 after birth (Fig. 1B).

Immunohistochemistry with a pan-cytokeratin (a general epithelial marker) antibody revealed aspects of epithelial organization in the early postnatal VP. Epithelial structures from both the wild-type and the MMP-2$^{-/-}$ ventral prostate were already branched at the end of the first postnatal week, but, unlike the wild-type ventral prostate, the MMP-2$^{-/-}$ samples showed dilated profiles in the distal epithelium. Accordingly, the MMP-2$^{-/-}$ ventral prostate showed fewer epithelial tips compared to the wild-type (Fig. 1C).

The normal mouse ventral prostate epithelium grows extensively during the first postnatal week (Sugimura et al., 1986b). The MMP-2-deficient ventral prostate showed fewer proliferating epithelial cells than the wild-type gland (Fig. 1D). No statistical differences in the rate of proliferating mesenchymal cells were found between the wild type and MMP-2 null groups (results not shown). We could detect no difference between the MMP-2$^{-/-}$ and the wild-type mice, in the rate of epithelial cell death (Fig. 1E). No apoptotic cells were found in the stromal compartment.

MMP-2 contributes to adult ventral prostate size and structure

The MMP-2$^{-/-}$ mice showed a lower body weight, as previously reported (22.5 ± 1.1 g *vs* 18 ± 2.7 g; *p*<0.05) (Kato et al., 2001). By calculating the relative weight, we noted that the growth of the ventral prostate gland was compromised in MMP-2$^{-/-}$ compared to the wild-type ventral prostate (0.032 ± 0.004 % *vs* 0.023% ± 0.002 %; *p*<0.05), suggesting that MMP-2 is essential for the normal development of the prostate gland.

MMP-2 was identified in the adult mouse VP, and was located in the epithelium and around smooth-muscle cells (Fig. 2A). As expected, MMP-2 staining was absent in the VP of the MMP-2$^{-/-}$ mice (Fig. 2A).

The stereological analysis of the adult animals revealed that the volume density of the epithelium was smaller in MMP-2$^{-/-}$ ventral prostate than in wild-type samples (Fig. 2B). The resulting volumes of the epithelium and stroma were reduced (Fig. 2B). We also noted that the volume density and volume of the smooth-muscle cells were reduced in the adult VP (results not shown).

In spite of the lack of variation in luminal volume, the histological analysis of the adult ventral prostate showed that the MMP-2$^{-/-}$ ventral prostate epithelial acini were dilated and the epithelium was folded in some microscope fields, aspects not observed in the wild-type mouse (Fig. 2C).

No difference was found in both the number of proliferating cells (Fig. 2D) and in the rate of epithelial apoptosis between the MMP-2$^{-/-}$ and wild-type mice (Fig. 2E). Neither proliferating nor apoptotic cells were found in the stromal compartment.

Enhanced endogenous MMP-9 expression does not rescue the MMP-2 null VP phenotype

Previous studies have suggested that the ablation of MMPs can result in compensatory expression of other MMPs (Rudolph-Owen et al., 1997; Esparza et al., 2004). Since MMP-2 ECM substrate specificities share a significant overlap with those of MMP-9, we examined the localization and expression of MMP-9 in the wild type and MMP-2 null neonatal and adult ventral prostates. Immunohistochemistry revealed the presence of MMP-9 in the early postnatal developing VP, in agreement with previous results for the rat (Bruni-Cardoso et al., 2008) but it appeared that there were no differences in the intensity of staining (Figure 3A and B). In adults, MMP-9 protein could not be detected in the ventral prostate of the adult mice, as assessed by immunohistochemistry, an observation that is in agreement with our previous results examining adult rat ventral prostates (Bruni-Cardoso et al., 2009b), (Fig. 3C). However, the MMP-2$^{-/-}$ samples showed intense staining for this enzyme in the stroma, particularly in the smooth muscle cells (Fig. 3D). This suggests that MMP-9 partially compensates for MMP-2 activity in the ventral prostate of MMP-2$^{-/-}$ mice but that the enhanced expression does not rescue the MMP-2 null phenotype since the MMP-2$^{-/-}$ ventral prostates do not reach the same size as their wild-type counterparts.

MMP-2 is critical for ECM remodeling during VP development

Considering the critical function of MMP-2 for the processing of ECM components abundant in the prostate stroma, we examined whether the observed effects on the VP in neonatal and adult mice were due to a failure of MMP-2 to mediate ECM remodeling by assessing reticulin fiber deposition. In wild type neonatal animals, reticulin fibers were observed surrounding the epithelial cords in the developing mouse ventral prostate (Fig. 4A). Additionally,

these fibers were thinner and fewer in the distal regions of the wild-type samples (Fig. 4A). In contrast, the neonatal MMP-2$^{-/-}$ ventral prostate showed thicker and more-abundant reticulin fibers (Fig. 4A), suggesting that MMP-2 has an important role in the remodeling of these ECM elements, and that the accumulation of these fibers might be responsible for the smaller number of epithelial tips and also the dilated epithelial cords in the distal regions of the developing gland. This failure of appropriate ECM remodeling in MMP-2$^{-/-}$ ventral prostates persisted into adulthood (Figure 4A) and also potentially explains why the MMP-2$^{-/-}$ adult ventral prostates are significantly smaller than their wild type counterparts. Quantitative assessment of these results showed increased content of reticulin per sectional area (Fig. 4B) as well as an increased reticulin/epithelium area ratio (Fig. 4C), which achieved statistical significance at adulthood.

Taken together, these data suggest that MMP-2 mediated remodeling of ECM is critical for appropriate prostate development.

Discussion

We investigated the role of MMP-2 in the mouse ventral prostate morphogenesis, by studying the MMP-2$^{-/-}$ mice. We showed that MMP-2 is expressed in the early post-natal and adult VP, and contributes to epithelial cell proliferation and normal branching morphogenesis: the MMP-2 KO showed a smaller gland with altered tissue organization, in spite of a partial compensation by MMP-9, in adulthood.

Using an *in vitro/ex vivo* organogenesis model, we previously reported that the activities of MMP-2 and -9 are higher and localized in the distal ductal region and at the epithelial/stromal interface of rat VP during the first postnatal week (Bruni-Cardoso et al., 2008). Subsequently, we showed that MMP-2 modulates the morphogenesis of the rat ventral prostate *in vitro* by

influencing the epithelial cell proliferation rate, branching, and the canalization of the epithelium, and the remodeling of collagen fibers (Bruni-Cardoso et al., 2009a). Although these results indicate that MMP-2 activity and the resulting ECM remodeling are necessary for VP morphogenesis, in particular to accommodate epithelial growth and its projection into the surrounding stroma, a more physiological examination of this hypothesis was needed. Therefore, in the current study, we examined the effect of MMP-2 on prostate development *in vivo* using MMP-2 null mice.

Studies have reported the involvement of MMPs during the branching morphogenesis of many organs, such as the kidney (Lelongt et al., 1997), mammary gland (Wiseman and Werb, 2002), lung (Kheradmand et al., 2002), and submandibular salivary gland (Steinberg et al., 2005; Rebustini et al., 2009).

MMP-2-null mice have smaller body size and reduced neovascularization (Kato et al., 2001). The present findings are in agreement with those examining the role of MMP-2 in the development of other organs such as the mammary gland (Wiseman et al., 2003) and lung (Kheradmand et al., 2002) for the which decreased primary ductal invasion and saccular development were observed, respectively.

As in the rat, the wild-type mouse ventral prostate on day 6 after birth expresses MMP-2 in both the mesenchyme and epithelium. In the epithelium, MMP-2 was concentrated at the epithelial tips, indicating a possible contribution of the enzyme to the epithelial invasion through the prostate stroma. As a result of knocking out MMP-2, we found fewer epithelial tips, a reduced rate of epithelial cell proliferation, and accumulation of reticulin fibers around the epithelium, suggesting that MMP-2 contributes to the branching morphogenesis, by remodeling

some extracellular matrix proteins and consequently creating spaces for the bifurcation and elongation of the epithelial structures and influencing cell proliferation.

Studies of the adult VP showed that the MMP-2$^{-/-}$ mice have lower ventral-prostate weight and decreased epithelial (and smooth-muscle cell) volume. The epithelial and smooth-muscle cells play crucial roles in the prostate physiology. Luminal epithelial cells are responsible for the gland secretory activity, while smooth-muscle cells help to eliminate the secretion accumulated in the lumen during ejaculation (McNeal et al., 1988). In addition, paracrine signaling between these two cell types is essential in all stages of the gland development and homeostasis (Cunha and Chung, 1981). These interactions might be compromised in the MMP-2$^{-/-}$, as the thickened basement membrane, which normally acts as a physical and chemical barrier between the epithelium and the surrounding smooth-muscle cells, could obstruct the diffusion of regulatory molecules between the two compartments. Because epithelial cell proliferation and apoptosis rates were not affected by the absence of MMP-2 in the adult samples, we conclude that the smaller size is a result of reduced cell proliferation and compromised morphogenesis during development.

MMPs are transcriptionally regulated by a variety of growth factors and cytokines (Qin et al., 1999). In addition, post-transcriptional mechanisms can contribute to this regulation (Borden and Heller et al., 1997). Although MMP-2 expression is constitutive, the levels of this enzyme can change during normal development, inflammation, and tumor progression (Qin et al., 1999). The rodent prostate gland shows three main growth phases. After an initial embryonic stage, early postnatal growth takes place during the first three postnatal weeks, in response to a testosterone surge (Corbier et al., 1992). We believe that the high testosterone levels in this period might regulate the expression of MMPs, especially MMP-2. In fact, Liao et al. (2003)

showed that testosterone regulates MMP-2 expression in LNCaP and LAPC-4 in a dose-dependent manner. Furthermore, there is an androgen-responsive element (ARE) in the MMP-2 promotor gene (Li et al., 2007), indicating that MMP-2 expression might be regulated by androgens during prostate development.

Our current findings and previous reports clearly demonstrate a role for MMP-2 in mediating prostate gland development, despite compensation by proteinases with similar substrate specificities such as MMP-9. It is important to note however, that MMP-2 may not just contribute to ECM degradation, but specific cleavages in ECM components may reveal neoepitopes within the ECM substrates that provide critical information for the invading epithelial cells. We have suggested previously that matrix remodeling is essential for the epithelium to grow and invade the stroma (Bruni-Cardoso et al., 2009a). In this context, we found that inhibition of MMP-2 by siRNA resulted in a more effective impairment of prostate growth than the use of the broadly specific inhibitor GM6001, and therefore we could not rule out the possibility that some MMPs may have an inhibitory effect on branching morphogenesis. The inhibitory effect may result from the degradation of essential extracellular matrix or non-matrix components such as growth factors and cytokines that contribute to prostate gland development, as demonstrated for tenascin in the lung (Gebb and Jones, 2003) and type III collagen in the salivary gland (Nakanishi et al., 1998). For example, MT2-MMP activity results in the release of the NC1 fragment of collagen IV, which regulates cell behavior, in particular angiogenesis (Rebustini et al., 2009).

In conclusion, the present *in vivo* results for the mouse model indicate that MMP-2 plays an important role in epithelial growth and morphogenesis in the mouse ventral prostate, through a mechanism involving ECM remodeling.

1
2
3
4
5
6
7
8
9
10
11
12
13
14
15
16
17
18
19
20
21
22
23
24
25
26
27
28
29
30
31
32
33
34
35
36
37
38
39
40
41
42
43
44
45
46
47
48
49
50
51
52
53
54
55
56
57
58
59
60

Acknowledgments

References

Antonioli E, Della-Colleta HH, Carvalho HF. 2004. Smooth muscle cell behavior in the ventral prostate of castrated rats. J Androl 25: 50-56.

Antonioli E, Bruni-Cardoso A, Carvalho HF. 2007. Effects of long-term castration on the smooth muscle cell phenotype of the rat ventral prostate. J Androl 28: 777-783.

Borden P, Heller RA. 1997. Transcriptional control of matrix metalloproteinases and the tissue inhibitors of matrix metalloproteinases. Crit Rev Eukaryot Gene Exp 7: 159-178.

Bruni-Cardoso A, Carvalho HF. 2007. Dynamics of the epithelium during canalization of the rat ventral prostate. Anat Rec 290: 1223-1232.

Bruni-Cardoso A, Vilamaior PSL, Taboga SB, Carvalho HF. 2008. Localized matrix metalloproteinase (MMP)-2 and MMP-9 activity in the rat ventral prostate during the first week of postnatal development. Histochem Cell Biol 129: 805-815.

Bruni-Cardoso A, Rosa-Ribeiro R, Pascoal VDB, Thomaz AA, Cesar, CL, Carvalho, HF. 2009a. MMP-2 Regulates prostate development *in vitro*. Dev Dyn (in press)

Bruni-Cardoso A, Augusto TA, Pravatta H, Damas-Souza DM, Carvalho HF. 2009b. Stromal remodeling is required for progressive involution of the rat ventral prostate after castration: Identification of a matrix metalloproteinase-dependent apoptotic wave. Int. J. Androl. DOI=10.1111/j.1365-2605.2009.01004.x

Corbier P, Edwards DA, Roffi J. 1992. The neonatal testosterone surge: a comparative study. Arch Int Physiol Biochem Biophys 100: 127-131.

Cunha GR, Chung LWK. 1981. Stromal-epithelial interactions: I. Induction of prostatic phenotype in urothelium of testicular feminized (Tfm/y) mice. J Steroid Biochem 14: 1317-1321.

Donjacour AA, Cunha GR. 1988. The effect of androgen deprivation on branching morphogenesis in the mouse prostate. Dev Biol 128: 1-14.

Esparza J, Kruse M, Lee J, Michaud M, Madri JA. 2004. MMP-2 null mice exhibit an early onset and severe experimental autoimmune encephalomyelitis due to an increase in MMP-9 expression and activity. FASEB J 18: 1682:1691.

Garcia-Florez M, Oliveira CA, Carvalho HF. 2005. Early effects of estrogen on the rat ventral prostate. Braz Med Biol Res 38: 487-497.

Hayward SW, Baskin LS, Haughney PC, Cunha AR, Foster BC, Dahiya R, Prins GS, Cunha GR. 1996. Epithelial development in the rat ventral prostate, anterior prostate and seminal vesicle. Acta Anat 155: 81–93.

Huttunen E, Romppanen T, Helminen HJ. (1981. A histoquantitative study on the effects of castration on the rat ventral prostate. J. Anat. 132, 357-370.

Gebb SA, Jones PL. 2003. Hypoxia and lung branching morphogenesis. Adv Exp Med Biol 543: 117-125.

Kato T, Kure T, Chang J, Gabison EE, Itoh T, Itohara S, Azar DT. 2001. Diminished corneal angiogenesis in gelatinase A-deficient mice. FEBS Lett 508: 187–190.

Kheradmand F, Rishi K, Werb Z. 2002. Signaling through the EGF receptor controls lung morphogenesis in part by regulating MT1-MMP-mediated activation of gelatinase A/MMP2. J Cell Sci 115: 839–848.

Lelongt B, Trugnan G, Murphy G, Ronco PM. 1997. Matrix metalloproteinases MMP2 and MMP9 are produced in early stages of kidney morphogenesis but only MMP9 is required for renal organogenesis in vitro. J Cell Biol 136: 1363-1373.

Li BY, Liao XB, Fujito A, Thrasher JB, Shen FY, Xu PY. 2007. Dual androgen-response elements mediate androgen regulation of MMP-2 expression in prostate cancer cells. Asian J Androl 9: 41-50.

Liao X, Thrasher JB, Pelling J, Holzbeierlein J, Sang XQ, Li B. 2003. Androgen stimulates matrix metalloproteinase-2 expression in human prostate cancer. Endocrinology 144: 1656-1663.

Lynch CC, Hikosaka A, Acuff BH, Martin MD, Kawai N, Singh RK, Vargo-Gogola TC, Begtrup JL, Peterson TE, Fingleton B, Tomoyuki S, Matrisian LM, Futakuchi M. 2005. MMP-7 promotes prostate cancer-induced osteolysis via the solubilization of RANKL. Cancer Cell 7: 485-496.

Matrisian LM, Bowden GT. 1990. Stromelysin/transin and tumor progression. Semin. Cancer Biol. 1: 107-115.

McNeal JE, Stamey TA, Hodge KK. 1988. The prostate gland: morphology, pathology, ultrasound anatomy. Monogr Urol 9: 36-54.

Nakanishi Y, Nogawa H, Hashimoto Y, Kishi J, Hayakawa T. 1988. Accumulation of collagen III at the cleft points of developing mouse submandibular epithelium. Development 104: 51-59.

Nuttall RK, Sampieri CL, Pennington CJ, Gill SE, Schultz GA, Edwards DR. 2004. Expression analysis of the entire MMP and TIMP gene families during mouse tissue development. FEBS Lett 563: 129-134.

Page-McCaw A, Ewald AJ, Werb Z. 2007. Matrix metalloproteinases and the regulation of tissue remodeling. Nat Rev Mol Cell Biol 8: 221-233.

Putz O, Schwartz CB, Kim S, LeBlanc GA, Cooper RL, Prins GS. 2001. Neonatal low- and high-dose exposure to estradiol benzoate in the male rat: I. Effects on the prostate gland. Biol Reprod 65: 1496-1505.

Qin H, SunY, Benveniste EN. 1999. The transcription factors Sp1, Sp3, and AP-2 are required for constitutive matrix metalloproteinase-2 gene expression in astroglioma cells. J Biol Chem 274: 29130-29137.

Rebustini IT, Myers C, Lassiter KS, Surmak A, Szabova L, Holmbeck K, Pedchenko V, Hudson BG, Hoffman MP. 2009. MT2-MMP-dependent release of collagen IV NC1 domains regulates submandibular gland branching morphogenesis. Dev Cell 17: 482-493.

Risbridger GP, Almahbobi GA, Taylor RA. 2005. Early prostate development and its association with late-life prostate disease. Cell Tissue Res 322: 173-181.

Rudolph-Owen LA, Hulboy DL, Wilson CL, Mudgett J, Matrisian LM. 1997. Coordinate expression of matrix metalloproteinase family members in the uterus of normal, matrilysin-deficient, and stromelysin-1-deficient mice. Endocrinology 138: 4902-4911.

Steinberg Z, Myers C, Heim VM, Lathrop CA, Rebustini IT, Stewart JS, Larsen M, Hoffman MP. 2005. FGFR2b signaling regulates ex vivo submandibular gland epithelial cell proliferation and branching morphogenesis. Development 132: 1223-1234.

Sternlicht MD, Werb Z. 2001. How matrix metalloproteinases regulate cell behavior. Annu. Rev Cell Dev Biol 17: 465-516.

Sugimura Y, Cunha GR, Donjacour AA. 1986a. Morphogenesis of ductal networks in the mouse prostate. Biol Reprod 34: 961-971.

Sugimura Y, Cunha GR, Donjacour AA, Bigsby RM, Brody JR. 1986b. Whole-mount autoradiography study of DNA synthetic activity during postnatal development and androgen-induced regeneration in the mouse prostate. Biol Reprod 34: 985-995.

VanSaun MN, Matrisian LM. 2006. Matrix metalloproteinases and cellular motility in development and disease. Birth Defects Res. C Embryo Today 78: 69-79.

Wiseman BS, Werb Z. 2002. Stromal effects on mammary gland development and breast cancer. Science 296: 1046-1049.

Wiseman BS, Sternlicht MD, Lund LR, Alexander C.M, Mott J, Bissell MJ, Soloway P, Itohara S, Werb Z. 2003. Site-specific inductive and inhibitory activities of MMP-2 and MMP-3 orchestrate mammary gland branching morphogenesis.. J. Cell Biol. 162, 1123-1133.

Legends for the figures

Figure 1. Structural aspects of the neonatal mouse VP and the effect of MMP-2 knocking out. A. Immunohistochemistry showed the presence of MMP-2 (green fluorescence) in the proximal and distal region of the neonatal prostate. The enzyme concentrates in the epithelial tips at the distal regions. Nuclei (blue fluorescence) were stained with DAPI. Scale bar = 20 µm. **B.** Stereology revealed no difference in the volume densities ($V_{v\%}$) of the epithelium, lumen, and stroma at day 6 after birth. **C.** Pan-cytokeratin staining of wild-type and MMP-2$^{-/-}$ mice was used to identify the epithelial organization and to count the number of distal tips in each situation. Besides revealing a reduced number of epithelial tips ($p<0.05$), the stain also showed the existence of dilated epithelial structures in the knockout mice VP (asterisk). Scale bar = 100 µm. **C.** Mitotic cells were identified through immunohistochemistry for phospho-histone H3 in neonate ventral prostate sections. Phospho-histone H3-positive epithelial and stromal cell nuclei (green fluorescence) were found in both strains, and their counts revealed fewer mitotic cells in the epithelium of the MMP-2$^{-/-}$ mice VP ($p<0.05$), whereas no difference was found in the stroma. Scale bar = 50 µm. **D.** Apoptotic cells were counted after TUNEL reaction. TUNEL-positive epithelial cell nuclei (green fluorescence) were observed in the center of the epithelial cords in the ventral prostate of both strains. Epithelial structures are outlined by dashed white lines. Nuclei (blue fluorescence) were stained with DAPI. No difference in apoptotic rates was found between the wild-type and MMP-2$^{-/-}$ mice. Scale bar = 20 µm.

Figure 2. Structural aspects of the neonatal mouse VP and the effect of MMP-2 knocking out. A. Immunohistochemistry revealed that MMP-2 (green fluorescence) was found in normal ventral prostate epithelial and stromal tissues. As expected, MMP-2 was not present in MMP2$^{-/-}$ mouse ventral prostates. Nuclei (blue fluorescence) were stained with DAPI. Scale bars: left panel = 50 µm, middle panel = 20 µm, right panel = 50 µm. **B.** Hematoxylin-eosin stained sections of adult ventral prostates. Unlike the wild-type samples, MMP2$^{-/-}$ VP acini were more dilated (asterisk). Scale bars = 50 µm. **C**. Stereology showed a reduced (p<0.05) epithelial volume density (upper panel). The epithelial and stromal compartments of MMP2$^{-/-}$ had smaller volumes (p<0.05) than the wild-type VP. **D**. Phospho-histone H3 staining identified mitotic cells in the adult VP, but their counts showed no difference between the wild-type and MMP2$^{-/-}$ mice. Scale bars = 100 µm, detail = 20 µm. **E.** TUNEL reaction (green fluorescence) was used to identify apoptotic cells with respect to the total number of nuclei (DAPI staining, blue fluorescence). Scale bars = 20 µm. No statistical differences in the number of dying epithelial cells were found between the strains.

Figure 3. MMP-9 compensates for MMP-2 in the adult MMP-2$^{-/-}$ mice. Immunohistochemistry for MMP-9 showed the enzyme to be widely distributed in the VP stroma of both wild-type (upper left panel) and MMP-2$^{-/-}$ (upper right panel) samples from 6-day-old animals. No reaction was found in the adult wild-type mice (lower left panel), but appeared concentrated in the stroma, more particularly on smooth muscle cells of the MMP-2$^{-/-}$ mice (lower right panel). Scale bar: 50 µm.

Figure 4. Reticulin fiber accumulation in the absence of MMP-2. A. After Gömöri´s silver impregnation, reticulin fibers (in black) were thinner and fewer in the distal regions of the wild-type samples (upper left panel). The MMP-2$^{-/-}$ ventral prostate showed thicker and more abundant reticulin fibers in association with the dilated epithelial structures (upper right panel) than did the wild-type samples. Scale bar: 50 μm, detail 20 μm. **F.** In the adult mouse, Gömöri´s silver impregnation revealed the presence of reticulin fibers (in black) in the boundary between epithelium and stroma. These fibers were thicker in the MMP-2$^{-/-}$ VP (lower right panel) than in the wild-type samples (lower left panel). Scale bar: 20 μm. **B**. The sectional are occupied by reticulin was measured for both 6-day-old and adult mice. Reticulin occupied a larger area of the prostate section in both ages, but achieved significance only in the adults (*, $p<0.05$). **C**. The reticulin/epithelium area ratio was also determined for both ages in the wild type and MMP-2$^{-/-}$ mice and the results confirmed a larger area occupied by reticulin fibers in the knockout mice, particularly in the adults.

1
2
3
4
5
6
7
8
9
10
11
12
13
14
15
16
17
18
19
20
21
22
23
24
25
26
27
28
29
30
31
32
33
34
35
36
37
38
39
40
41
42
43
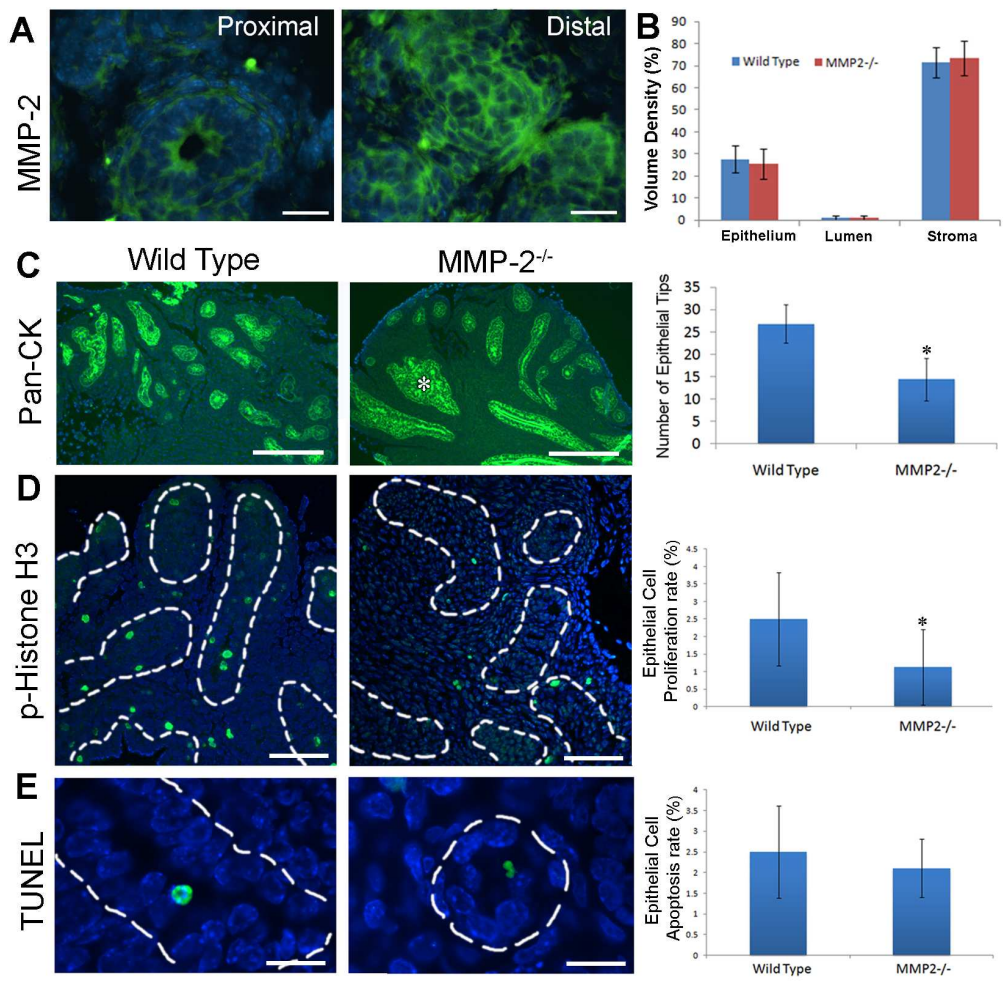44
45
46
47
48
49
50
51
52
53
54
55
56
57
58
59
60

Figure 1
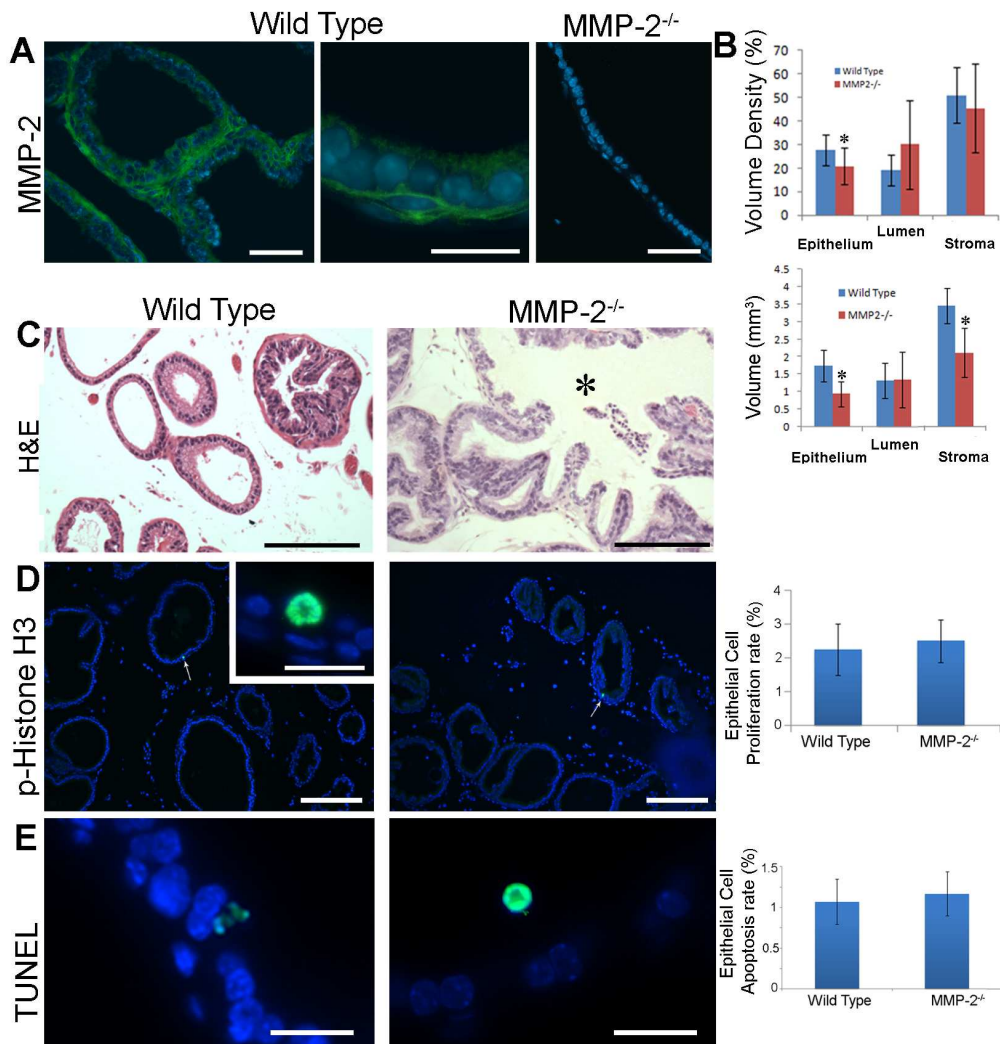138x135mm (300 x 300 DPI)

Figure 2
137x143mm (300 x 300 DPI)

1
2
3
4
5
6
7
8
9
10
11
12
13
14
15
16
17
18
19
20
21
22
23
24
25
26
27
28
29
30
31
32
33
34
35
36
37
38
39
40
41
42
43
44
45
46
47
48
49
50
51
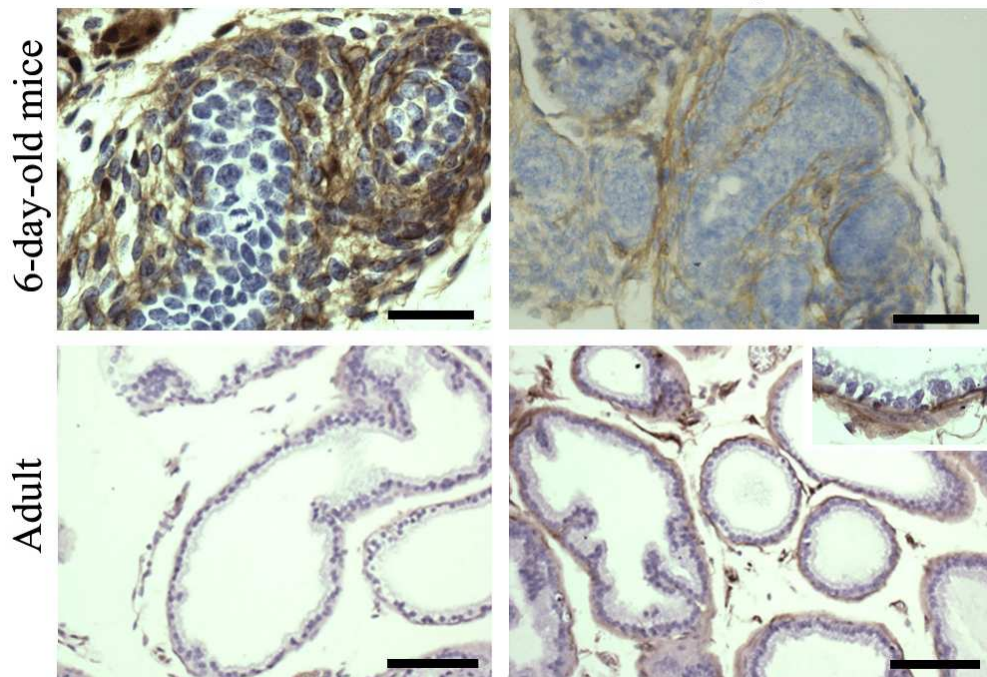52
53
54
55
56
57
58
59
60

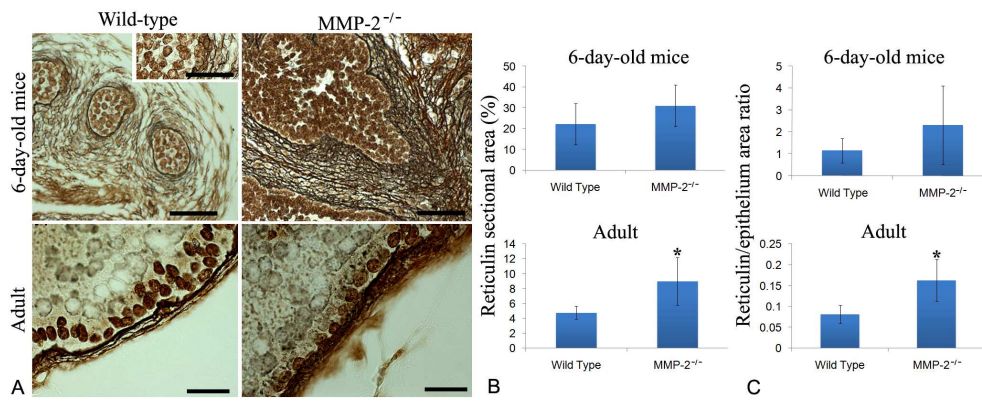## MMP-9 immunohistochemistry

Figure 3
84x61mm (300 x 300 DPI)

Figure 4
177x69mm (300 x 300 DPI)

ORIGINAL ARTICLE

Stromal remodelling is required for progressive involution of the rat ventral prostate after castration: Identification of a matrix metalloproteinase-dependent apoptotic wave

A. Bruni-Cardoso,[1] T. M. Augusto,[1] H. Pravatta, D. M. Damas-Souza and H. F. Carvalho

Department of Anatomy, Cell Biology, Physiology, and Biophysics, Institute of Biology, State University of Campinas (UNICAMP), SP, Brazil

Summary

Prostate epithelial-cell apoptosis occurs in response to androgen deprivation. We have hypothesized that continued regression would require stromal changes. Studying apoptosis kinetics up to the 14th day after castration, we identified successive waves of apoptosis, with a prominent peak on day 11. This peak was associated with caspase-3 activity, nuclear translocation of apoptosis-inducing factor and clusterin expression. The apoptosis peak on day 11 was preceded by increased MMP-2 and MMP-7 activation, and MMP-9 expression on days 9 and 10. Treatment with the matrix metalloproteinases inhibitors doxycyclin, hydrocortisone, or GM6001 caused significant reduction in the apoptosis rate on day 11. The present data demonstrate that prostatic epithelial-cell deletion at the 11th day after castration was induced by focal degradation of the extracellular matrix associated with stromal remodelling.

Introduction

Prostate cancer usually progresses very slowly, but is ranked as the second cause of non-accidental death among Occidental men, despite a wider range of diagnostic and therapeutic options. The ever-increasing incidence of prostate cancer can be attributed to the progressive extension in males' life expectancy, together with increased awareness of and screening for the disease. Antiandrogen therapies, including surgical or chemical castration, are the first choices in treatment of primary tumours. However, it is common that after remission, some androgen-independent tumour cells will begin aggressive proliferative growth (Feldman & Feldman, 2001; Jin *et al.*, 2008).

The antiandrogen treatment is based on the clear dependence of prostate growth and maintenance on androgen stimulation, so that androgen deprivation causes a progressive reduction in prostatic function and weight. The regressive changes in response to androgen deprivation involve a sudden drop in synthetic activity, continuous elimination of the secretory products present in the lumen, the deletion of a large number of epithelial cells by apoptosis and changes in the stromal compartment.

In rodents, epithelial-cell apoptosis peaks 72 h after castration (Kerr & Searle, 1973; Sandford *et al.*, 1984; Isaacs, 1984; Kyprianou & Isaacs, 1988; Garcia-Flórez *et al.*, 2005). The reason for this delay in apoptosis is not yet clear, but may be related to the existence of a buffering mechanism that protects the organ against occasional oscillation in androgen levels, which may occur in response to a series of environmental and stress factors. In contrast to the epithelium, prostate endothelial cells respond rather quickly to the reduction in circulating testosterone (Lekås *et al.*, 1997; Shabsigh *et al.*, 1998). Part of the endothelial cells die by apoptosis, and there is a reduction in blood flow to the gland, an increase in vascular permeability and the development of a hypoxic condition. Accordingly, it was suggested that the death of the

epithelial cells in response to androgen deprivation results from the poor vascular supply of nutrients and oxygen (Shabsigh *et al.*, 2001). Recovery of the initial size and function is readily achieved after androgen administration (Lesser & Bruchovsky, 1974).

In a previous study, we showed that oestrogen treatment together with orchiectomy causes different rates of epithelial cell death, and, most importantly, that the different rates of epithelial cell death cause no additional reduction in the volume density of the epithelium within the first week post-castration (Garcia-Flórez *et al.*, 2005). These results led us to hypothesize that the reduction in the prostatic weight after the first week of androgen deprivation would also require a reorganization of the stromal compartment, and would depend on the active remodelling of the basement membrane and stromal extracellular matrix by the activation of extracellular matrix-degrading enzymes, especially matrix metalloproteinases (MMP), as was shown for the mammary-gland regression after weaning (Lund *et al.*, 1996).

To test this hypothesis, we examined the content and/or activity of MMP 2, 7 and 9, and the effects of their inhibition on the rate of apoptotic cell death in the regressing prostate after bilateral surgical castration, following a 14-day experimental timeline. The results presented here demonstrate the existence of a second major peak of apoptosis at the 11th day after castration, which was preceded by a peak of MMPs expression, accumulation and/or activation, with different contributions from the epithelial and stroma cells. In addition, pharmacological inhibition of MMP activity reduced the rate of apoptosis at day 11. Taken together, these results indicate that different mechanisms contribute to epithelial apoptosis during rat ventral prostate (VP) involution, with a clear role of extracellular matrix-degrading enzymes and consequent stromal remodelling.

Materials and methods

Animals and treatments

A total of 158 90-day-old Wistar male rats were used in this study. Fourteen animals were maintained as sham-operated controls, and 126 animals were castrated under anaesthesia with 80 mg/kg body weight ketamine hydrochloride and 10 mg/kg body weight xylazine hydrochloride, and assigned to 14 groups (nine animals per group), one of which was killed on each day (day 1 through 14 after castration) by anaesthetic overdose. An additional 18 castrated animals were treated either with hydrocortisone succinate (500 mg/kg i.p., twice a day, in sterilized water) (Eurofarma, São Paulo, SP, Brazil) or doxycycline [1.42 mg/kg orally, twice a day, in phosphate buffered solution (PBS)] (Henrifarma, Ribeirão

Preto, SP, Brazil) administered at days 9–11 after castration; or were treated with GM6001 (0.7 mg/kg/day in PBS) (Sigma Chemical Co., St Louis, MO, USA) given at days 9 and 10. Six animals received only PBS, and were designated as the Cas11 group. All animals were killed at day 11, and had their VPs dissected and processed for paraffin embedding and submitted to terminal deoxynucleotidyl transferase-mediated -dUTP nick end labelling (TUNEL) reaction (as below) for the counting of apoptotic cells. The VPs were then immediately dissected, freed of adherent tissue, weighed and fixed for paraffin embedding or snap-frozen in liquid nitrogen for the biochemical analysis. Animal-handling and experimental procedures were approved by the State University of Campinas Committee for Ethics in Animal Experimentation (Protocol no. 1490-1).

Apoptotic cell counting: Feulgen reaction and TUNEL

The Feulgen reaction was performed on histological sections after blocking of aldehyde groups by treatment with 100 mM sodium borohydride. In brief, sections were hydrolysed in 4 M HCl at room temperature for 1 h 15 min before incubation with Schiff's reagent for 40 min at room temperature in the dark. After three rinses, the sections were dehydrated and mounted in Entellan. Morphologically identified nuclei were counted with respect to the total epithelial cells in six microscope fields taken at random from three animals; the numbers of nuclei were expressed as percentages of the total epithelial cell nuclei (Garcia-Flórez *et al.*, 2005). The TUNEL assay was performed using the in situ cell-death detection kit (Roche Diagnostics, Indianopolis, IN, USA), according to the manufacturer's instructions, including the peroxidase converter and methyl-green counterstaining. Microscope fields from an equatorial section of a single VP lobe from each of three animals were taken at random, and the frequency of apoptotic cells was counted and expressed as a percentage of the total number of epithelial-cell nuclei. At least 1000 cells were counted per experimental group.

Immunohistochemistry

We performed immunostaining for MMP-2, MMP-7, MMP-9, and apoptosis induction factor (AIF). The antigens were retrieved from the dewaxed sections by either boiling in a microwave oven in 10 mM citrate buffer, pH 6.0, for 10 min, or digestion in 0.1% pepsin (Sigma Chemical Co.) in 0.01 N HCl for 20 min at room temperature. The sections were blocked with 3% H_2O_2 for 10 min, followed by incubation with either 1% pre-immune serum in PBS or 3% bovine serum albumin in Tris-buffered saline with 0.2% Tween 20 (TBS-T) for

1 h, and were incubated overnight with rabbit anti-human MMP-7 diluted 1 : 100 (Chemicon, Temecula, CA, USA), rabbit anti-mouse MMP-9 and MMP-2 diluted 1 : 500 (Abcam, Cambridge, MA, USA), and rabbit anti-AIF diluted 1 : 50 (Cell Signaling Technology, Danvers, MA, USA). Negative controls were established by omitting the primary antibody step. The specificity of the antibodies was guaranteed by the manufacturers. Tissue-bound primary antibody against AIF was detected using the ABC kit (NCL-ABCu; Novocastra, Newcastle-upon-Tyne, UK) according to the manufacturer's instructions. The sections were counterstained with Harris haematoxylin. Antibodies against MMP-2, - 7, and -9 were localized by Alexa-488 conjugated secondary antibodies, and nuclei were stained with 4′-6-diamidino-2-phenylindole (DAPI).

Protein extraction

For MMP analysis, VPs were dissected from three animals per group, immediately frozen in liquid nitrogen and stored at −80 °C until used. The frozen tissue was homogenized in 50 mM Tris-HCl, pH 7.4, containing 0.2 M NaCl, 0.1% Triton, 10 mM $CaCl_2$ and 1% protease-inhibitor cocktail (Sigma Chemical Co.) using a Polytron homogenizer (Kinematica, Lucerne, Switzerland). The homogenates were incubated for 2 h at 4 °C and centrifuged at 2080 g for 20 min at 4 °C. The supernatants were removed and the pellets resuspended in the same solution as described above, heated to 60 °C for 5 min, centrifuged at 2080 g for 20 min at 4 °C, and the two supernatants were pooled. The protein concentration was determined by using the Bradford reagent (Bio-Rad Laboratories, Hercules, CA, USA) following the manufacturer's instructions.

Gelatin zymography

Twenty micrograms of protein extract was electrophoresed in 10% SDS polyacrylamide gel containing 0.1% gelatin (used as protein substrate) at 4 °C under non-reducing conditions. After electrophoresis, the gel was washed twice under gentle shaking at room temperature with 2.5% Triton X-100 for 30 min to remove SDS. The gel was incubated overnight in a 50 mM Tris-HCl, pH 7.4, containing 10 mM $CaCl_2$ and 0.1 M NaCl at 37 °C. The gel was then stained with Coomassie brilliant blue R (0.5% dye in 20% methanol and 10% acetic acid) for 1 h. Unstained bands indicating gelatinolytic activity were seen after a series of washes with 30% ethanol and 10% acetic acid. The intensity of the bands was determined using the Scion Image Analysis software (Scion Corporation, Frederick, MD, USA). The activity determined for the VP of non-castrated rats was used as the

reference (100%). The experiments were performed in triplicate.

Western blotting (WB)

The protein extracts obtained as described above were used in this assay. A total of 60 micrograms of protein was electrophoresed on polyacrylamide gels at different concentrations, followed by electric transfer (Hoefer, San Francisco, CA, USA) onto nitrocellulose membranes (Amersham, Buckinghamshire, UK). The membranes were blocked in 5% non-fat milk in TBS-T for 1 h, followed by overnight incubation with 1% non-fat milk in TBS-T and rabbit anti-MMP-7 (Chemicon) diluted 1 : 500, mouse anti-clusterin (Upstate Technologies, Lake Placid, NY, USA) (1 : 1000) or rabbit anti-AIF diluted 1 : 2000 (Cell Signaling Technology, Beverly, MA, USA). The membranes were washed in TBS-T and incubated for 1 h with peroxidase-conjugated goat anti-rabbit Ig (Zymed, San Francisco, CA, USA) or goat anti-mouse Ig (Sigma Chemical Co.) each diluted 1 : 2000, followed by detection with the Luminol system (Santa Cruz Biotechnology, Santa Cruz, CA, USA). The intensity of the bands was determined using the Scion Image Analysis software. The values determined for the control were used as the reference (100%) (except for clusterin). The experiments were performed in triplicate.

Caspase-3 activity assay

Caspase-3 activity was determined with a colorimetric test (Sigma Chemical Co.), according to the manufacturer's instructions. This assay is based on the hydrolysis of the peptide substrate acetyl-Asp-Glu-Val-Asp p-nitroanilide (Ac-DEVD-pNA) by caspase-3, resulting in the release of p-nitroaniline (pNA) which has an absorbance at 405 nm. In brief, 50 μg of protein from two VPs for each experimental point was assayed in duplicate in a 96-well plate. The samples were incubated for 90 min with the assay buffer in the presence of substrate with or without a caspase-3 inhibitor (AC-DVDE-CHO). The concentration of the pNA released from the substrate was calculated from the absorbance values measured in an ELISA reader, and a calibration curve was prepared with defined pNA solutions.

Statistical analysis

Statistical analyses were performed by ANOVA followed by the multi-comparison post-hoc Tukey's or Fisher's tests, at $p < 0.05$, using a free trial version of the software Minitab (Minitab Inc., State College, PA, USA). Results are presented as the mean of measurements for at least three

animals per group. Error bars were omitted from some graphs for the sake of clarity.

Results

Drastically reduced prostate weight after castration is associated with successive peaks of apoptosis

In non-castrated animals, the prostate weight was approximately 0.1% of the animal's body weight (Fig. 1A). After 14 days of androgen deprivation, the prostate weight was reduced to about 0.016% of the animal's weight. Seventy-six per cent of this reduction took place within the first week, and 34% within the second week post-castration. Interestingly, daily variation in prostatic weight revealed three major points of weight reduction, at days 3, 7 and 11 after androgen ablation (Fig. S1). Moreover, the gland gained weight at days 1 and 10 after castration.

To evaluate the kinetics of cell death in the prostatic involution, we used both Feulgen staining and TUNEL reaction for counting apoptotic cell nuclei and nuclei containing fragmented DNA. Three days after castration, characteristic apoptotic nuclei and nuclei containing fragmented DNA were found (Fig. S2). The counts were very similar, with two major waves of apoptosis detected at the 3rd and 11th day, with a less-prominent count at the 7th day after surgery (Fig. 1B). No statistical difference was observed between the percentage of apoptosis identified by each procedure at each time point. It was apparent that these successive peaks of epithelial cell death were associated with the marked points of prostatic weight reduction (Fig. S1).

Caspase-3 activation is considered a key factor in apoptosis, and a converging element in both intrinsic and extrinsic apoptotic pathways. Therefore, we investigated the variation in caspase-3 amounts and activity throughout the timeline of the experiment, using WB and a colorimetric assay. The caspase-3 content showed an increase centred at days 6 to 8, but no clear association with the apoptosis peaks (Fig. S3). Under the experimental conditions used, we could not detect the cleaved active band. However, caspase-3 activity (peak activity at days 2 and 9-11) (Fig. 1C) correlated with the observed kinetics of apoptosis and preceded DNA fragmentation.

Clusterin is known as a testosterone-repressed message in the rat VP and is associated with apoptosis (Rouleau et al., 1990). It was also found in association with apoptosis in the mammary gland (Lund et al., 1996). However, its specific function is unknown. To determine whether clusterin expression was correlated with the different apoptosis peaks detected up to day 14, we investigated the variation in clusterin content within the timeline of the experiment by WB. We found that the amount of clusterin increased in response to castration up to day 5,

overlapped the apoptosis peak at day 3, and also exhibited a second peak at days 8 and 9, preceding the apoptosis peak at day 11 (Fig. 1D).

Apoptosis-inducing factor is a mitochondrial protein that is released from mitochondria and translocated to the cell nucleus, where it binds to DNA and elicits DNA fragmentation (Lipton & Bossy-Wetzel, 2002). AIF was found in the VP by WB, and its content dropped abruptly after castration (Fig. 1E–H). Nonetheless, it was located by immunohistochemistry in the cytoplasm of the luminal epithelial cells of the VP in non-castrated animals (Fig. 1F) and in the nuclei of apoptotic cells after castration (Fig. 1G,H).

Matrix-remodelling enzymes accumulate and are activated before the apoptotic peak at day 11

The stromal compartment undergoes noticeable changes after castration (Vilamaior et al., 2000; Antonioli et al., 2004, 2007; Augusto et al., 2008). To verify if a correlation existed between the changes in the extracellular matrix components and the kinetics of apoptosis, we investigated the variations in the amounts and/or activation of MMP-2, MMP-9, and MMP-7 in the regressing prostate. Figure 2A presents a representative zymogram showing the variation in MMP-2 and MMP-9 content and its densitometric quantification. The MMP-2 amounts varied after castration, but reached a peak on day 10 (Fig. 2A). This coincided with the peak activation of this enzyme (measured as the percentage of the active 62 KDa band with respect to the total). The amount of MMP-9 increased at days 10 and 11, with no association with the first peak found on the 3rd day after castration (Fig. 2A).

Figure 2B presents a representative WB for MMP-7 in the VP of castrated rats, and the densitometric quantification of the data, revealing a clear drop in MMP-7 content during the first three days after castration and a progressive increase after day 8, with a maximum amount observed at day 10. Nevertheless, for the proteolysis-derived active MMP-7, we found a peak of activation at day 9.

Stromal and epithelial cells contribute to the increased MMP activity at day 11

To determine which cells contribute to the enzymes preceding the peak in epithelial-cell apoptosis at day 11, we used immunohistochemistry to locate MMP-2, MMP-7 and MMP-9. Figure 3 shows the location of these three enzymes in the VP at day 10 after castration. MMP-2 (Fig. 3A) and MMP-7 were found predominantly in the epithelium, but were also observed at the surface of smooth-muscle cells in the stroma. At least part of the epithelial staining for MMP-2 may be attributable to
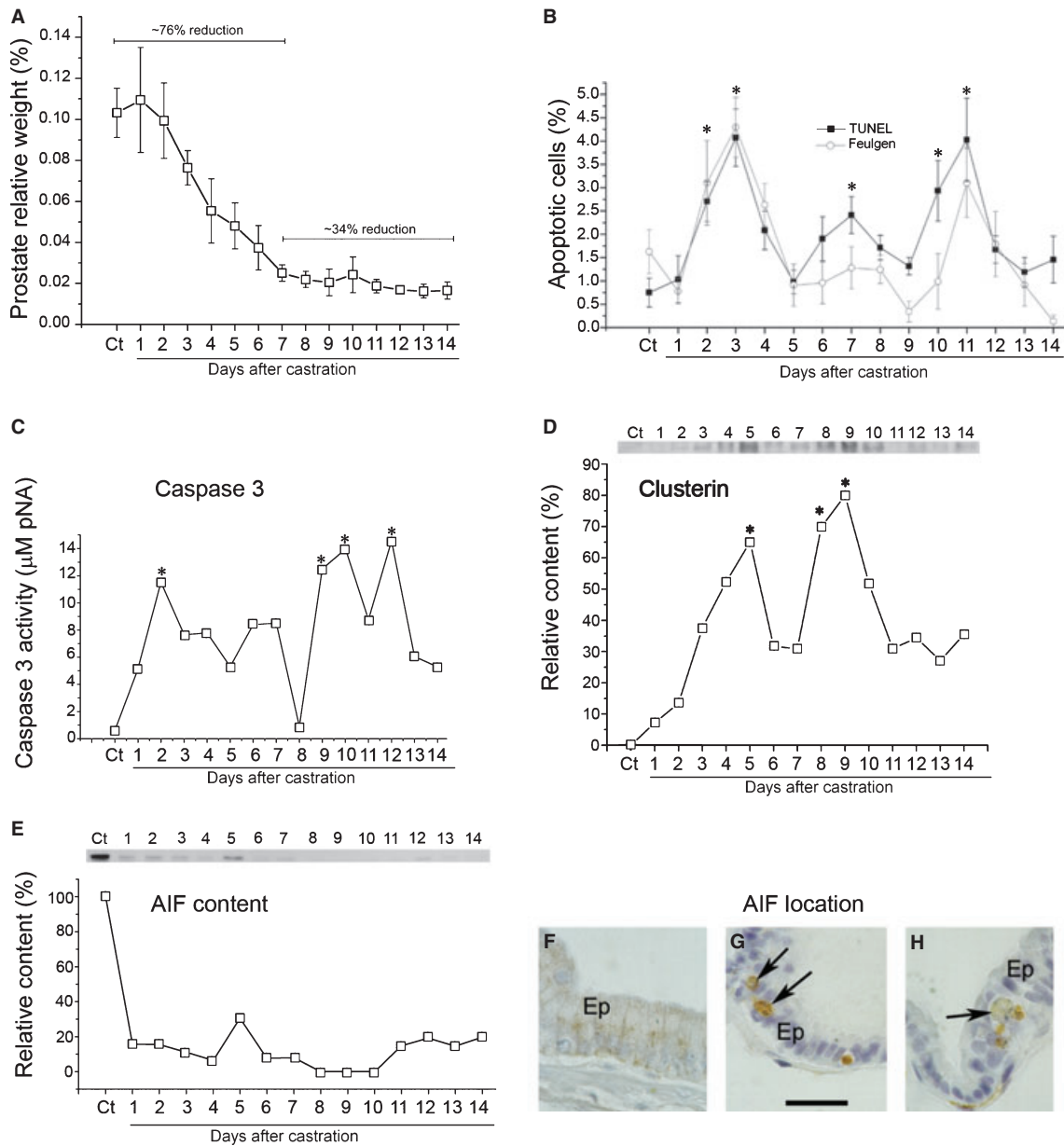
Figure 1 (A) Variation in the rat ventral prostate (VP) relative weight (shown as a percentage of the total body weight) up to the 14th day after castration. There was a 76% reduction within the first 7 days, and a further 34% reduction within the next 7 days (*n* = 4). (B) Kinetics of apoptosis in the rat VP after castration, up to the 14th day after surgery, as determined by the percentage of morphologically recognized nuclei after the Feulgen reaction and after terminal deoxynucleotidyl transferase-mediated -dUTP nick end labelling (TUNEL) reaction. (C) Caspase-3 activity as determined by a colorimetric assay in extracts of the VP of control and castrated rats up to the 14th day after surgery. Peak activity was detected at days 2, 5 and 9–11. Data are the means of measurements for two animals. (D) Representative western blotting (WB) for clusterin in VP extracts and its relative variation after castration. Two peaks were found at days 5 and 9 after castration. Significant increases in clusterin amounts were found at days 5, 8 and 9 after castration. Maximum expression was found at days 5 or 9 in different gels and defined as 100%. The expression in the control was fixed at zero. (E) Representative WB for apoptosis induction factor (AIF) in the rat VP before and up to the 14th day after castration and its quantification, showing a marked reduction in response to androgen deprivation. Immunohistochemical localization of AIF in the VP epithelium of non-castrated rats, showing its cytoplasmic location (F) and its translocation to the cell nucleus of apoptotic cells on the 3rd (G) and 11th (H) day after castration, showing the nuclear localization in apoptotic cells. Results are the mean ± SEM. The asterisks indicate significant differences from the control after TUNEL reaction, following anova and Tukey's or Fisher's test. F-H, scale bar = 20 μm.
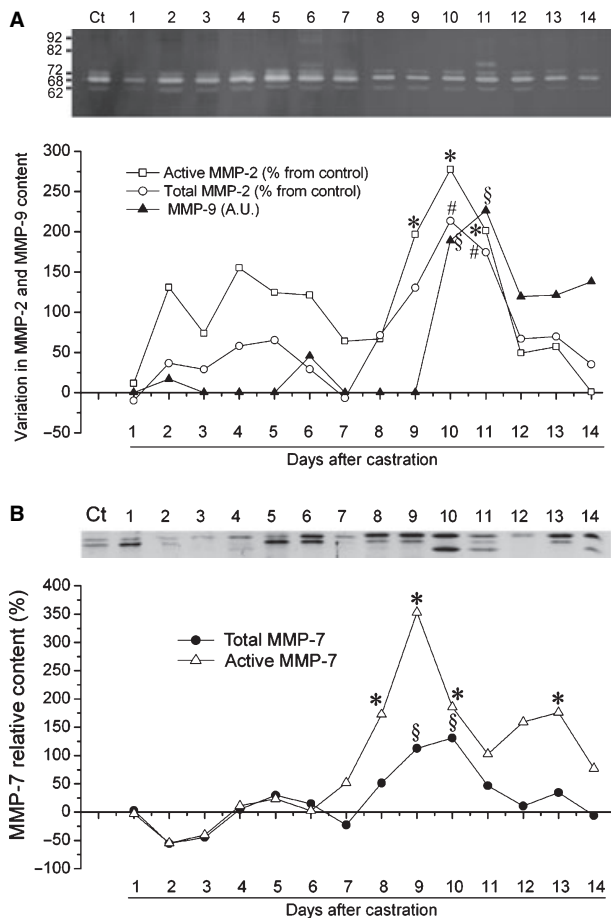
Figure 2 (A) Representative gelatin zymogram of VP extracts showing the identification of MMP-2 (72 KDa, 68 KDa, and 62 KDa) and MMP-9 (92 KDa and 82 KDa) and variation in the amount of the total and active band (62 KDa) (as a percentage of the controls) and in MMP-9 (arbitrary units). MMP-2 increased after castration. MMP-9 was not expressed in the control prostate, but was highly expressed at days 10 and 11. (B) Representative WB for MMP-7 in VP extracts from control (Ct) and castrated rats, depicting the native (29 KDa) and cleaved forms (23 KDa and 20 KDa), and the percentage variation of the total and active MMP-7, showing that the content and activation dropped below control levels immediately after castration; and a subsequent increase, starting at day 7, with a peak of the total content at day 10 and a peak of the active form at day 9. Symbols represent significant changes with respect to controls for active MMP-2 (*), total MMP-2 (#) and MMP-9 (§).

macrophages. MMP-9 occurred in different locations: in fibroblasts and smooth-muscle cells in the stroma, but not in the epithelium (Fig. 3C).

Inhibition of MMP activity results in decreased apoptosis at day 11

The time association between MMP-2 and MMP-7 activation, MMP-9 expression and the apoptosis peak at day 11
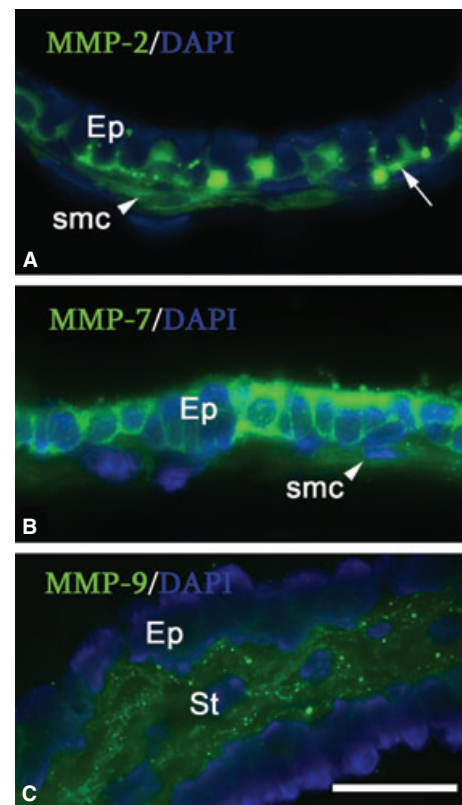
Figure 3 Immunohistochemical location of MMP-2 (A), MMP-7 (B) and MMP-9 (C). MMP-2 was found in both epithelial (Ep) and stromal compartments, particularly in smooth-muscle cells (SMC). At least part of the epithelial staining was due to macrophages (arrow). MMP-7 was predominantly located in the epithelial cells, even though minimal staining could be observed around the smooth muscle cells. By contrast, MMP-9 was exclusive to the stroma, in association with the surface of cells. Scale bar = 25 μm.

led us to question if a causal relationship exists between these two events. To approach this question, we blocked MMP activity using non-specific (hydrocortisone and doxycycline) (Mignatti & Rifkin, 1993; Saikali & Singh, 2003) and broadly specific (GM6001) (Gupta *et al.*, 2007) inhibitors during days 9 through 11, and checked their influence on the apoptosis rate at day 11. It was then apparent that MMP inhibition caused a reduction in the percentage of epithelial-cell apoptosis at day 11 (Fig. 4), demonstrating a causal relationship between MMP activity and cell death.

Discussion

Using a combination of morphological and biochemical analysis associated with pharmacological intervention, we have identified a second wave of apoptosis in the regressing VP in response to castration, which is dependent on

Figure 4 Effects of non-specific and broadly specific MMP inhibition on the apoptotic rate at day 11. Doxycycline (Dox), hydrocortisone (HC), and GM6001 were administered to castrated rats, and the percentage of apoptotic cells was determined when compared with the percentage of apoptotic cells found in the VP of castrated rats at day 11 (Cas11). A significant reduction in apoptosis rate (*; $p < 0.05$) was found for the three inhibitors.
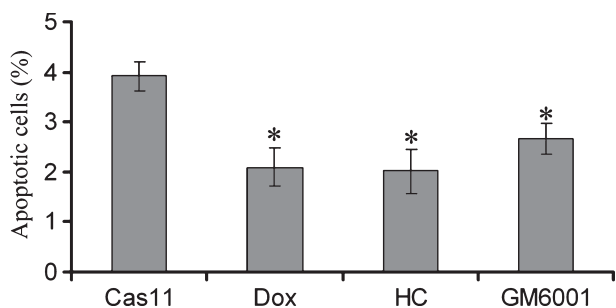
extracellular-matrix degradation, and demonstrates that matrix remodelling is a prerequisite for continued deletion of epithelial cells.

The prostate gland is highly dependent on androgens for its development, growth and functioning, and castration results in active and progressive regression of the gland (Isaacs, 1984; Kyprianou & Isaacs, 1988; Isaacs *et al.*, 1994). Analyses of long-term (100 days) androgen deprivation showed that the organ corresponds to about 5% of the prostate weight in the control animals (Antoni-oli *et al.*, 2007). The weight reduction observed within the first week post-castration results from the elimination of the accumulated secretions, the reduction in the synthetic organelles such as the endoplasmic reticulum and the Golgi complex, reduced blood flow and extensive deletion of epithelial cells by apoptosis. Nonetheless, weight gain occurred at days 1 and 10. It has been reported previously that increased blood-vessel permeability results in vascular extravasation, and this might contribute to the weight gain observed at day 1 after castration. This increased vascular permeability results from the deletion of endothelial cells, which is a primary event occurring after castration (Shabsigh *et al.*, 1998). It remains to be determined whether another series of vascular changes similar to those observed early after castration takes place and might be responsible for the weight gain at day 10. It is also interesting to note from the present results that both time points preceded peaks of epithelial-cell apoptosis.

Extending the analysis period to 14 days, we could identify two further increases in apoptosis on days 7 and 11. Both methods (Feulgen and TUNEL) showed identical kinetics of cell death, demonstrating that accurate identification of apoptotic nuclei might provide good estimates of tissue apoptosis, at least in the rat VP, confirming

previous findings by our group (Garcia-Flórez *et al.*, 2005). These results demonstrate that prostatic regression results from multiple waves of apoptosis. Sandford *et al.* (1984) reported the occurrence of successive waves of apoptosis, but they referred to the ability of the gland to recover after the administration of testosterone and to show the major apoptotic peak at day 3 (appearing at day 2 after repeated cycles of testosterone administration). However, they failed to discriminate the additional peaks observed in this study, perhaps because they did not carry out analyses in the day 8–12 period.

We have shown that caspase-3 activity and the translocation of AIF to the cell nucleus are events shared by the apoptosis peaks at days 3 and 11. Both these events are related to apoptosis induction, but represent components of the caspase-dependent and caspase-independent pathways respectively. AIF translocation to the cell nucleus is a factor associated with induction of LNCaP apoptosis in response to cisplatin (Zhang *et al.*, 2007). A search for other members of each pathway with respect to each apoptosis peak is underway in our laboratory.

Clusterin has been reported to correlate with androgen deprivation and epithelial apoptosis in the rat VP. Indeed, it was first described as TRPM-2, because it is strongly induced in the VP of castrated animals. It is also involved with mammary-gland regression (Lund *et al.*, 1996). However, the present results demonstrated that the clusterin content is increased in the regressing prostate, but showed no clear correlation with apoptotic cell death or even a direct correlation with androgen deprivation. This pattern suggests that clusterin expression has a temporal association but apparently no causal relationship with epithelial apoptosis, reinforcing the notion that this molecule is closely associated with specific events leading to tissue remodelling, and most specifically with signal transduction and DNA repair (Trougakos & Gonos, 2002). Furthermore, we have reason to believe that one possible function of clusterin (at least of its secreted sulphated form) is the inhibition of an inflammatory response, orchestrating the recruitment of inflammatory cells (macrophages, lymphocytes and mast cells) with maintenance of the non-inflamed condition, perhaps by recruiting and stimulating regulatory T cells. This possibility is currently under investigation in our laboratory.

We have previously reported that, regardless of the kinetics of apoptosis within the first week post-castration, the maximum regression of the epithelium was about the same (~24% of the original weight) (Garcia-Flórez *et al.*, 2005). This led us to hypothesize that stromal changes occur to allow further regression of the epithelium to take place.

In fact, the regressive changes of the mammary gland involve a second wave of apoptosis, which was demon-

strated to be dependent on the stromal production of matrix-degrading enzymes, particularly gelatinase-A and -B (MMP-2 and -9 respectively), by stromal fibroblasts, and that blocking MMP activity with hydrocortisone reduced the apoptosis rate and the regressive changes of the gland (Lund et al., 1996). Furthermore, we and others have reported later changes in stromal organization and in the content of extracellular matrix components, from tenascin expression (Vollmer et al., 1994) to fibrillar and microfibrillar collagen reorganization (Carvalho et al., 1997; Vilamaior et al., 2000), from variations in heparan sulphate (Augusto et al., 2008) to the altered ultrastructure of the basement membrane (Carvalho & Line, 1996; Ilio et al., 2000).

The VP differs from the mammary gland, where stromal fibroblasts produce the MMP presumed to degrade the epithelial basement membrane (Lund et al., 1996), by showing a contribution from both epithelial and stromal cells. Immunolocation of macrophages demonstrated that these cells contribute part of the epithelial staining for MMP-2 (results not shown). On the other hand, based on the present data, we cannot rule out the participation of MMPs in the first peak at day 3.

MMP-7 has been implicated in the cleavage and liberation of the FAS ligand (FAS-L), which would result in the induction of apoptosis of the epithelial cells (Powell et al., 1996); this was associated with a change in the vectorial secretion of the enzyme from the lumen to the basal membrane of the cell (Ilio et al., 2000; Powell et al., 1996, 1999; Felisbino et al., 2007). However, we could not observe either MMP-7 expression or activation in association with the apoptotic peak on the 3rd day after apoptosis. The reason for this discrepancy might be the inherent differences between mice and rats. Another possibility is that the MMP-7 knockout mice used to show that the absence of MMP-7 results in diminished apoptosis at day 3 after castration might have an intrinsically reduced rate of apoptosis. Because no apoptosis rates were estimated for the non-castrated mice, this possibility should be examined further in the future. However, the opposite was true for the apoptosis peak at day 11, when MMP-7 activation reached a marked peak.

It is not possible to ascertain at the moment whether these enzymes are involved with extracellular-matrix remodelling to accommodate a progressively smaller volume of the epithelium, which was demonstrated earlier to be associated with the pleated and folded basement membrane (Carvalho & Line, 1996), or whether their activity would result in the activation of a paracrine mechanism responsible for causing epithelial cells to undergo apoptosis, such as the liberation of growth factors or cryptic signals from the extracellular matrix. The existence of a paracrine mechanism was proposed for the induction of apoptosis in epithelial cells in the context of androgen deprivation, because epithelial cells lacking androgen receptors also underwent apoptosis in chimeric-tissue experiments (Kurita et al., 2001). However, this consideration should be placed in the context of the findings presented here. It is consistent that epithelial apoptosis after the first peak at the third day after castration does not result directly from the drop in androgen levels, because the additional peaks after castration occur long after the levels of testosterone and dihydrotestorene fall below the level of detection (Kashiwagi et al., 2005). It is possible that basement-membrane degradation, by the action of MMP-2, MMP-7 and MMP-9, results in epithelial-cell anoikis which triggers apoptosis, as has been suggested for the mammary-gland regression (Lund et al., 1996). Because pharmacological blocking of MMP activity by any of the compounds employed here (hydrocortisone, doxycyclin, and GM6001) did not result in complete inhibition of epithelial-cell apoptosis, other superimposing mechanisms responsible for matrix degradation or for inducing apoptosis may contribute to the death of epithelial cells.

In conclusion, to the best of our knowledge, this is the first study to report (i) the existence of multiple apoptotic waves in the regressing VP; (ii) the dependence on extracellular-matrix remodelling for regressive changes to progress after the first week after castration; and (iii) the causal relationship between MMP activity and the day-11 apoptosis peak. These observations will certainly have an impact on the methodological approaches for studying prostate regression, as well as on the use of androgen-deprivation therapies.

Acknowledgements

Supporting Information

Additional Supporting Infomation may be found in the online version of this article:

Figure S1 Daily variation in prostatic weight (percentage reduction within a 24-h interval). Maximum reduction was achieved at day 7, followed by marked reductions at days 4 and 11 (arrowheads). Weight gain was observed at day 1 and 10. Ct = control.

Figure S2 Representative microscope images of a Feulgen-stained section of the VP 3 days after castration. Arrows indicate fragmented nuclei with compact chromatin. (B) Representative microscope image of TUNEL-positive nuclei in the epithelium of the VP 3 days after castration. Arrows indicate TUNEL-positive nuclei. A and B, scale bar = 20 μm.
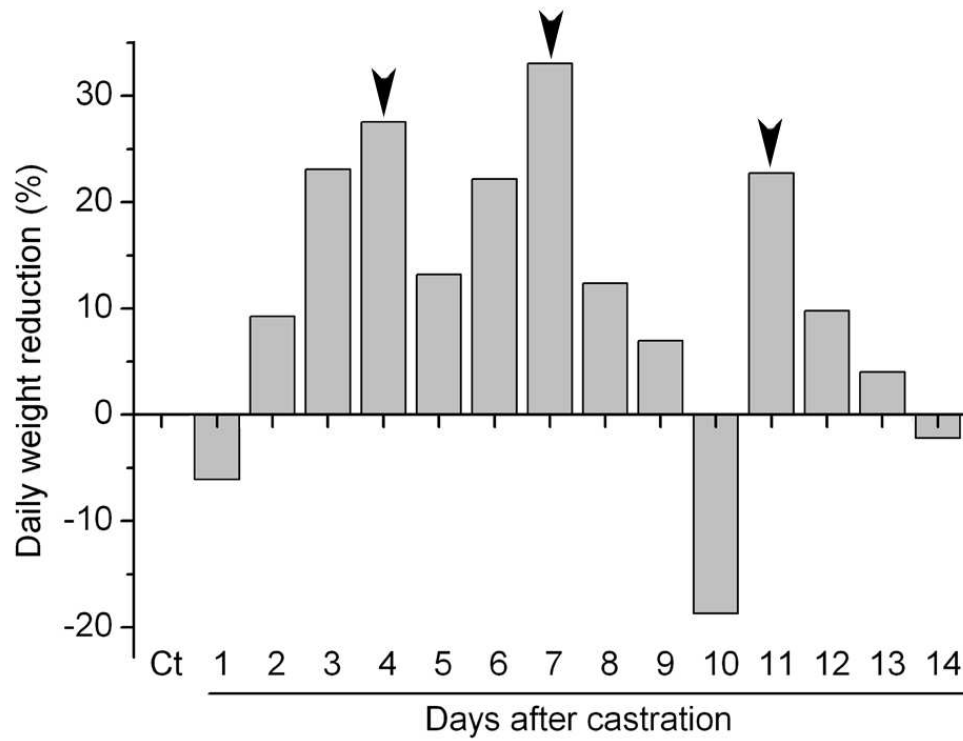
Figure S3 (A) Representative WB for caspase-3 in extracts from the rat VP before and after castration, indicating the uncleaved inactive band. (B) Quantification of the WB for caspase-3. There was an increase in the content of caspase-3 after castration, centred at days 6–8.

Please note: Wiley-Blackwell are not responsible for the content or functionality of any supporting materials supplied by the authors. Any queries (other than missing material) should be directed to the corresponding author for the article.

References

Antonioli, E., Della-Colleta, H. H. & Carvalho, H. F. (2004) Smooth muscle cell behavior in the ventral prostate of castrated rats. *Journal of Andrology* 25, 50–56.

Antonioli, E., Cardoso, A. B. & Carvalho, H. F. (2007) Effects of long-term castration on the smooth muscle cell phenotype of the rat ventral prostate. *Journal of Andrology* 28, 777–783.

Augusto, T. M., Felisbino, S. L. & Carvalho, H. F. (2008) Remodeling of rat ventral prostate after castration involves heparanase-1. *Cell and Tissue Research* 332, 307–315.

Carvalho, H. F. & Line, S. R. (1996) Basement membrane associated changes in the rat ventral prostate following castration. *Cell Biology International* 20, 809–819.

Carvalho, H. F., Taboga, S. R. & Vilamaior, P. S. (1997) Collagen type VI is a component of the extracellular matrix microfibril network of the prostatic stroma. *Tissue and Cell* 29, 163–170.

Feldman, B. J. & Feldman, D. (2001) The development of androgen-independent prostate cancer. *Nature Reviews Cancer* 1, 34–45.

Felisbino, S. L., Justulin, L. A. Jr, Carvalho, H. F. & Taboga, S. R. (2007) Epithelial-stromal transition of MMP-7 immunolocalization in the rat ventral prostate following bilateral orchiectomy. *Cell Biology International* 31, 1173–1178.

Garcia-Flórez, M., Oliveira, C. A. & Carvalho, H. F. (2005) Early effects of estrogen on the rat ventral prostate. *Brazilian Journal of Medical and Biological Research* 38, 487–497.

Gupta, G. P., Nguyen, D. X., Chiang, A. C., Bos, P. D., Kim, J. Y., Nadal, C., Gomis, R. R., Manova-Todorova, K. & Massagué, J. (2007) Mediators of vascular remodelling co-opted for sequential steps in lung metastasis. *Nature* 446, 765–770.

Ilio, K. Y., Nemeth, J. A., Sensibar, J. A., Lang, S. & Lee, C. (2000) Prostatic ductal system in rats: changes in regional distribution of extracellular matrix proteins during castration-induced regression. *Prostate* 43, 3–10.

Isaacs, J. T. (1984) Antagonistic effect of androgen on prostatic cell death. *Prostate* 5, 545–557.

Isaacs, J. T., Furuya, Y. & Berges, R. (1994) The role of androgen in the regulation of programmed cell death/apoptosis in normal and malignant prostatic tissue. *Seminars in Cancer Biology* 5, 391–400.

Jin, R. J., Lho, Y., Connelly, L., Wang, Y., Yu, X., Saint Jean, L. *et al.* (2008) The nuclear factor-κB pathway controls the progression of prostate cancer to androgen-independent growth. *Cancer Research* 68, 6762–6769.

Kashiwagi, B., Shibata, Y., Ono, Y., Suzuki, R., Honma, S. & Suzuki, K. (2005) Changes in testosterone and dihydrotestosterone levels in male rat accessory sex organs, serum, and seminal fluid after castration: establishment of a new highly sensitive simultaneous androgen measurement method. *Journal of Andrology* 26, 586–591.

Kerr, J. F. R. & Searle, J. W. (1973) Deletion of cells by apoptosis during castration-induced involution of the rat prostate. *Virchows Archives (Cell Pathology)*, 13, 87–102.

Kurita, T., Wang, Y. Z., Donjacour, A. A., Zhao, C., Lydon, J. P., O'Malley, B. V., Isaacs, J. T., Dahiya, T. & Cunha, G. R. (2001) Paracrine regulation of apoptosis by steroid hormones in the male and female reproductive systems. *Cell Death Differentiation* 8, 192–200.

Kyprianou, N. & Isaacs, J. T. (1988) Activation of programmed cell death in the rat ventral prostate after castration. *Endocrinology* 122, 552–562.

Lekås, E., Johansson, M., Widmark, A., Bergh, A. & Amber, J.-E. (1997) Decrement of blood flow precedes the involution of the rat ventral prostate in the rat after castration. *Urology Research* 25, 309–314.

Lesser, B. & Bruchovsky, N. (1974) Effect of duration of the period after castration on the response of the rat ventral prostate to androgens. *Biochemical Journal* 149, 429–431.

Lipton, S. A. & Bossy-Wetzel, E. (2002) Dueling activities of AIF in cell death versus survival: DNA binding and redox activity. *Cell* 111, 147–150.

Lund, L. R., Rømer, J., Thomasset, N., Solberg, H., Pyke, C., Bissell, M. J., Danø, K. & Werb, Z. (1996) Two distinct phases of apoptosis in mammary gland involution: proteinase-independent and -dependent pathways. *Development* 122, 181–193.

Mignatti, P. & Rifkin, D. B. (1993) Biology and biochemistry of proteinases in tumor invasion. *Physiological Reviews* 73, 161–195.

Powell, W. C., Domann, F. E. Jr, Mitchen, J. M., Matrisian, L. M., Nagle, R. B. & Bowden, G. T. (1996) Matrilysin expression in the involuting rat ventral prostate. *Prostate* 29, 159–168.

Powell, W. C., Fingleton, B., Wilson, C. L., Boothby, M. & Matrisian, L. M. (1999) The metalloproteinase matrilysin proteolytically generates active soluble Fas ligand and potentiates epithelial cell apoptosis. *Current Biology* 9, 1441–1447.

Rouleau, M., Léger, J. & Tenniswood, M. (1990) Ductal heterogeneity of cytokeratins, gene expression, and cell death in the rat ventral prostate. *Molecular Endocrinology* 4, 2003–2013.

Saikali, Z. & Singh, G. (2003) Doxycycline and other tetracyclines in the treatment of bone metastasis. *Anti-Cancer Drugs* 14, 773–778.

Sandford, N. L., Searle, J. W. & Kerr, J. F. R. (1984) Successive waves of apoptosis in the rat prostate after repeated withdrawal of testosterone stimulation. *Pathology* 16, 406–410.

Shabsigh, A., Chang, D. T., Heitjan, D. F., Kiss, A., Olsson, C. A., Puchner, P. J. & Buttyan, R. (1998) Rapid reduction in blood flow to the rat ventral prostate gland after castration: preliminary evidence that androgens influence prostate size by regulating blood flow to the prostate gland and prostatic endothelial cell survival. *Prostate* 36, 201–206.

Shabsigh, A., Ghafar, M. A., de la Taille, A., Burchardt, M., Kaplan, S. A., Anastasiadis, A. G. & Buttyan, R. (2001) Biomarker analysis demonstrates a hypoxic environment in the castrated rat ventral prostate gland. *Journal of Cellular Biochemistry* 81, 437–444.

Trougakos, I. P. & Gonos, E. S. (2002) Clusterin/apolipoprotein J in human aging and cancer. *International Journal of Biochemistry and Cell Biology* 34, 1430–1448.

Vilamaior, P. S. L., Felisbino, S. L., Taboga, S. R. & Carvalho, H. F. (2000) Collagen fiber reorganization in the rat ventral prostate following androgen deprivation: a possible role for smooth muscle cells. *Prostate* 45, 253–258.

Vollmer, G., Michna, H., Ebert, K. & Knuppen, R. (1994) Androgen ablation induces tenascin expression in the rat prostate. *Prostate* 25, 81–90.

Zhang, W., Zhang, C., Narayani, N., Du, C. & Balaji, K. C. (2007) Nuclear translocation of apoptosis inducing factor is associated with cisplatin induced apoptosis in LNCaP prostate cancer cells. *Cancer Letters* 255, 127–134.

1
2
3
4
5
6
7
8
9
10
11
12
13
14
15
16
17
18
19
20
21
22
23
24
25
26
27
28
29
30
31
32
33
34
35
36
37
38
39
40
41
42
43
44
45
46
47
48
49
50
51
52
53
54
55
56
57
58
59
60

Daily variation in prostate weight after castration. Major points of weight loss and episodes of weigh gain are noted
80x60mm (300 x 300 DPI)
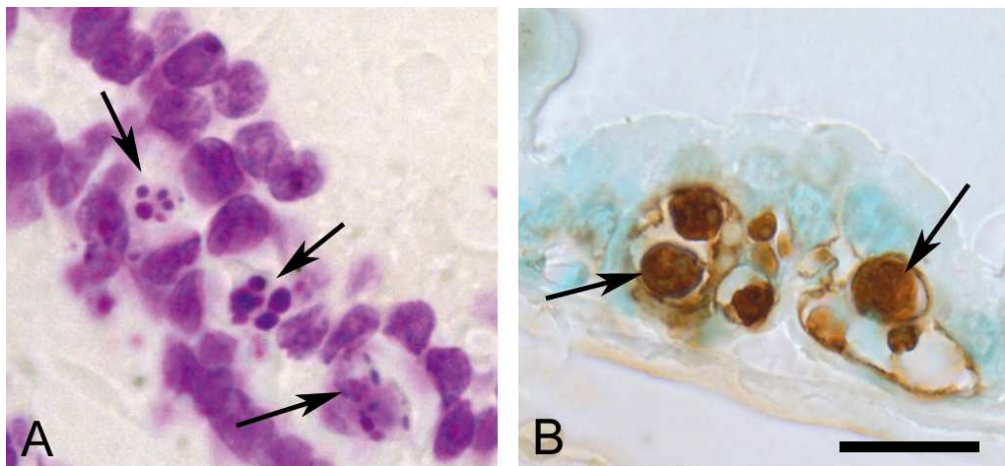
Apoptotic epithelial cells were identified by the characteristic morphology of their nuclei after Feulgen staining or by the presence of fragmented DNA, as indicated by TUNEL reaction.
86x39mm (300 x 300 DPI)
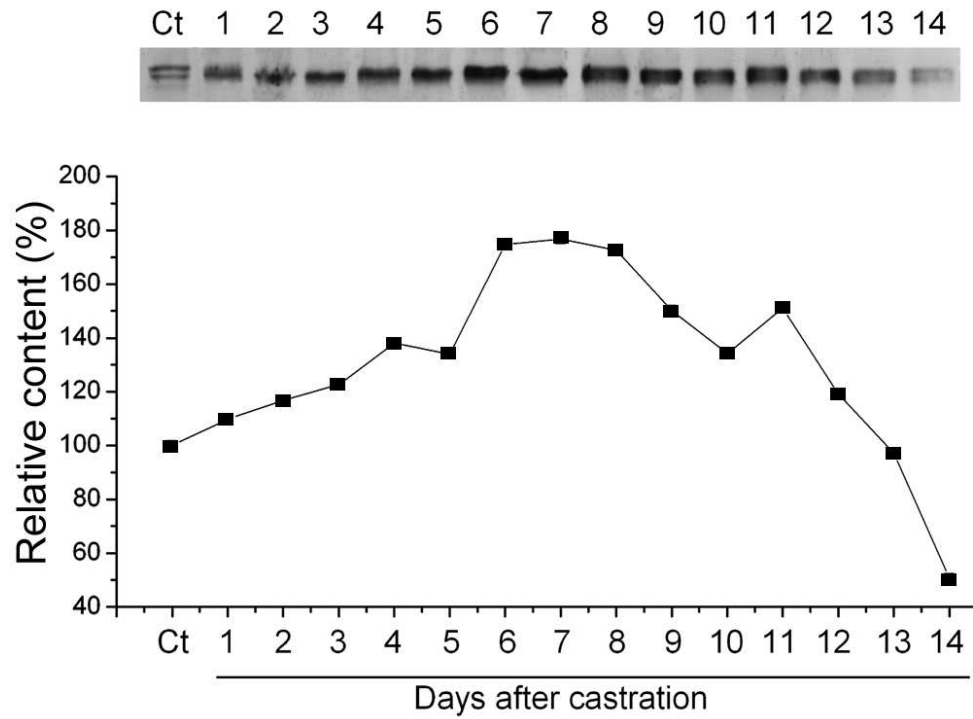
Caspase-3 accumulates in the rat VP after castration, with an increase centered on days 6-8.
87x64mm (300 x 300 DPI)

4. DISCUSSÃO

No presente trabalho, foram investigados o papel da MMP-2 durante as primeiras fases do desenvolvimento prostático pós-natal em roedores e o envolvimento das MMP-2, -7 e -9 na regressão prostática após a castração cirúrgica. Utilizando-se de diversas metodologias de biologia celular e de bioquímica, demonstrou-se que a MMP-2 contribui para a morfogênese epitelial da PV de ratos e camundongos, e que a progressiva regressão da PV de ratos pós-castração cirúrgica é dependente de remodelação estromal associada à atividade de MMPs.

A degradação da matriz extracelular e a remodelação tecidual são necessárias para a criação de espaços que permitem o crescimento e a invasão de tecidos em desenvolvimento ou tumorais (VanSaun e Matrisian, 2006; Page-McCaw *et al*., 2007). As proteinases em geral e as MMPs em particular têm um papel essencial nesses processos. A morfogênese da PV de roedores é caracterizada por eventos dinâmicos, tais como crescimento epitelial, ramificação e canalização das estruturas epiteliais (Sugimura *et al*., 1986a; Sugimura *et al*., 1986b; Hayward *et al*., 1996; Bruni-Cardoso *et al*., 2007), que necessitam de remodelação estromal e, conseqüentemente, da atividade de MMPs. Além disso, a maioria desses eventos é completada até a terceira semana após o nascimento (Hayashi *et al*., 1991; Vilamaior *et al*., 2006; Huang *et al*., 2005; Pu *et al*., 2004, Bruni-Cardoso e Carvalho, 2007). Nesse contexto, o papel da MMP-2 na morfogênese da PV de roedores foi investigado, inibindo-se a expressão e atividade dessa enzima na PV de ratos em cultura de órgão ou utilizando-se de uma linhagem de camundongo nocaute para MMP-2 (MMP-2$^{-/-}$). Esses estudos demonstraram pela primeira vez que a MMP-2 é essencial para o desenvolvimento normal da PV, no que diz respeito à proliferação de células epiteliais, ramificação epitelial, assim como na sua organização tecidual e acúmulo de fibras colagênicas.

Vários trabalhos documentaram o envolvimento de MMPs no desenvolvimento de órgãos ramificados, tais como rim (Lelongt *et al*., 1997), glândula mamária (Wiseman e Werb, 2002), pulmão (Kheradmand *et al*., 2002), e glândula salivar submandibular (Steinberg *et al*., 2005). Camundongos MMP-2$^{-/-}$ apresentam reduzido tamanho corporal, reduzida neovascularização (Kato et., 2001), diminuída invasão ductal primária na glândula mamária (Wiseman *et al*., 2003), e

reduzido desenvolvimento sacular dos pulmões (Kheradmand *et al*., 2002). Nosso grupo mostrou recentemente que as atividades de MMP-2 e -9 são mais altas e localizadas no epitélio e na interface epitélio/estroma na PV de ratos durante a primeira semana pós-natal, e sugeriu que a atividade gelatinolítica destas enzimas estaria correlacionada com a remodelação da MEC necessária para morfogênese da PV, especificamente permitindo o crescimento e projeção das estruturas epiteliais em direção ao estroma adjacente (Bruni-Cardoso *et al*.,2008).

No presente trabalho, encontrou-se que a inibição de MMPs com 20 μM de GM6001 prejudicou de forma significativa o crescimento e morfogênese da próstata ventral de ratos até o dia 2 em cultura. A despeito de ter mostrado um efeito de dose-dependência, o tratamento com o GM6001 não afetou significativamente o desenvolvimento da PV nos estágios mais tardios. Considerando-se o fato de GM6001 ser um inibidor de amplo espectro, é possível que a atividade de algumas MMPs possa ter um efeito inibitório na morfogênese da glândula e que o bloqueio dessas enzimas possa contribuir para o crescimento. Sabe-se que alguns componentes da MEC promovem a ramificação epitelial, tais como a tenascina no pulmão (Gebb e Jones, 2003) e o colágeno tipo III na glândula salivar (Nakanishi *et al*., 1998). De modo que o efeito inibitório seria manifestado através da degradação em excesso de componentes da MEC que poderiam contribuir para o desenvolvimento do órgão.

O papel da MMP-2 na morfogênese da PV foi analisado com o emprego do "small interference" RNA (siRNA) específico para MMP-2 com o uso de controles apropriados (somente o agente de transfecção, lipofectamina, ou siRNA específico para GFP). O silenciamento pós-transcricional da MMP-2 com siRNA foi altamente eficiente, alcançando 90% de redução da quantidade de RNAm (conforme demonstrado por RT-PCR quantitativo) e aproximadamente 60% da atividade de MMP-2 (conforme demonstrado por zimografia). Provavelmente, a discrepância entre essas porcentagens seja resultado da estabilidade da proteína MMP-2 no ambiente extracelular. O silenciamento da MMP-2 reduziu o crescimento do órgão (dia 6) e comprometeu a morfogênese prostática durante o período experimental. Conforme avaliação histológica, as PVs desenvolvidas *in vitro* apresentaram arquitetura semelhante às desenvolvidas *in vivo* (Bruni-Cardoso & Carvalho, 2007; Bruni-Cardoso *et al*., 2008). Células apoptóticas foram encontradas no epitélio em canalização. Embora tenham apresentado células apoptóticas, não houve formação do

lúmen no grupo siMMP-2, indicando que em adição a criação de espaços em conseqüência da deleção de células epiteliais, a expansão e consolidação do lúmen requer atividade de MMP-2 na periferia das estruturas epiteliais. Este resultado é consistente com a atividade gelatinolítica e a localização da MMP-2 não somente nas estruturas epiteliais distais, mas também na base do epitélio ao longo das estruturas epiteliais (Bruni-Cardoso *et al*., 2008).

A despeito dos resultados *in vitro* mostrarem que a atividade de MMP-2 e a conseqüente remodelação da matriz sejam necessárias para a morfogênese da PV, havia a necessidade de uma avaliação mais sistêmica desta hipótese. Portanto, decidiu-se examinar o papel da MMP-2 no desenvolvimento prostático *in vivo*, utilizando-se a linhagem de camundongo MMP-2$^{-/-}$ como modelo biológico.

Assim como demonstrado para ratos, a MMP-2 foi encontrada tanto no estroma como no epitélio da PV do camundongo selvagem no dia 6. No epitélio, a MMP-2 foi concentrada nas estruturas epiteliais distais. Como resultado da ausência de MMP-2, encontrou-se um menor número de extremidades distais ("tips"), uma taxa reduzida de proliferação de células epiteliais, um maior acúmulo de fibras reticulares ao redor do epitélio, sugerindo que a MMP-2 contribua para a ramificação epitelial, através da remodelação de algumas proteínas da MEC. Portanto, esse processo criaria espaços para a bifurcação e elongação das estruturas epiteliais e influenciaria na proliferação das células epiteliais

Os camundongos MMP-2$^{-/-}$ adultos apresentaram um menor peso da PV e reduzido volume do epitélio e das células musculares lisas (CML). O epitélio e as CML exercem função crucial na fisiologia prostática. As células epiteliais luminais são responsáveis pela atividade secretora da glândula, enquanto as CML ajudam a eliminar a secreção acumulada no lúmen no momento da ejaculação (McNeal *et al*., 1988). Além disso, há a sinalização parácrina entre esses dois tipos celulares que é essencial em todos os estágios do desenvolvimento e homeostase da glândula (Cunha e Chung, 1981). Essas interações devem estar comprometidas no camundongo MMP-2$^{-/-}$, devido ao espessamento da membrana basal que normalmente atua como uma barreira química e fisiológica entre o epitélio e as CML.

Tanto a taxa de proliferação como a de morte celular não foram afetadas nos camundongos MMP-2$^{-/-}$ adultos, indicando então, que o menor tamanho da PV nesses animais seja conseqüência da reduzida taxa de proliferação celular e morfogênese alterada durante a primeira semana de desenvolvimento pós-natal.

No geral, as MMPs são reguladas em nível transcricional por uma ampla variedade de fatores de crescimento e citocinas (Qin *et al*., 1999). Entretanto, mecanismos pós-transcricionais também contribuem para essa regulação (Borden e Heller *et al*., 1997). A expressão de MMP-2 é constitutiva, no entanto, as concentrações dessa enzima podem variar durante o desenvolvimento, inflamação e progressão tumoral (Qin *et al*., 1999).

A próstata de roedores apresenta três fases principais de crescimento. Depois da fase inicial no estágio embrionário, um crescimento acentuado ocorre no início da vida pós-natal em resposta a um pico de testosterona (Corbier *et al*., 1992). Nós acreditamos que as altas concentrações de testosterona nesse período possam influenciar a expressão de MMPs, especialmente MMP-2. Nesse contexto, Liao *et al*., (2003) demonstraram que a testosterona regula a expressão de MMP-2 em células LNCaP e LAPC-4 de uma maneira dose-dependente. Além disso, há um elemento responsivo ao andrógeno (ARE) no promotor do gene da MMP-2 (Li *et al*., 2007), indicando que a expressão de MMP-2 possa ser regulada por andrógenos durante o desenvolvimento da próstata. De forma contraditória, tanto a MMP-2 como as MMP-7 e -9, de acordo com os resultados aqui apresentados e com estudos anteriores (Limaye *et al*., 2008), tiveram a sua expressão e atividade aumentadas em um ambiente privado de andrógenos, sugerindo que a regulação daexpressão das MMPs por andrógenos, particularmente a MMP-2, seja realizada de uma forma complexa e dependa do modelo utilizado.

Ao contrário do que ocorre nos camundongos selvagens, a PV de animais MMP-2$^{-/-}$ adultos apresentou a expressão de MMP-9 conforme demonstrado por imunohistoquímica, o que sugere que a ausência da MMP-2 seja compensada por essa enzima ou até mesmo por outras proteinases nesse modelo. Entretanto, a presença da MMP-9 nos animais deficientes em MMP-2 não foi suficiente para suprimir as alterações causadas pela ausência da MMP-2. De forma interessante, a quantidade de RNAm de MMP-9, conforme detectados em experimento de RT-PCR em tempo

real, não foi aumentado após a inibição de MMP-2 por siRNA em cultura de PV neonatal. Esse efeito não compensatório pode ser explicado pelo curto período experimental, o que difere do modelo "knockout", onde os animais têm a MMP-2 ausente desde o início do desenvolvimento embrionário.

Há a possibilidade de que as MMPs não somente contribuam para a degradação de componentes da MEC, mas também na clivagem específica de proteínas que poderia produzir neoepítopos contidos na MEC e prover informações para as células epiteliais. Como exemplo, na glândula salivar submandibular, a atividade MT2-MMP resulta na liberação do fragmento NC1 do colágeno IV. Esse fragmento possui uma interessante atividade biológica, regulando o comportamento celular e, em particular, a angiogênese (Rebustini *et al*., 2009).

Utilizando-se de uma combinação de análise morfológica e bioquímica associada com intervenção farmacêutica, foi identificado no presente trabalho, uma segunda onda de apoptose na regressão da PV em resposta à castração cirúrgica, que é dependente de degradação da MEC, demonstrando que a remodelação da MEC é um pré-requisito para a deleção das células epiteliais.

A próstata é altamente dependente de andrógenos para seu desenvolvimento, crescimento e funcionamento, e a castração leva a uma ativa e progressiva regressão da glândula (Isaacs, 1984; Kyprianou & Isaacs, 1988; Isaacs *et al*., 1994). Análises de privação androgênica de longa duração (100 dias) mostraram que o órgão regride a aproximadamente 5% do peso da próstata de animais controle (Antonioli *et al*., 2007). A redução de peso observada dentro da primeira semana pós-castração resulta da eliminação secreção, a redução das organelas de síntese, tais como o reticulo endoplasmático, complexo de Golgi e vesículas de secreção, reduzido fluxo sanguíneo e extensiva deleção de células epiteliais por apoptose. De forma inesperada, ganhos de peso ocorreram nos dias 1 e 10 depois da castração. Foi relatado anteriormente que a permeabilidade aumentada dos vasos sanguíneos resulta em extravasamento vascular e que isso poderia resultar no ganho de peso observado 1 dia após a cirurgia. O aumento da permeabilidade vascular resulta da deleção de células endoteliais, que é um dos primeiros eventos após a castração (Shabsigh *et al*., 1998). Ainda é necessário investigar se há mudanças vasculares similares às que ocorrem no estágio

inicial da castração e se elas seriam responsáveis pelo ganho de peso no dia 10. É importante ressaltar que esses ganhos de peso precedem os picos de apoptose de células epiteliais.

Por estender o período de análise para 14 dias, pôde-se identificar dois picos extras de apoptose nos dia 7 e 11 com o uso das técnicas de Feulgen e TUNEL. Ambas as metodologias mostraram cinética idêntica de morte celular, demonstrando que a identificação precisa de núcleos apoptóticos pode gerar boas estimativas de índices de morte celular, ao menos para PV, confirmando resultados publicados pelo nosso grupo (Garcia-Florez *et al.*, 2005). Esses resultados demonstraram que a regressão prostática após a castração cirúrgica resulta de múltiplas ondas de apoptose.

No presente trabalho foi demonstrado que a atividade de caspase-3 e a translocação de AIF ("apoptosis-inducing factor") para o núcleo são eventos compartilhados pelos picos de apoptose nos dias 3 e 11. Ambos os eventos estão relacionadas à indução de apoptose, entretanto representam vias dependente e independente de caspase respectivamente. A translocação do AIF para o núcleo é um mecanismo associado à indução de apoptose em células LNCaP como resposta ao tratamento com a cisplatina (Zhang *et al.*, 2007). A identificação de outros componentes que participam na via de morte celular em cada um dos picos de apoptose está em curso no nosso laboratório.

Sabe-se que a expressão de clusterina é diretamente correlacionada com a privação androgênica. Essa molécula foi primeiramente descrita como TRPM-2 ("Testosterone-Repressed Prostate Message"-2), por ser fortemente induzida na PV de animais castrados (Buttyan *et al.*, 1989). Ela é também envolvida com a regressão da glândula mamária. (Lund *et al.*, 1996). Embora o presente estudo tenha demonstrado que o conteúdo de clusterina é aumentado na regressão prostática, não foi encontrada uma associação direta entre a cinética de apoptose ou mesmo com a ausência de andrógeno. Esse padrão de expressão sugere que a clusterina tenha uma associação temporal, mas aparentemente não causal com a morte celular epitelial, o que reforça a noção de que essa molécula esteja associada com eventos específicos de remodelação tecidual e, mais especificamente, com a transdução de sinal e reparo de DNA (Trougakos & Gonos, 2002). Além disso, nós acreditamos que uma possível função da clusterina na regressão prostática seja a

inibição da resposta inflamatória, controlando o recrutamento de células inflamatórias (macrófagos, linfócitos e mastócitos) com a manutenção da condição não inflamada, talvez por estimular céulas T regulatórias. Essa possibilidade está sendo atualmente investigada no nosso laboratório.

Um estudo anterior de nosso grupo associando castração cirúrgica e a administração de estrógeno demonstrou que, independente da cinética de apoptose dentro da primeira semana pós-castração, a regressão máxima do epitélio era aproximadamente a mesma (24% do peso original) (Garcia-Flórez *et al.*, 2005). Isso nos levou a hipotetizar que alterações no estroma ocorreriam no sentido de permitir a regressão adicional do epitélio. De fato, a regressão da glândula mamária após o desmame envolve uma segunda onda de apoptose que é dependente da produção estromal (por fibroblastos) de enzimas que degradam MEC, particularmente MMP-2 e -9. Ainda nesse modelo, o bloqueio da atividade de MMPs por hidrocortisona reduziu a taxa de apoptose e as alterações de regressão da glândula (Lund *et al.,* 1996). Além disso, nosso grupo e outros pesquisadores documentaram mudanças tardias na organização estromal e no conteúdo de componentes da MEC, de expressão da tenascina à reorganização fibrilar e microfibrilar de colágeno (Carvalho *et al.*, 1997; Vilamaior *et al.*, 2000), de variação do heparam sulfato (Augusto *et al.*, 2008) às alterações ultraestruturais na membrana basal (Carvalho & Line, 1996; Ilio *et al.*, 2000).

A PV apresenta a contribuição de ambas as células epiteliais e estromais na produção de MMPs, o que difere da glândula mamária, onde os fibroblastos produzem as MMPs que supostamente degradam a membrana basal. A imunolocalização de macrófagos demonstrou que essas células contribuem parcialmente para marcação imunohistoquímica da MMP-2 (resultados não apresentados). Por outro lado, no presente estudo, não se descarta a participação de MMPs no primeiro pico de apoptose. A MMP-7 é implicada na clivagem e liberação do ligante FAS (FAS-L) na PV de camundongos, o que resulta na indução de apoptose das células epiteliais (Powell *et al.*, 1996); isso foi associado com uma mudança vetorial na secreção dessa enzima, da porção luminal para a porção basal das células epiteliais (Ilio *et al.*, 2000; Powell *et al.*, 1996, 1999; Felisbino *et al.*, 2007). Entretanto, nós não observamos a expressão ou ativação da MMP-7 em associação com o pico de apoptose no 3º dia. A razão para essa discrepância poderia ser inerente a diferenças entre

ratos e camundongos. Outra possibilidade seria o fato do camundongo "knockout" para MMP-7 usado para como modelo da ausência de MMP-7 resultou em diminuída taxa de apoptose no dia 3 após a castração poderia ter uma taxa intrinsecamente reduzida de apoptose. Desde que as quantidades células apoptóticas não foram estimadas para os animais não castrados, essa possibilidade poderia ser analisada no futuro. O oposto foi verdade para o pico de apoptose do dia 11 após a castração, quando a atividade de MMP-7 alcançou um pico. Até o presente momento, não é possível dizer com certeza se essas enzimas estão envolvidas com a remodelação da matriz extracelular para acomodar a regressão epitelial, o qual foi demonstrado previamente ser associada com o pregueamento da membrana basal (Carvalho e Line, 1996), ou se a atividade dessas enzimas resultaria na ativação de mecanismos parácrinos que poderiam levar à apoptose das células epiteliais, tais como a liberação de fatores de crescimento ou sinais crípticos da MEC.

A existência de mecanismos parácrinos foi proposto para a indução de apoptose de células epiteliais num ambiente sem andrógeno após experimentos com tecidos quiméricos (epitélio que não expressa AR recombinado com um mesênquima selvagem), onde células epiteliais que não expressam AR sofreram apoptose num ambiente provado de andrógenos. Contanto, essa consideração deve ser contextualizada frente aos achados do presente trabalho (Kurita *et al*., 2001). É fato que a apoptose de células epiteliais que ocorre após o primeiro pico de apoptose (ao 3º dia após a cirurgia) não resulta diretamente da queda da concentração de andrógeno, isso porque os picos adicionais de apoptose acontecem após um longo tempo de ausência quase que total da testosterona e da diidrotestosterona (Kashiwagi *et al*., 2005). Portanto, é possível que a degradação da membrana basal, pela ação das MMP-2, -7 e -9, resulte de um estado de *anoikis* das células epiteliais que ativaria o processo de apoptose, conforme já sugerido para a regressão da glândula mamária (Lund *et al*., 1996). Estudos em andamento no nosso laboratório indicam que o tratamento com o GM6001 estabiliza a fosforilação da FAK (quinase de adesão focal) na porção basal das células epiteliais, ao contrário do que ocorre com a PV dos animais não tratados com a droga, indicando que as MMPs possam afetar a interação entre as células epiteliais e a MEC, comprometendo assim, a adesão celular.

O bloqueio da atividade de MMPs pelos inibidores farmacológicos empregados aqui (hidrocortisona, doxiciclina, e GM6001) não ocasionaram a completa inibição da apoptose de

células epiteliais, sugerindo que outros mecanismos celulares possam atuar no processo de apoptose das células epiteliais. Dentre esses, temos evidências da participação da heparanase (Augusto *et al.,* em preparação)

Apesar de distintos, os modelos de desenvolvimento prostático e regressão prostática compartilham diversas características. Ambos os modelos apresentam dinamismo nas mudanças fenotípicas e no comportamento celular (proliferação e diferenciação celular durante o desenvolvimento e atrofia e morte celular durante a regressão) e também intensa remodelação da MEC. De acordo com os resultados apresentados no presente trabalho, conclui-se que as MMPs exercem papel crucial tanto no crescimento como na regressão da PV.

5. CONCLUSÕES

a. A MMP-2 exerce um importante papel no crescimento epitelial e morfogênese da próstata ventral de roedores;

b. A inibição da MMP-2 por siRNA compromete o crescimento, ramificação, formação de lúmen e a proliferação de células epiteliais da PV de ratos *in vitro*, ao menos em parte devido à estabilização da matriz colagênica;

c. A PV do camundongo "knockout" para MMP-2 apresenta peso relativo reduzido e alterações estruturais decorrentes de menor proliferação epitelial, menor ramificação ductal e acúmulo da matriz colagênica no período neonatal;

d. Na regressão da próstata ventral de ratos após a castração há múltiplas ondas de morte celular e a progressiva regressão prostática que ocorre após a primeira semana depois da castração é dependente da remodelação da matriz extracelular;

e. Há uma relação direta entre a expressão e atividade das MMP-2, -7 e -9 e o pico de apoptose que ocorre 11 dias após a castração.

1. REFERÊNCIAS BIBLIOGRÁFICAS

Aggarwal S, Thareja S, Verma A, Bhardwaj TR, Kumar M (2010) An overview on 5alpha-reductase inhibitors. *Steroids* 75:109-53

Alexander CM, Werb Z (1991) Extracellular Matrix Degradation. *In Hay ED. Cell Biology of the Extracellular Matrix. Plenum Press, New York*. p. 225-302

Alarid ET, Rubin JS, Young P, Chedid M, Ron D, Aaronson SA, Cunha GR (1994) Keratinocyte growth factor functions in epithelial induction during seminal vesicle development. *Proc Natl Acad Sci USA* 91:1074-1088

Altundag O, Altundag K, Gunduz (2004) DNA methilation inhibitor, procainamide, may decrease the tamoxifeno resistance by inducing overexpression of the estrogen receptor beta in breast câncer patients. *Medical Hypotheses* 63:684-687

Andersson S, Berman DM, Jenkins EP, Russell DW (1991) Deletion of steroid 5 alpha-reductase 2 gene in male pseudohermaphroditism. *Nature* 354:159-61

Antonioli E, Della-Colleta, HH, Carvalho HF (2004) Smooth muscle cell behavior in the ventral prostate of castrated rats. *J Androl* 25:50-56

Antonioli E, Bruni-Cardoso A, Carvalho HF (2007) Effects of long-term castration on the smooth muscle cell phenotype of the rat ventral prostate. *J Androl* 28:777-783

Almahbobi G, Hedwards S, Fricout G, Jeulin D, Bertram JF, Risbridger GP (2005) Computer-based detection of neonatal changes to branching morphogenesis reveals different mechanisms of and predicts prostate enlargement in mice haplo-insufficient for bone morphogenetic protein 4. *J Pathol* 206:52–61

Augusto TM, Felisbino SL, Carvalho, HF (2008) Remodeling of rat ventral prostate after castration involves heparanase-1. *Cell Tissue Res* 332:307-315

Augusto TM, Bruni-Cardoso A, Damas-Souza DM, Zambuzzi WF, Kühne F, Lourenço LB, Ferreira CV, Carvalho HF (2009) Oestrogen imprinting causes nuclear changes in eptilhelial cells and overall inhibition of gene transcription and protein synthesis in rat ventral prostate. *Int J Androl* Doi= 10.1111/j.1365-2605.2009.01008.x

Aümuller G (1979) Prostate gland and seminal vesicles. In: Handbuch der mikroskopischen Anatomie des Menschen. Edited by A. Okche and L. Vollrath. *Berlin-Heidelberg-New York: Springer-Verlag* vol. VII/6.p.1

Bhatia-Gaur R, Donjacour AA, Sciavolino PJ, Kim M, Desai N, Young P, Norton CR, Gridley T, Cardiff RD, Cunha GR, Abate-Shen C, Shen MM (1999) Roles for Nkx3.1 in prostate development and cancer. *Genes Dev* 13:966-977

Balbín M, Fueyo A, Tester AM, Pendás AM, Pitiot AS, Astudillo A, Overall CM, Shapiro SD, Lopéz-Otín C (2003) Loss of collagenase-2 confers increased skin tumor susceptibility to male mice. *Nat Genet* 35:252-257

Bagavandoss P (1998) Differential distribution of gelatinases and tissue inhibitor of metalloproteinase-1 in the rat ovary. *J Endocrinol* 158:221-228

Berman DM, Desai N, Wang X, Karhadkar SS, Reynon M, Abate-Shen C, Beachy PA, Shen MM (2004) Roles for Hedgehog signaling in androgen production and prostate ductal morphogenesis. *Dev Biol* 267:387-398

Borden P, Heller RA (1997) Transcriptional control of matrix metalloproteinases and the tissue inhibitors of matrix metalloproteinases. *Crit Rev Eukaryot Gene Ex* 7:159-178

Brown TR, Lubahn DB, Wilson EM, Joseph DR, French FS, Migeon CJ (1988) Deletion of the steroid-binding domain of the human androgen receptor gene in one family with complete androgen insensitivity syndrome: evidence for further genetic heterogeneity in this syndrome. *Proc Natl Acad Sci USA* 85:8151-8155

Bruni-Cardoso A, Carvalho HF (2007) Dynamics of epithelium during canalization of the rat ventral prostate. *Anat Rec* 290:1223-1232

Bruni-Cardoso A, Vilamaior PSL, Taboga SB, Carvalho HF (2008) Localized matrix metalloproteinase (MMP) 2 and MMP-9 activity in the rat ventral prostate during the first week of postnatal development. *Histochem Cell Biol* 129:805-815

Bruni-Cardoso A, Rosa-Ribeiro R, Pascoal VDB, Thomaz AA, Cézar CL, Carvalho HF (2010) MMP-2 Regulates Prostate Development *in vitro. Dev Dyn* 239:737-746

Bruni-Cardoso A, Augusto TA, Pravatta H, Damas-Souza DM, Carvalho HF (2009) Stromal remodeling is required for progressive involution of the rat ventral prostate after castration:

Identification of a matrix metalloproteinase-dependent apoptotic wave. *Int J Androl* DOI=10.1111/j.1365-2605.2009.01004.x

Buttyan R, Olsson CA, Pintar J. Chang C, Bandyk M, Ng PY, Sawczuk IS (1989) Induction of the TRPM-2 gene in cells undergoing programmed death. *Mol Cell Biol* 9:3473-3481

Cancilla B, Jarred RA, Wang H, Mellor SL, Cunha GR, Risbridger GP (2001) Regulation of prostate branching morphogenesis by activin A and follistatin. *Dev Biol* 237:145-58

Carvalho HF, Line SR (1996) Basement membrane associated changes in the rat ventral prostate following castration. *Cell Biol Int* 20:809-819

Carvalho HF, Taboga SR, Vilamaior PSL (1997a) Collagen type VI is a component of the microfibrils of the prostatic stroma. *Tissue Cell* 29:163-170

Carvalho HF, Vilamaior PSL, Taboga SR (1997b).The elastic system of the rat ventral prostate and its modification following orchidectomy. *Prostate* 32:27-34

Chang C, Werb Z. (2001) The many faces of metalloproteases: cell growth, invasion, angiogenesis and metastasis. *Trends Cell Biol* 11:S37-43

Charest NJ, Zhou ZX, Lubahn DB, Olsen KL, Wilson EM, French FS (1991) A frameshift mutation destabilizes androgen receptor messenger RNA in the Tfm mouse. *Mol Endocrinol* 5:573-81

Chuang P-T, McMahon AP (2003) Branching morphogenesis of the lung: new molecular insights into an old problem. *Trends Cell Biol* 13:86- 91

Cook C, Vezina CM, Allgeier SH, Shaw A, Yu M, Peterson RE, Bushman W (2007) Noggin is required for normal lobe patterning and ductal budding in the mouse prostate. *Dev Biol* 312: 217-230

Corbier P, Edwards DA, Roffi J (1992) The neonatal testosterone surge: a comparative study. *Arch Int Physiol Biochim Biophys* 1 100:127-31

Cunha GR, Chung LWK (1981) Stromal-epithelial interactions: I. Induction of prostatic phenotype in urothelium of testicular feminized (Tfm/y) mice. *J Steroid Biochem.* 14:1317-1321

Cunha GR, Donjacour AA, Cooke PS, Mee S, Bigsby RM, Higgins SJ, Sugimura Y (1987) The endocrinology and developmental biology of the prostate. *Endocrinol Rev* 8: 338-362

Cunha GR, Ricke W, Thomson, Marker P, Risbridger G, Hayward SW, Wang YZ, Donjacour AA, Kurita T (2004) Hormonal, cellular, and molecular regulation of normal and neoplastic prostatic development. *J Steroid Biochem Mol Biol* 92:221-236

DeKlerk DP, Coffey DS (1978) Quantitative determination of prostatic epithelial and stromal hyperplasia by a new technique biomorphometrics. *Invest Urol* 16:240-245

Doles J, Cook C, Shi X, Valosky J, Lipinski R, BushmanW (2006) Functional compensation in Hedgehog signaling during mouse prostate development. *Dev Biol* 295:13-25

Donjacour AA, Cunha GR (1988) The effect of androgen deprivation on branching morphogenesis in the mouse prostate. *Dev Biol* 128:1-14

Donjacour AA, Cunha GR (1993) Assessment of prostatic protein secretion in tissue recombinants made of urogenital sinus mesenchyme and urothelium from normal or androgen-insensitive mice. *Endocrinology* 132:2342-50

Donjacour AA, Thomson AA, Cunha, GR (2003) FGF-10 plays na essential role in the growth of the fetal prostate. *Dev Biol* 261:39-54

Economides KD, Capecchi MR (2003) Hoxb13 is required for normal differentiation and secretory function of the ventral prostate. *Development* 130:2061-2069

Esparza J, Kruse M, Lee J, Michaud M, Madri JA (2004) MMP-2 null mice exhibit an early onset and severe experimental autoimmune encephalomyelitis due to an increase in MMP-9 expression and activity. *FASEB J* 18:1682-1691

Feldman BJ, Feldman D (2001) The development of androgen-independent prostate cancer. *Nat Rev Cancer* 1:34-45

Felisbino SL, Justulin LA Jr Carvalho HF, Taboga SR (2007) Epithelial-stromal transition of MMP-7 immunolocalization in the rat ventral prostate following bilateral orchiectomy. *Cell Biol Int* 31:1173-1178

Feng X, Clark RA, Galanakis D, Tonnesen MG (1999) Fibrin and collagen differentially regulate human dermal microvascular endothelial cell integrins: stabilization of alphav/beta3 mRNA by fibrin1. *J Invest Dermatol* 113:913-9

Freeman SN, Rennie PS, Chao J, Lund LR, Andreasen PS (1990) Urokinase- and tissue-type plasminogen activators are suppressed by cortisol in the involuting prostate of castrate rats. *Biochem J* 269:189-193

Freestone SH, Marker P, Grace OC, Tomlinson DC, Cunha GR Harnden P, Thomson AA (2003) Sonic hedgehog regulates prostatic growth and epithelial differentiation. *Dev Biol* 264:352-362

Gao N, Ishii K, Mirosevich J, Kuwajima S, Oppenheimer SR, Roberts RL, Jiang M, Yu X, Shappell SB, Caprioli RM, Stoffel M, Hayward SW, Matusik RJ (2005) Forkhead box A1 regulates prostate ductal morphogenesis and promotes epithelial cell maturation. *Development* 132:3431-3443

García-Flórez M, Oliveira CA, Carvalho HF (2005) Early effects of estrogen on the rat ventral prostate. *Braz J Med Biol Res* 38:487-497

Gaspar ML, Meo T, Bourgarel P, Guenet JL, Tosi M (1991) A single base deletion in the Tfm androgen receptor gene creates a short-lived messenger RNA that directs internal translation initiation. *Proc Natl Acad Sci USA* 88:8606-10

Gebb SA, Jones PL (2003) Hypoxia and lung branching morphogenesis. *Adv Exp Med Biol* 543:117-125

Gelmann E (2002) Molecular Biology of the Androgen Receptor. *Biol Neoplasia* 20:3001-3015

Giambernardi TA, Grant GM, Taylor GP, Hay RJ, Maher VM, Mccormick JJ, Klebe RJ (1998) Overview of matrix metalloproteinase expression in cultured human cells. *Matrix Biol* 16:483-496

Gordon KJ, Kirkbride KC, How T, Blobel GC (2008) Bone morphogenetic proteins induce pancreatic cancer cell invasiveness through a Smad1-dependent mechanism that involves matrix metalloproteinase protein-2. *Carcinogenesis* 30:238-248

Grant GM, Giambernardi TA, Grant AM, Klebe RJ (1999) Overview of expression of matrix metalloproteinases (MMP-17, MMP-18, and MMP-20) in cultured human cells. *Matrix Biol* 18:145-148

Grishina IB, Kim SY, Ferrara C, Makarenkova HP, Walden PD (2005) BMP7 inhibits branching morphogenesis in the prostate gland and interferes with Notch signaling. *Dev Biol* 288:334-347

Gupta GP, Nguyen D X, Chiang AC, Bos PD, Kim JY, Nadal C, Gomis RR, Manova-Todorova K, Massagué J (2007) Mediators of vascular remodelling co-opted for sequential steps in lung metastasis. *Nature* 446:765-770

Hannas AR, Pereira JC, Granjeiro JM, Tjäderhane L(2007) The role of matrix metalloproteinases in the oral environment. *Acta Odontol Scand* 65:1-13

Hashimoto K, Kihira Y, Matuo Y, Usui T (1998) Expression of matrix metalloproteinase-7 and tissue inhibitor of metalloproteinase-1 in human prostate. *J Urol* 160:1872-19876

Haraguchi R, Mo R, Hui C, Motoyama J, Makino S, Shiroishi T, Gaffield W, Yamada G (2001) Unique functions of Sonic hedgehog signaling during external genitalia development. *Development* 128:4241-425

Hayward SW, Baskin LS, Haughney PC, Cunha AR, Foster BA, Dahiya R, Prins GS, Cunha GR (1996a) Epithelial development in the rat ventral prostate, anterior prostate and seminal vesicle. *Acta Anat (Basel)* 155:81-93

Hayward SW, Baskin LS, Haughney PC, Foster BA, Cunha AR, Dahiya R, Prins GS, Cunha GR (1996b) Stromal development in the ventral prostate, anterior prostate and seminal vesicle of the rat. *Acta Anat (Basel)* 155:94-103

Hayward SW, Rosen MA, Cunha GR (1997) Stromal-epithelial interactions in the normal and neoplastic prostate. *Br J Urol* 79:18-26

He WW, Kumar MV, Tindall DJ (1991) A frame-shift mutation in the androgen receptor gene causes complete androgen insensitivity in the testicular-feminized mouse. *Nucleic Acids Res* 19:2373-2378

Heikinheimo K, Salo T (1995) Expression of basement membrane type IV collagen and type IV collagenases (MMP-2 and MMP-9) in human fetal teeth. *J Dent Res* 74:1226-1234

Huang L, Pu Y, Alam S, Birch L, Prins GS (2004) Estrogenic regulation of signaling pathways and homeobox genes during rat prostate development. *J Androl* 25:330-337

Huang L, Pu Y, Alam S, Birch L, Prins GS (2005) The role of Fgf10 signaling in branching morphogenesis and gene expression of the rat prostate gland: lobe-specific suppression by neonatal estrogens. *Dev Biol* 278:396–414

Huang L, Pu Y, Hu WY, Birch L, Luccio-Camelo D, Yamaguchi T, Prins GS (2009) The role of Wnt5a in prostate gland development. *Dev Biol* 328:188-199

Huttunen E, Romppanen T, Helminen HJ (1981) A histoquantitative study on the effects of castration on the rat ventral prostate. *J Anat* 132:357-370

Ilio KY, Nemeth JA, Sensibar JA, Lang S, Lee C (2000) Prostatic ductal system in rats: changes in regional distribution of extracellular matrix proteins during castration-induced regression. *Prostate* 43:3-10

Isaacs JT (1984) Antagonistic effect of androgen on prostatic cell death. *Prostate* 5:545-557

Isaacs JT, Furuya Y, Berges R (1994) The role of androgen in the regulation of programmed cell death∕apoptosis in normal and malignant prostatic tissue. *Semins Cancer Biol* 5:91-400

Ishizuya-Oka A, Li Q, Amano T, Damjanovski S, Ueda S, Shy YB (2000) Requirement for matrix metalloproteinase stromelysin-3 in cell migration and apoptosis during tissue remodeling in Xenopus laevis. *J Cell Biol* 150:1177-1188

Itoh N, Patel U, Cupp AS, Skinner MK (1998) Developmental and hormonal regulation of transforming growth factor-beta-1 (TGFbeta1), -2, and -3 gene expression in isolated prostatic epithelial and stromal cells: epidermal growth factor and TGFbeta interactions. *Endocrinology* 139:1378-138

Itoh T, Tanioka M, Yoshida H, Yoshioka T, Nishimoto H, Itohara S (1998) Reduced angiogenesis and tumor progression in gelatinase A-deficient mice. *Cancer Res* 58:1048-1051

Jacobs MN, Dickins M, Lewis DF (2003) Homology modelling of the nuclear receptors: human oestrogen receptorbeta (hERbeta), the human pregnane-X-receptor (PXR), the Ah receptor (AhR) and the constitutive androstane receptor (CAR) ligand binding domains from the human oestrogen receptor alpha (hERalpha) crystal structure, and the human peroxisome proliferator activated receptor alpha (PPARalpha) ligand binding domain from the human PPARgamma crystal structure. *J Steroid Biochem Mol Biol* 84:117-132

Jarred RA, Cancilla B, Prins GS, Thayer KA, Cunha GR, Risbridge GP (2000) evidence that estrogens directly alter androgen-regulated prostate development. *Endocrinology* 141:3471-3478

Jin RJ, Lho Y, Connelly L, Wang Y, Yu X, Saint Jean L Case TC, Ellwood-Yen K, Sawyers CL, Bhowmick NA, Blackwell TS, Yull FE, Matusik RJ (2008) The nuclear factor-κB pathway controls the progression of prostate cancer to androgen-independent growth. *Cancer Research* 68:6762–6769

Joesting MS, Cheever TR, Volzing KG, Yamaguchi TP, Wolf V, Naf D, Rubin JS, Marker PC (2008) Secreted frizzled related protein 1 is a paracrine modulator of epithelial branching morphogenesis, proliferation, and secretory gene expression in the prostate. *Dev Biol* 317:161-73

Kambara T, Oyama T, Segawa A, Fukabori Y, Yoshida KI (2009) Prognostic significance of global grading system of Gleason score in patients with prostate cancer with bone metastasis. *BJU Int* (Epub ahead of print)

Kashiwagi B, Shibata Y, Ono Y, Suzuki R, Honma S, Suzuki K (2005) Changes in testosterone and dihydrotestosterone levels in male rat accessory sex organs, serum, and seminal fluid after castration: establishment of a new highly sensitive simultaneous androgen measurement method. *J Androl* 26:586-591

Kato T, Kure T, Chang J, Gabison EE, Itoh T, Itohara S, Azar DT (2001) Diminished corneal angiogenesis in gelatinase A-deficient mice. *FEBS Lett* 508:187-190

Kerr JFR, Searle JW (1973) Deletion of cells by apoptosis during castration-induced involution of the rat prostate. *Virchows Arch (Cell Path)* 13:87-102

Kheradmand F, Rishi K, Werb Z (2002) Signaling through the EGF receptor controls lung morphogenesis in part by regulating MT1-MMP-mediated activation of gelatinase A/MMP2. *J Cell Sci* 115:839-48

Kim HG, Kassis J, Souto JC, Turner T, Wells A (1999) EGF receptor signaling in prostate morphogenesis and tumorigenesis. *Histol Histopathol* 14:1175-82

Kofoed JA, Houssay AB, Tocci AA, Curbelo HM, Gamper CH (1971) Effects of testosterone on glycosaminoglycans in the prostate, seminal vesicles and salivary glands of the rat. *J Endocrinol* 51:465-471

Kurita T, Wang YZ, Donjacour AA, Zhao C, Lydon JP, O'Malley BW, Isaacs JT, Dahiya R, Cunha GR (2001). Paracrine regulation of apoptosis by steroid hormones in the male and female reproductive system. *Cell Death Differentiation* 8:192-200

Kyprianou N, Isaacs JT (1988) Activation of programmed cell death in the rat ventral prostate after castration. *Endocrinology* 122:552-562

Lamm ML, Podlasek CA, Barnett DH, Lee J, Clemens JQ, Hebner CM, Bushman W (2001) Mesenchymal factor bone morphogenetic protein 4 restricts ductal budding and branching morphogenesis in the developing prostate. *Dev Biol* 232:301-314

Lamm ML, Catbagan WS, Laciak RJ, Barnett DH, Hebner CM, Gaffield W, Walterhouse D, Iannaccone P, BushmanW (2002) Sonic hedgehog activates mesenchymal Gli1 expression during prostate ductal bud formation. *Dev Biol* 249:349-366

Lee BH, Seo JW, Han YH, Kim YH, Cha SJ. Primary mucinous adenocarcinoma of a seminal vesicle cyst associated with ectopic ureter and ipsilateral renal agenesis: a case report (2007) *Korean J Radiol* 8:258-61

Lee C, Sensibar JA, Dudek SM, Hiipakka RA, Liao S (1990) Prostatic ductal system in rats: Regional variation in morphological and functional activities. *Biol Reprod* 43:1079-1086

Lekås E, Johansson M, Widmark A, Bergh A, Amber JE (1997) Decrement of blood flow precedes the involution of the rat ventral prostate in the rat after castration. *Urol Res* 25:309-314

Lelongt B, Trugnan G, Murphy G, Ronco PM (1997) Matrix metalloproteinases MMP2 and MMP9 are produced in early stages of kidney morphogenesis but only MMP-9 is required for renal organogenesis in vitro. *J Cell Biol* 136:1363-1373

Lesser B, Bruchovsky N (1974) Effect of duration of the period after castration on the response of the rat ventral prostate to androgens. *Biochem J* 149:429-431

Li BY, Liao XB, Fujito A, Thrasher JB, Shen FY, Xu PY (2007) Dual androgen-response elements mediate androgen regulation of MMP-2 expression in prostate cancer cells. *Asian J Androl* 9:41-50

Li J, Al-Azzawi F. Mechanism of androgen receptor action (2009) *Maturitas* 63:142-148

Liao X, Thrasher JB, Pelling J, Holzbeierlein J, Sang QX, Li B (2003) Androgen stimulates matrix metalloproteinase-2 expression in human prostate cancer. *Endocrinology* 144:1656-1663

Limaye AM, Desai KV, Chavalmane AK, Kondaiah P (2008) Regulation of mRNAs encoding MMP-9 and MMP-2, and their inhibitors TIMP-1 and TIMP-2 by androgens in the rat ventral prostate. *Mol Cell Endocrinol* 294:10-8

Lipton SA, Bossy-Wetzel E (2002) Dueling activities of AIF in cell death versus survival: DNA binding and redox activity. *Cell* 111:147-150

Llano E, Pendas AM, Knauper V, Sorsa T, Salo T, Salido E, Murphy G, Simmer JP, Bartlett JD, Lopez-Otin C (1997) Identification and structural and functional characterization of human enamelysin (MMP-20) *Biochemistry* 36:15101-15108

Lohi J, Lehti K, Valtanen H, Parks WC, Keski-Oja J (2000) Structural analysis and promoter characterization of the human membrane-type matrix metalloproteinase-1 (MT1-MMP) gene. *Gene*. 242:75-86

Lopes ES, Foster BA, Donjacour AA, Cunha GR (1996) Initiation of secretory activity of rat prostatic epithelium in organ culture. *Endocrinology* 137:4225-4234

Lubahn DB, Tan JA, Quarmby VE, Sar M, Joseph DR, French FS, Wilson EM (1989) Structural analysis of the human and rat androgen receptors and expression in male reproductive tract tissues. *Ann N Y Acad Sci* 564:48-56

Lund LR, Rømer J, Thomasset N, Solberg H, Pyke C, Bissell MJ, Danø K, Werb Z (1996) Two distinct phases of apoptosis in mammary gland involution: proteinase-independent and -dependent pathways. *Development* 122:181-193

Lynch CC, Hikosaka A, Acuff BH, Martin MD, Kawai N, Singh RK, Vargo-Gogola TC, Begtrup, JL, Peterson TE, Fingleton B, Tomoyuki S, Matrisian LM, Futakuchi, M (2005) MMP-7 promotes prostate cancer-induced osteolysis via the solubilization of RANKL. *Cancer Cell* 7:485-496

Mahendroo MS, Cala KM, Hess DL, Russell DW (2001) Unexpected virilization in male mice lacking steroid 5 alpha-reductase enzymes. *Endocrinology* 142:4652-4662

Marchenko GN, Strongin AY (2001) MMP-28, a new human matrix metalloproteinase with an unusual cysteine-switch sequence is widely expressed in tumors. *Gene* 265:87-93

Matrisian LM (1990) Metalloproteinases and their inhibitors in matrix remodeling. *Trends Genet* 6:121-125

Matrisian, LM, Bowden GT (1990) Stromelysin/transin and tumor progression. *Semin Cancer Biol* 1:107-115

McNeal JE (1980) Anatomy of the prostate: an historical survey of divergent views. *Prostate* 1:3-13

McNeal JE, Stamey TA, Hodge KK (1988) The prostate gland: morphology, pathology, ultrasound anatomy. *Monogr Urol* 9:36-54

McCawley LJ, Crawford HC, King LE Jr, Mudgett J, Matrisian LM (2004) A protective role for matrix metalloproteinase-3 in squamous cell carcinoma. *Cancer Res* 64: 6965-6972

Mignatti P. Rifkin DB (1993) Biology and biochemistry of proteinases in tumor invasion. *Physiol Rev* 73:161–195

Moalli PA, Klingensmith WL, Meyn LA, Zyczynski HM 2002 Regulation of matrix metalloproteinase expression by estrogen in fibroblasts that are derived from the pelvic floor. *Am J Obstet Gynecol* 187:72-79

Mott JD, Werb Z (2004) Regulation of matrix biology by matrix metalloproteinases. *Curr Opin Cell Biol* 16:558-564

Nagakawa O, Murakami K, Yamaura T, Fujiuchi Y, Murata J, Fuse H, Saiki I (2000) Expression of membrane-type 1 matrix metalloproteinase (MT1-MMP) on prostate cancer cell lines. *Cancer Lett* 155:73-179

Nakanishi Y, Nogawa H, Hashimoto Y, Kishi J, Hayakawa T (1988) Accumulation of collagen III at the cleft points of developing mouse submandibular epithelium. *Development* 104:51-59

Nelson CM, Vanduijn MM, Inman JL, Fletcher DA, Bissell MJ (2006) Tissue geometry determines sites of mammary branching morphogenesis in organotypic cultures. *Science* 314:298-300

Nelson CM, Khauv D, Bissell MJ, Radisky DC (2008) Change in cell shape is required for matrix metalloproteinase-induced epithelial-mesenchymal transition of mammary epithelial cells. *J Cell Biochem* 105:25-33

Nemeth, Ha, Lee C (1996) Prostatic ductal system in rats: Regional variation in stromal organization. *Prostate* 28:124-128

Nonneman DJ, Ganjam VK, Welshons WV, Vom Saal FS (1992) Intrauterine position effects on steroid metabolism and steroid receptors of reproductive organs in male mice. *Biol Reprod* 47:723-729

Nuttall RK, Sampieri CL, Pennington CJ, Gill SE, Schultz GA, Edwards DR (2004) Expression analysis of the entire MMP and TIMP gene families during mouse tissue development. *FEBS Lett* 563:129-134

Omoto Y, Imamov O, Warner M, Gustafsson JA (2005) Estrogen receptor alpha and imprinting of the neonatal mouse ventral prostate by estrogen. *Proc Natl Acad Sci USA* 102:1484-1489

Ohtani H (1998) Stromal reaction in cancer tissue: pathophysiologic significance of the expression of matrix-degrading enzymes in relation to matrix turnover and immune/inflammatory reactions. *Pathol In* 48:1-9

Page-McCaw A, Ewald AJ, Werb Z (2007) Matrix metalloproteinases and the regulation of tissue remodeling. *Nat Rev Mol Cell Biol* 8:221-233

Pendás AM, Knäuper V, Puente XS, Llano E, Matter MG, Apte S, Murphy G, Lopéz-Otín C (1997) Identification and characterization of a novel human matrix metalloproteinase with unique structural characteristics, chromosomal location, and tissue distribution. *J Biol Chem* 272:4281-4286

Pereira TC, Bittencourt VDP, Secolin R, Rocha CS, Maia IG, Lopes-Cendes I (2007) Strand Analysis, a free online program for the computational identification of the best RNA interference (RNAi) targets based on Gibbs free energy. *Genet Mol Biol* 30:1206-1208

Pfau A, Caine M (1980) In: Spring-Mills E, Hafez ESSE (eds) Male Accessory Sex Glands. *Elsevier-North-Holland, New York*, p. 357

Powell WC, Domann FE Jr, Mitchen JM, Matrisian LM, Nagle RB, Bowden GT (1996) Matrilysin expression in the involuting rat ventral prostate. *Prostate* 29:159-168

Powell WC, Fingleton B, Wilson CL, Boothby M, Matrisian LM (1999) The metalloproteinase matrilysin proteolytically generates active soluble Fas ligand and potentiates epithelial cell apoptosis. *Curr Biol* 9:1441-1447

Podlasek CA, Duboule D, Bushman W (1997) Male accessory sex organ morphogenesis is altered by loss of function of Hoxd-13. *Dev Dyn* 208:454-65

Podlasek CA, Seo RM, Clemens JQ, Ma L, Maas RL, Bushman W (1999a) Hoxa-10 deficient male mice exhibit abnormal development of the accessory sex organs. *Dev Dyn* 214:1-12

Podlasek CA, Clemens JQ, Bushman W (1999b) Hoxa-13 gene mutation results in abnormal seminal vesicle and prostate development. *J Urol* 161:1655-1661

Podlasek CA, Barnett DH, Clemens JQ, Bak PM, Bushman W (1999c) Prostate development requires Sonic hedgehog expressed by the urogenital sinus epithelium. *Dev Biol* 209:28-39

Poulsom R, Pignatelli M, Stetler-Stevenson WG, Liotta LA, Wright PA, Jeffery RE, Longcroft JM, Rogers L, Stamp GW (1992) Stromal expession of 72 Kda type IV collagenase (MMP-2) and TIMP-2 mRNAs in colorectal neoplasia. *Am J Pathol* 141:389-394

Prins GS, Birch L, Habermann H, Chang WY, Christopher T, Oliver P, Bieberich C (2001) Influence of neonatal estrogens on rat prostate development. *Reprod Fertil Dev* 13:241-252

Prins G, Putz O (2008) Molecular signaling pathways that regulate prostate gland development. *Differentiation* 76:641-659

Price D (1963) Comparative aspects of development and structure in the prostate. *Natl Cancer Inst Monogr* 12:1-27

Pu Y, Huang L, Prins GS (2004) Sonic hedgehog-patched Gli signaling in the developing rat prostate gland: lobe-specific suppression by neonatal estrogens reduces ductal growth and branching. *Dev Biol* 273:257-75

Pu Y, Huan L, Birch L, Prins GS (2007) Androgen Regulation of Prostate Morphoregulatory Gene Expression: *Fgf*10-Dependent and -Independent Pathways. *Endocrinology* 148:1697-1706

Putz O, Schwartz CB, Kim S, LeBlanc GA, Cooper RL, Prins GS (2001) Neonatal low- and high-dose exposure to estradiol benzoate in the male rat: I. Effects on the prostate gland. *Biol Reprod.* 65:1496-1505

Pyke C, Ralfkiaer E, Tryggvason K, Dano K (1993) Messenger RNA for two type IV collagenases is located in stromal cells in human colon cancer. *Am J Pathol* 142: 359-365

Qin H Sun, Y, Benveniste EN (1999) The transcription factors Sp1, Sp3, and AP-2 are required for constitutive matrix metalloproteinase-2 gene expression in astroglioma cells. *J Biol Chem* 274:29130-29137

Rebustini IT, Myers C, Lassiter KS, Surmak A, Szabova L, Holmbeck K, Pedchenko V, Hudson BG, Hoffman MP (2009) MT2-MMP-dependent release of collagen IV NC1 domains regulates submandibular gland branching morphogenesis. *Dev Cell* 17:482-493

Risbridger GP, Almahbobi GA, Taylor RA (2005) Early prostate development and its association with late-life prostate disease. *Cell Tissue Res* 322: 173-181

Rouleau M, Léger J, Tenniswood M (1990) Ductal heterogeneity of cytokeratins, gene expression, and cell death in the rat ventral prostate. *Mol Endocrinol* 4:2003-2013

Ruan W, Powell-Braxton L, Kopchick JJ, Kleinberg DL (1999) Evidence that insulin-like growth factor I and growth hormone are required for prostate gland development. *Endocrinology* 140:1984-1989

Saikali Z, Singh G (2003) Doxycycline and other tetracyclines in the treatment of bone metastasis. *Anti-Cancer Drugs* 14:773-778

Sandford NL, Searle JW, Kerr JF (1984) Successive waves of apoptosis in the rat prostate after repeated withdrawal of testosterone stimulation. *Pathology* 16:406-410

Sasaki M, Enami J (1999) Hepatocyte growth factor supports androgen stimulation of growth of mouse ventral prostate epithelial cells in collagen gel matrix culture. *Cell Biol Int* 23:373-37

Sasaki M, Kaneuchi M, Fujimoto S, Tanaka Y, Dahiya R (2003) Hypermethylation can selectively silence multiple promoters of steroid receptors in cancers. *Molecular and Cellular Endocrinology* 202:201-207

Schneider A, Brand T, Zweigerdt R, Arnold H (2000) Targeted disruption of the Nkx3.1 gene in mice results in morphogenetic defects of minor salivary glands: parallels to glandular duct morphogenesis in prostate. *Mech Dev* 95:163-174

Shabsigh A, Chang DT, Heitjan, DF, Kiss A, Olsson, CA Puchner PJ Buttyan R (1998) Rapid reduction in blood flow to the rat ventral prostate gland after castration: preliminary evidence that androgens influence prostate size by regulating blood flow to the prostate gland and prostatic endothelial cell survival. *Prostate* 36:201-206

Shabsigh A, Tanji N, D'agati V, Burchardt T, Burchardt M, Hayek O, Shabsigh R, Buttyan R (1999) Vascular anatomy of the rat ventral prostate. *Anat Rec* 256:403-411

Shabsigh A, Ghafar MA, de la Taille A, Burchardt M, Kaplan SA Anastasiadis AG, Buttyan R (2001) Biomarker analysis demonstrates a hypoxic environment in the castrated rat ventral prostate gland. *J Cell Biochem* 81:437444

Signoretti S, Waltregny D, Dilks J, Isaac B, Lin D, Garraway L, Yang A, Montironi R, McKeon F, Loda M (2000) p63 is a prostate basal cell marker and is required for prostate development. *Am J Pathol* 157:1769-1775

Simpson E, Rubin G, Clyne C (1999) Local estrogens biosynthesis in males and females. *Endocrine-Related Cancer* 6:131-137

Stearns ME, Wang M (1993) Type IV collagenase (M(r) 72,000) expression in human prostate: benign and malignant tissue. *Cancer Res* 53:878-883

Stearns M, Stearns ME (1996) Evidence for increased activated metalloproteinase 2 (MMP-2a) expression associated with human prostate cancer progression. *Oncol Res* 8:69-75

Stegemann H, Stalder K (1967) Determination of hydroxyproline. *Clin Chim Acta* 18: 267-273

Steinberg Z, Myers C, Heim VM, Lathrop CA, Rebustini IT, Stewart JS, Larsen M, Hoffman MP (2005) FGFR2b signaling regulates ex vivo submandibular gland epithelial cell proliferation and branching morphogenesis. *Development* 132:1223-1234

Sternlicht MD, Werb Z (2001) How matrix metalloproteinases regulate cell behavior. *Annu Rev Cell Dev Biol* 17:463-516

Sugimura Y, Cunha GR, Donjacour AA (1986a) Morphogenesis of ductal networks in the mouse prostate. *Biol Reprod* 34:961-971

Sugimura Y, Cunha GR, Donjacour AA, Bigsby RM, Brody JR (1986b) Whole-mount autoradiography study of DNA synthetic activity during postnatal development and androgen-induced regeneration in the mouse prostate. *Biol Reprod* 34:985-995

Sugimura Y, Foster BA, Hom YK, Lipschutz JH, Rubin JS, Finch PW, Aaronson SA, Hayashi N, Kawamura J, Cunha GR (1996) Keratinocyte growth factor (KGF) can replace testosterone in the ductal branching morphogenesis of the rat ventral prostate. *Int J Dev Biol* 40:941–951

Takeda H, Lasnitzki I, Mizuno T (1986) Analysis of prostatic bud induction by brief androgen treatment in the fetal rat urogenital sinus. *J Endocrinol* 110:467-470

Tanaka M, Komuro I, Inagaki H, Jenkins NA, Copeland NG, Izumo S (2000) Nkx3.1, a murine homolog of Ddrosophila bagpipe, regulates epithelial ductal branching and proliferation of the prostate and palatine glands. *Dev Dyn* 219:248-60

Tanney DC, Feng L, Pollok AS, Lovett DH (1998) Regulated expression of matrix metalloproteinases and TIMP in nephrogenesis. *Dev Dyn* 213:121-129

Tsugaya M, Harada N, Tozawa K (1996) Aromatase mRNA levels in benign prostatic hyperplasia and prostate cancer. *Int J urol* 3:292-296

Terry DE, Clark AF (1997) Glycosaminoglycans in the three lobes of the rat prostate following castration and testosterone treatment. *Biochem Cell Biol* 74:653-658

Thomson, AA, Cunha, GR (1999) Prostatic growth and development are regulated by FGF10. *Development* 126:3693-3701

Thomson AA (2001) Role of androgens and fibroblast growth factors in prostatic development. *Reproduction* 121:187-195

Tomlinson DC, Grindley JC, Thomson AA (2004) Regulation of Fgf10 gene expression in the prostate: identification of transforming growth factor-beta1 and promoter elements.

Endocrinology 145:1988-1995

Timms TL, Truong LD, Merz VW, Krebs T, Kadmon D, Flanders KC, Park SH, Thompson TC (1994) Mesenchymal-epithelial interactions and transforming growth factor-b expression during mouse prostate morphogenesis. *Endocrinology* 134:1039-1045

Uchida K, Kanai M, Yonemura S, Ishii K, Hirokawa Y, Sugimura Y (2007) Proprotein convertases modulate budding and branching morphogenesis of rat ventral prostate. *Int J Dev Biol* 51:229-33

Upadhyay J, Shekarriz B, Nemeth JA, Dong Z, Cummings GD, Fridman R, Sakr W, Grignon DJ, Cher ML (1999) Membrane type 1-matrix metalloproteinase (MT1-MMP) and MMP-2 immunolocalization in human prostate: change in cellular localization associated with high-grade prostatic intraepithelial neoplasia. *Clin Cancer Res* 5:4105-4110

VanSaun, MN, Matrisian, LM (2006) Matrix metalloproteinases and cellular motility in development and disease. Birth Defects Res. *C Embryo Today* 78:69-79

Velasco G, Pendas AM, Fueyo A, Knauper V, Murphy G, Lopez-Otin C (1999) Cloning and characterization of human MMP-23, a new matrix metalloproteinase predominantly expressed in reproductive tissues and lacking conserved domains in other family members. *J Biol Chem* 274: 4570-4576

Vezina CM, Allgeier SH, Fritz WA, Moore RW, Strerath M, Bushman W, Peterson RE (2008) Retinoic acid induces prostatic bud formation. *Dev Dyn* 237:1321-1333

Vezina CM, Lin TM, Peterson RE (2009) AHR signaling in prostate growth, morphogenesis, and disease. *Biochem Pharmacol* 77:566-576

Vilamaior PS, Taboga SR, Carvalho HF (2006) Alternating proliferative and secretory activities contribute to the postnatal growth of rat ventral prostate. *Anat Rec A Discov Mol Cell Evol Biol* 288:885-892

Wang Y, Hayward S, Cao M, Thayer K, Cunha G (2001) Cell differentiation lineage in the prostate. *Differentiation* 68:270-279

Wang BE, Shou J, Ross S, Koeppen H, De Sauvage FJ, Gao WQ (2003) Inhibition of epithelial ductal branching in the prostate by sonic hedgehog is indirectly mediated by stromal cells. *J Biol Chem* 278:18506-18513

Wang XD, Leow CC, Zha J, Tang Z, Modrusan Z, Radtke F, Aguet M, de Sauvage FJ, Gao WQ (2006) Notch signaling is required for normal prostatic epithelial cell proliferation and

differentiation. *Dev Biol* 290:66-80

Webber MM (1981) Polypeptide hormones and the prostate. *Prog Clin Biol Res* 75:63-88

Weihua Z, Lathe R, Warner M, Gustafsson J-A (2002) An endocrine pathway in the prostate, ERβ, AR, 5α- androstane-3β, 17β-diol and CYP7B1, regulates the prostate growth. *Proc Natl Acad Sci USA* 99:13589-13594

Wilson CL, Heppner KJ, Labosky PA, Hogan BL, Matrisian LM (1997) Intestinal tumorigenesis is suppressed in mice lacking the metalloproteinase matrilysin. *Proc Natl Acad Sci USA* 94:1402-1407

Wiseman BS, Werb Z (2002) Stromal effects on mammary gland development and breast cancer. *Science* 296:1046-1049

Wiseman BS, Sternlicht MD, Lund LR, Alexander CM, Mott J, Bissell MJ, Soloway P, Itohara S, Werb Z (2003) Site-specific inductive and inhibitory activities of MMP-2 and MMP-3 orchestrate mammary gland branching morphogenesis. *J Cell Biol* 162:1123-1133

Wood M, Fudge K, Mohler JL, Frost AR, Garcia F, Wang M, Stearns ME (1997) In situ hybridization studies of metalloproteinases 2 and 9 and TIMP-1 and TIMP-2 expression in human prostate cancer. *Clin Exp Metastasis* 15:246-258

Yoshimoto M, Itoh F, Yamamoto H, Hinoda Y, Imai K, Yachi (1993) A Expression of MMP-7(PUMP-1) mRNA in human colorectal cancers. *Int J Cancer* 54:614-618

Zhao C, Dahlman-Wright K, Gustafsson JA (2008) Estrogen receptor beta: an overview and update. *Nucl Recept Signal* 1;6:e003
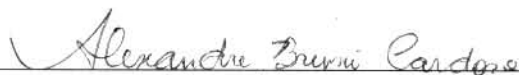
DECLARAÇÃO

Declaro para os devidos fins que o conteúdo de minha **Tese de Doutorado** intitulada "Envolvimento de Metaloproteinases de Matriz no Desenvolvimento e na regressão da próstata ventral de roedores".

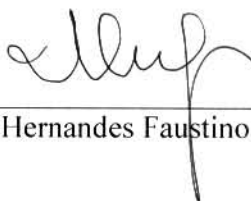( ) não se enquadra no Artigo 1º, § 3º da Informação CCPG 01/2008, referente a bioética e biossegurança.

( ) está inserido no Projeto CIBio (Protocolo nº), intitulado
_____

(X) tem autorização da Comissão de Ética em Experimentação Animal (Protocolo nº 1490-1).

( ) tem autorização do Comitê de Ética para Pesquisa com Seres Humanos (?) (Protocolo nº _____).

_____
Aluno: Alexandre Bruni Cardoso

_____
Orientador: Hernandes Faustino de Carvalho

Para uso da Comissão ou Comitê pertinente:

(X) Deferido   ( ) Indeferido

_____
Nome:
Função: Profa. Dra. ANA MARIA A. GUARALDO
                        Presidente
        Comissão de Ética na Experimentação Animal
                    CEEA/IB - UNICAMP